ABSTRACT

Title of Document: PERFORMANCE OF RESIDENTIAL
                                       HEATING AND COOLING CONTROL
                                       STRATEGIES USING DISTRIBUTED
                                       WIRELESS SENSOR NETWORKS

                                       Michael Siemann, M.S., 2010

Directed By: Professor Jungho Kim, Department of
                                       Mechanical Engineering
                                       Assistant Professor Nikhil Chopra, Department
                                       of Mechanical Engineering

        Previous work has suggested that residential space heating and cooling control

strategies that partition the structure into individual zones using wireless sensor

networks might result in lower energy consumption compared to systems using a

single-sensor thermostat. Questions have been posed as to whether these strategies

can achieve the same level of performance in a variety of geographic locations and

climates. This study compared four control strategies that utilized a wireless

temperature and humidity sensor network to regulate the comfort of a residence in the

mid-Atlantic region of the United States during the summer and winter. In particular,

the energy consumption and comfort levels of each multi-sensor strategy were

compared to a baseline strategy that mimicked a single thermostat. The difference in

energy usage measured by each control strategy was found to be statistically

insignificant. However, experiments indicated that these strategies may nevertheless

result in improvements in thermal comfort.

PERFORMANCE OF RESIDENTIAL HEATING AND COOLING CONTROL
STRATEGIES USING DISTRIBUTED WIRELESS SENSOR NETWORKS

By

Michael Siemann

Thesis submitted to the Faculty of the Graduate School of the
University of Maryland, College Park, in partial fulfillment
of the requirements for the degree of
Master of Science
2010

Advisory Committee:
Professor Jungho Kim, Chair
Assistant Professor Nikhil Chopra, Co-Chair
Professor Reinhard Radermacher
Research Associate Professor Yunho Hwang

Acknowledgements

I would like to thank my advisors Dr. Kim and Dr. Chopra for being constant sources of encouragement, guidance, and support from the initial beginnings of the project to the completion of this thesis. Their suggestions and questions pushed me to fully understand all the aspects of the experiment, and their patience was greatly appreciated. I also attribute a lot of what I have learned to the expert knowledge of my professors at the University of Maryland. My committee members, Dr. Radermacher and Dr. Hwang, have especially led my development in the field.

I appreciate the financial support from the Center for Energetic Concepts Development and the entire mechanical engineering department. I would also like to thank the Kim family for enduing several of the uncomfortable conditions introduced from control system errors, and for the tasty food.

I have been very fortunate to work with a number of current and former Phase Change Heat Transfer Lab personnel: Payam Delgoshaei, Rishi Raj, Bahman Abbasi, Thierry Some, Dongfang Chen, Steven Fuqua, Markus Nicklas, Funda Karatas, and Channing Tsai. The countless discussions and arguments in which we engaged in were invaluable to the progress and quality of this work. In particular, I would like to thank Rishi and Bahman for helping me determine if ideas presented in this thesis made sense, and thank many of my friends and engineering classmates for their support over the years. I am grateful to have loving parents who sparked my interest in science at a young age and taught me the value of hard work and being a good person.

Table of Contents

List of Tables

List of Figures

Chapter 1: Introduction

1.1 Background and Motivation

The energy revolution of the early twenty-first century is underway and energy technology is drawing interest from academia, industry, and even the rest of society. This revolution encompasses renewable and sustainable power sources, energy conservation, efficiency improvements, and integrated information sharing. An increasing number of people are realizing that current energy resources are limited, and are taking steps to search for alternatives and reduce consumption. Political leaders are calling for reductions in Carbon emissions and budgeted over 60 billion dollars for energy projects in the American Recovery and Reinvestment Act of 2009 (Recovery 2010).

According to the United States Department of Energy (DOE 2009), 21.6 quadrillion BTU's (quads) of total energy were consumed in the residential sector of the USA in 2008 (22% of the country's total). Of this, only about 0.6 quads came from renewable energy sources. Although renewable energy use is on the rise, reducing site energy consumption through low-energy building technologies will have the most significant contribution to balancing sustainable energy production with national consumption. Space heating and cooling accounts for the largest portion of residential primary energy end use at 39.4 percent, and has the potential to see the most significant reduction in energy consumption. In particular, 13 percent of the sector's energy goes to powering air conditioning and 26.4 percent is used to heat homes (2.9 % and 5.8% of the total national consumption respectively). Improving the efficiency of homes and finding

methods to cut-back the usage of heating and cooling systems can noticeably reduce the nation's energy consumption. A one percent efficiency improvement or energy reduction in residential systems would save 86 trillion BTU's or over 25 billion kWh a year, which is roughly the yearly capacity of Palo Verde Nuclear, America's largest power plant (US Nuclear 2009). There are also over 111 million existing homes in America, with only a few million being built each year; therefore, retrofitting constitutes the vast majority of the market.

There are several paths that research has taken to improve the efficiency and reduce the consumption of residential heating, ventilating, and air conditioning (HVAC) systems. Limiting energy waste during periods of light or no occupation can save substantial amounts of energy; however, designing programs and products that homeowners want to use has proven to be challenging. Higher efficiency components also show promise, but instillation and capital costs are often too high for homeowners to make the investment to improve existing systems. Wireless sensor network technology continues to become easier to install and operate while the price and operating power consumption is decreasing. This technology may provide HVAC control systems with more information, and detailed thermal environments can be used to optimize the thermal comfort and energy consumption to fit the needs of occupants.

1.2 Problem Statement

This thesis sets out to develop, test, and analyze residential HVAC control strategies that are designed to reduce energy consumption without sacrificing thermal comfort. Wireless sensor technology is used in an attempt to create a low-cost system

that will be easily deployable for the retrofit market. The greater the energy savings and ease of installation, the greater the impact it will have on national energy consumption. This thesis is a collection of two residential energy system studies: one performed in the summer for cooling systems, and another performed in the winter for heating systems. Conventional and contemporary heating and cooling systems are evaluated, and the existing literature is reviewed in Chapter 2. This background investigation identifies the most promising technology in the field and the need for new information. Chapter 3 explains the experimental design and setup, and the analytical methods used. Results for residential air conditioning are discussed in Chapter 4 and results for heating are discussed in Chapter 5. Chapter 6 summarizes the conclusions drawn from each individual study and their combination, and proposes what needs to be done in the future to reduce the country's residential energy consumption.

Chapter 2: Background and Literature Review

2.1 Brief Overview of Residential HVAC

2.1.1 Thermal Comfort

The main goal of a residential HVAC system is to control the thermal comfort of an indoor environment; therefore, it is important to establish metrics to quantify various levels of comfort. ASHRAE Standard 55 (ASHRAE 2004) describes thermal comfort as the "condition of mind that expresses satisfaction with the thermal environment." Intentionally vague, this loose definition captures more of the judgment call aspects of the sensation than an exact, rigid classification ever could. P. Ole Fanger's work over the last 40 years was successful in bringing the scientific world numerical values to count objective feelings such as "Hot" and "Cold" (Fanger 1972). ASHRAE and similar organizations worldwide have adopted Fanger's comfort metrics as the standard for thermal comfort (ASHRAE 2004 and ISO 7730 1994), and recommend considering them when designing all HVAC systems and components.

While the sensation is influenced by physical, physiological, and psychological inputs, it is an energy balance across the human body that offers the starting point for quantification. This balance can be described as equating the metabolic activity minus external work to the heat transferred to the environment. Equation 1 shows this energy balance, and Table 2.1 lists the thermoregulatory terms involved (all units can be expressed in W/m^2).

$$M - W = q_{sk} + q_{res} + S = (C + R + E_{sk}) + (C_{res} + E_{res}) + (S_{sk} + S_{cr}) \quad (1)$$

Table 2.1 Thermoregulatory Components

Symbol	Component Definition
M	Rate of metabolic heat production
W	Rate of mechanical work accomplished
q_{sk}	Total rate of heat loss from the skin
q_{res}	Total rate of heat loss through respiration
$C + R$	Sensible heat loss from skin
E_{sk}	Total rate of evaporative heat loss from skin
C_{res}	Rate of convective heat loss from respiration
E_{res}	Rate of evaporative heat loss from respiration
S_{sk}	Rate of heat storage in skin compartment
S_{cr}	Rate of heat storage in core compartment

These components, a clothing insulation factor, and environmental variables (air temperature and speed, mean radiant temperature, and water vapor pressure) reduce to equations defining Fanger's thermal comfort metrics the Predicted Mean Vote (PMV) and Predicted Percent Dissatisfied (PPD). Predicted Mean Vote uses a 7-point scale to rate levels of comfort experienced "hotter" or "colder" than the optimal level where the energy equation is balanced (PMV score of 0). Positive PMV values correspond to "hotter" conditions, while negative values equate to "colder" conditions. A slightly modified version of PMV ranges from -3.5 indicating "very cold" to 3.5 indicating "very hot" and can be explained using Table 2.2.

Table 2.2 Predicted Mean Vote

PMV	Thermal Sensitivity
< -3.5	very cold
-2.6 — -3.5	cold
-1.6 — -2.5	cool
-0.6 — -1.5	slightly cool
-0.5 — 0.5	neutral (comfortable)
0.6 — 1.5	slightly warm
1.6 — 2.5	warm
2.6 — 3.5	hot
> 3.5	very hot

Equations 2 and 3 are used to calculate the PMV, with the new terms introduced in Table 2.3, and solving for the clothing temperature iteratively.

$$\text{PMV} = \left[0.303\exp\left(-0.036M\right) + 0.028\right]L \tag{2}$$

$$T_{cl} = 35.7 - 0.028(M - W) - R_{cl}\{39.6 \times 10^{-9}f_{cl}[(T_{cl} + 273)^4 - T_r + 2734 + f_{cl}h_{cl}(T_{cl} - T_a) \tag{3}$$

Table 2.3 Predicted Mean Vote Parameters

Symbol	Parameter Definition
L	Thermal load on the body
T_{cl}	Clothing temperature
R_{cl}	Clothing thermal resistance
f_{cl}	Clothing area factor
$\bar{T}_r$	Mean radiant temperature
h_{cl}	Clothing heat transfer coefficient
T_a	Air temperature

Predicted Percent Dissatisfied relates the percentage of a population dissatisfied with a particular thermal comfort level to the PMV that comfort level is assessed. Minimal PPD is achieved at the neutral comfort level of 0 PMV, and is predicted to be 5 percent dissatisfied. Nearly one hundred percent of the population is predicted to be dissatisfied with the extreme comfort levels experienced at the edge of the range of PMV. Equation 4 relates PPD to PMV, with Figure 2.1 visualizing this relationship.

$$PPD = 100 - 95 \exp[-(0.03353 PMV^4 + 0.2179 PMV^2)] \qquad (4)$$
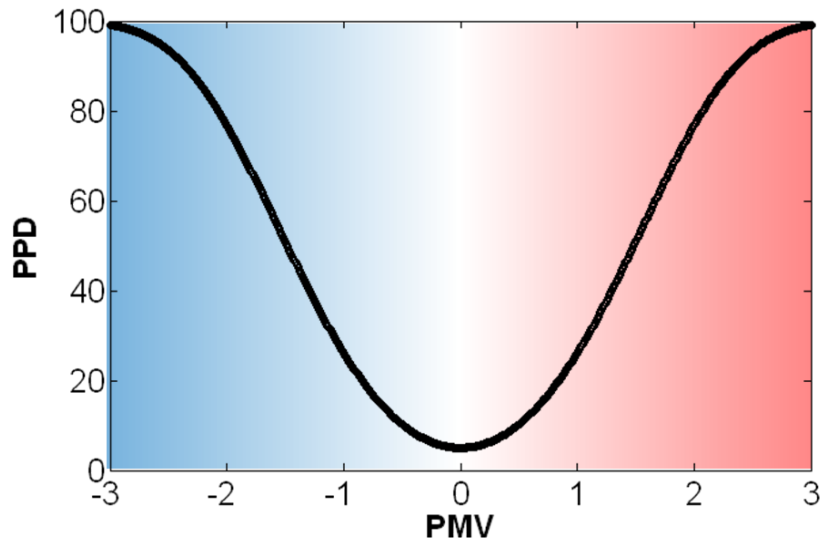
Figure 2.1 Predicted Percent Dissatisfied Verses Predicted Mean Vote

Research involving thermal comfort has continued since the 1970's and Fanger's PMV-PPD model. Fanger's original experiments in climate chambers did not show a discrepancy in the thermal comfort between the genders; however, the work of Parsons (2002) and Karjalainen (2007) found statistically significant differences in their test groups. At neutral conditions both studies observed slight differences in the thermal comfort between the genders, with women reporting cooler sensations than men in

cooler conditions. Karjalainen also observed that women experienced higher levels of discomfort in the summer due to being both cold and hot.

Studies have been conducted to characterize the transient and adaptive aspects of thermal comfort. Shorter time intervals between comfortable and uncomfortable conditions produced higher levels of measured discomfort, and triggered more adaptive responses by individuals (e.g., adding or removing clothing or opening a window) (Nicol 2002). Seasonal conditions are also shown to impact how an individual reports their thermal comfort. The PMV model accounts for different clothing levels (individuals would wear more clothes in the winter and less in the summer), but in the summer an individual is more acclimated to the heat and likely to elect a warmer temperature as being the most comfortable. de Dear and Brager (1998) assembled a large database of thermal comfort field studies comprised of over 21,000 observations, and correlated an adaptive PMV model with outdoor temperature. The study did suggest, however, that the model should mainly be used for naturally ventilated buildings, and that the results could be misleading for buildings with central systems because of the control. Humphreys and Nicol (2002) disagreed that the ability to control an environment should have an impact in assessing the actual comfort, and that PMV is successful in assessing conditions in buildings with central systems because they are often kept within a narrow range of comfort.

The thermal comfort models defined by Fanger and ASHRAE Standard 55 are still accepted in research, and recent studies have shown they are valid for application with central energy systems. The PMV-PPD model is used in this dissertation to assess thermal comfort for comparison and actuation purposes. The details about the particular

inputs and calibration associated with each individual study are presented in Section 3.4.1.

2.1.2 Conventional Technologies and Applications

Residential HVAC systems are implemented to provide general levels of thermal comfort to the occupants of a home. There are several conventional technologies used in a variety of applications to deliver the comfort. Central forced-air and hydronic, and zoned systems account for nearly 90 percent of the residential energy system usage (EERE 2009) with window/wall systems accounting for the majority of what remains (ASHRAE 2007). The most common energy sources, distribution medium and system, and terminal devises used in these main systems are given in Table 2.4.

Table 2.4 Residential Heating and Cooling Systems (ASHRAE 2007)

	Central Forced Air	*Central Hydronic*	*Zoned*
Most common energy sources	Gas Oil Electricity resistance and heat pump	Gas Oil Electricity resistance and heat pump	Gas Electricity resistance and heat pump
Distribution medium	Air	Water Steam	Air Water Refrigerant
Distribution systems	Ducting	Piping	Ducting Piping or Free Delivery
Terminal devices	Diffusers Registers Grilles	Radiators Radiant panels Fan-coil units	Included with product or same as forced-air or hydronic systems

Central forced-air systems condition spaces in the residence by delivering heated or cooled air. Figure 2.2 provides a condensed version of a typical central forced-air system, and the corresponding numbers can be used to identify the objects in the figure.

9
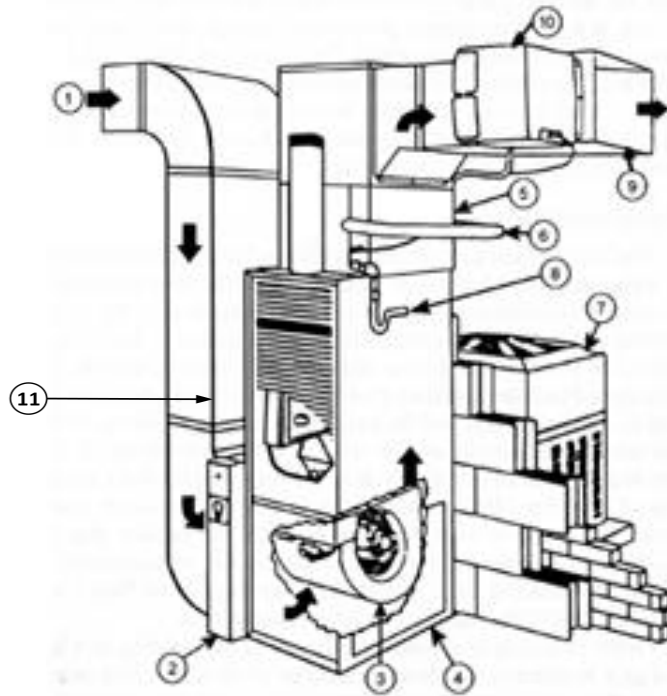
Figure 2.2 Typical Residential Installation of Heating, Cooling, Humidifying, and Air Filtering System (ASHRAE 2007)

Air is pulled into the system thought he return ducts (1) and an air filter (2) using the circulating blower (3). The conditioning air is generated in the air handling unit (AHU) (4) by forcing the air though a heat exchanger (evaporator for cooling 5 or furnace or electrical resistance coils for heating 11). When cooling is involved using the evaporator, refrigerant is cycled through the refrigerant pipe lines (6) to an outdoor condensing unit (7). The moisture that condenses from supply air onto the evaporator coil and is drained using the trap (8). Moisture can be added to the air when heating using the humidifier (10) before being distributed in the ductwork (9) to the space being conditioned in the house. Dampers, diffusers, registers and grills are used to balance and deliver the air flow to the various spaces being conditioned. Usually there exist one to two air delivery outlets per room and only one to two return inlets per floor or zone. The

cooling capacity of the heat exchanger is often expressed in refrigeration tons (1 RT =

enthalpy of fusion of 1 ton of ice to water at 32°F = 12,000 Btu/hr = 3.517 kW). Heating

capacity is expressed in Btu's per hour.

The cooling energy in the evaporator is generated using a vapor compression

cycle (VCC) and is explained in detail in any thermodynamics textbook (e.g., Çengel

2008). The basic premise of the cycle revolves around the ability of refrigerants to

absorb large quantities of heat during phase change processes.

The energy from the return air is removed by the evaporator of the VCC sensibly

in lowering the air temperature and latently in condensing the water vapor in the air. The

cooled conditioned air is then blown through the duct work, out individual registers, and

into the space being conditioned. The air in the conditioned space picks up energy from

the sun radiated through windows, occupants, appliances, lights, and infiltrated

convection and conduction through the building envelope (caused by a temperature

difference between the outdoor and indoor conditions, wind velocity, and incident solar

radiation). Figure 2.3 shows the energy flow for cooling applications with a VCC. In the

figure, solid red lines correspond to warmer air temperatures and blue represents lower

temperatures. Dashed lines represent the energy loads the air in the conditioned space

experiences. The AHU in the figure represents where the heat exchange between the

warmer return air and evaporator occurs to produce cooler conditioned air.
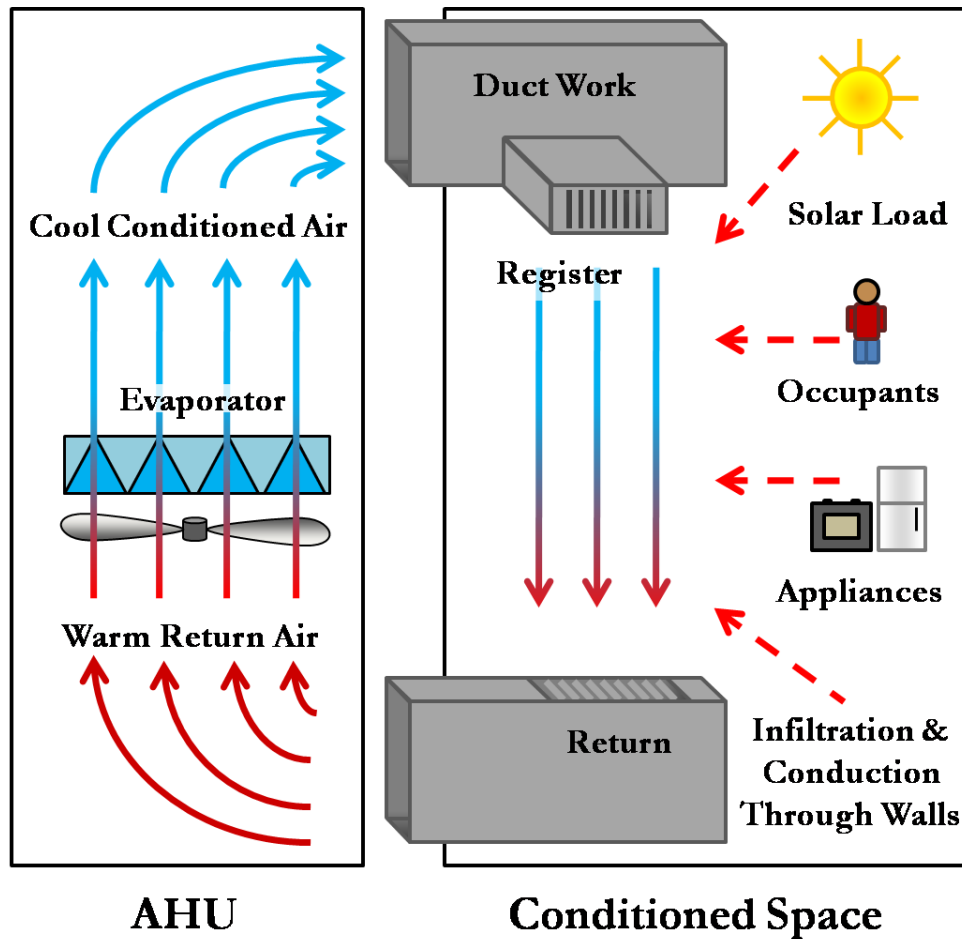
Figure 2.3 Cooling System Energy Cycle

Absorption cycle driven systems can be implemented instead of the VCC but often have too low of a coefficient of performance (COP) to warrant their use in residential systems; exceptions can be found when majorities of the input energy required is in the form of waste or cheap heat (Phillips 1984). Combining techniques to improve efficiency will be discussed in section 2.2.2. Evaporative cooling can also be advantageous in dry climates to cool air for space conditioning (Watt 1986).

There are several popular techniques employed to provide the heating energy in a central forced air system. Natural gas, oil, wood, and other combustible fueled furnaces provide the heat exchanger with high temperature air to heat the cool return air. A

detailed explanation about the combustion process can be found in any combustion

textbook (eg. Turns 2000). Once passed through the heat exchanger the combusted air is

ventilated out of the AHU and house. Heating can also be provided using an electric heat

pump; these systems are designed to utilize the equipment of a VCC cooling system,

only in reverse. Instead of the system rejecting heat to the outdoor environment, it is

dumped into the air of the AHU. These heat pumps can also have the

evaporator/condenser unit installed below ground to offer a different heat sink/source

than the outdoor ambient air and are known as ground-source geothermal heat pumps.

Figure 2.4 depicts the energy flow in a central forced air heating system with several of

the popular heating method options. In the figure, the red dashed lines also correspond to

the warm air energy sources and the blue dashed line is an energy sink.
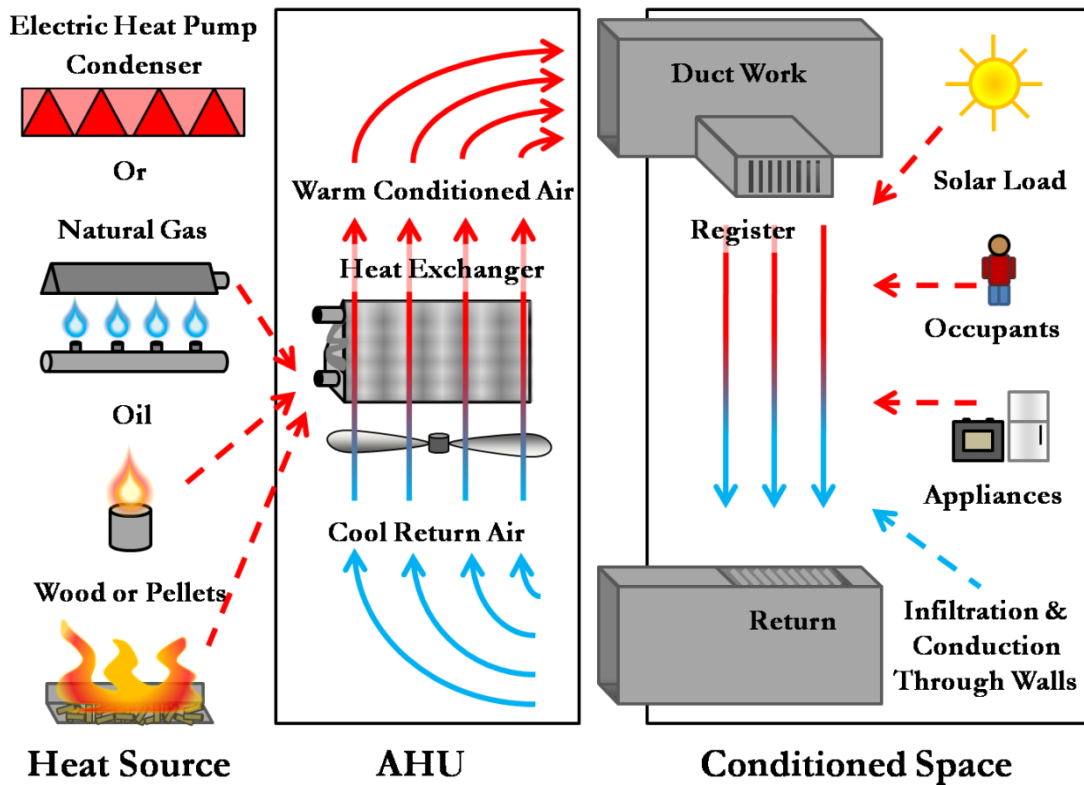
Figure 2.4 Heating System Energy Cycle

The primary distribution system used in central forced air system involves a constant speed blower fan. Constant speed fans deliver a constant volume of air (CAV) to the house. The fan is sized to balance the pressure drop in the duct network in an attempt to distribute air flow evenly. Opening and closing dampers, diffusers, and registers can redirect the air to produce alternate flow patterns; however, these are more effective with a variable speed fan system (VAV), but are less common residentially (Traister 1990).

Hydronic systems, also referred to as radiant heating systems, use conditioned water and piping instead of the air and duct work with forced air systems for the distribution medium and system. These systems involve similar heating sources to the central air with the water being heated in a boiler; one additional popular source for heat is to use radiation from the sun. Evacuated tubes or concentrated collectors can be used to heat either the supply water directly or a refrigerant that is passed through a heat exchanger to heat the supply water. The hot water is pumped to terminal radiators and baseboard convectors throughout the house where radiation and natural convection transfer the heat to the surrounding air in the space being conditioned. Figure 2.5 shows the energy flow found in a hydronic system with several of the heating energy sources. In the figure, the red and blue dotted lines show the flow of the hot or cool water in the supply and return pipes. The boiler in the figure is where the cool return water is heated using the heat source, stored, and pumped to the components.
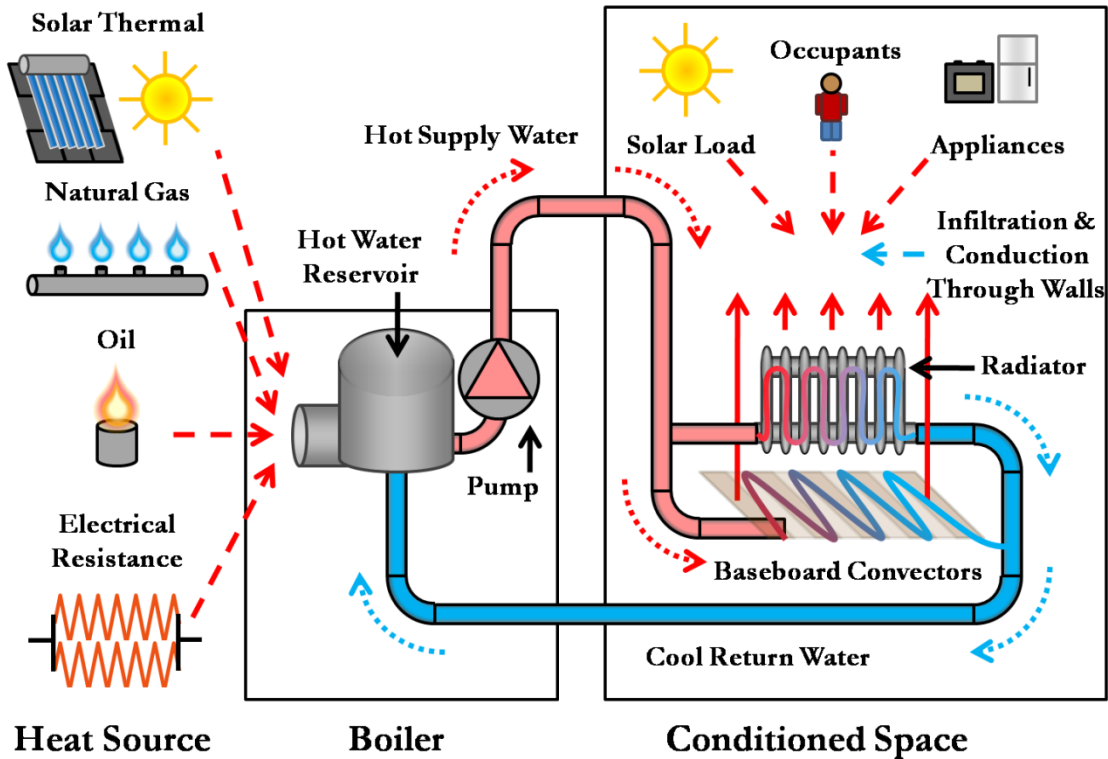
Figure 2.5 Hydronic Heating System Energy Cycle

Most modern homes are no long built with heat source such as a fireplace or furnace that only heat a single area (such as a living room) and not distribute the heat to other spaces in the house. These are powered by burning natural gas, oil, wood, coal, and other combustibles, and mostly serve as supplemental sources of heat or back-ups. This convention of only conditioning a small area can be seen with window mounted air conditioning units as well. More details about dividing up the home into individual spaces (zones) will be discussed in section 2.3.

Determining what capacity the heating and cooling system can deliver (sizing) is an important decision that can have a very large effect on the comfort capabilities and energy consumption of the system throughout its lifetime. Systems are properly sized by calculating the potential loads following local building codes for insulation, ASHRAE standards, and by using typical meteorological year (TMY) weather data. The system is

usually sized to be able to work most efficiently during the most common weather conditions, while still being able to be sufficient during almost any expected conditions (ASHRAE 2009).

2.1.3 Single Sensor Control

The previous section highlighted the basic technologies used to heat and cool residences to yield acceptable levels of thermal comfort, but there needs to be a control scheme in place to deliver the proper amounts of heating and cooling. With more primitive heating and cooling systems such as fireplaces and blocks of ice, the control was all user based. The user would perform the roles of many of the components in a control system, and at this level of simplicity, is able to perform them well. If modern systems are considered, such as a VCC driven cooling system with compressors, fans, and flow rates, performing all the same control system tasks would be quite daunting. Thermostats integrated with automated circuitry were invented to take the place of several of the occupant's tasks in these systems. The occupant provides the thermostat with their preferred comfort level (traditionally based on temperature) and the device performs all the tasks required to maintain it. This includes observing how the system is behaving, comparing that to the reference given by the occupant, determining the actions needed, and applying that input. The temperature observation is usually made by only one, local sensor. Depending on the energy system the thermostat is controlling (heating system in the winter or cooling system in the summer), the thermostat will decide an action for the system based on the measured temperature being lower or higher than the set point. If the system only has two modes of operation, ON and OFF, it is classified as a "two-position" system. The thermostat will trigger the heating system to turn on if the

sensor temperature is measured to be lower than the set point (during heating season) or trigger the cooling system to turn on if the sensor temperature is measured to be higher than the set point (during cooling season). Dead-bands and time delays are also utilized to keep the thermostat from actuating the system at too high of a frequency. Figure 2.6 visualizes this controlling scheme in a block diagram. The black colored text represents elements from the physical system and the blue text represents the controls terminology (Chen 1999).
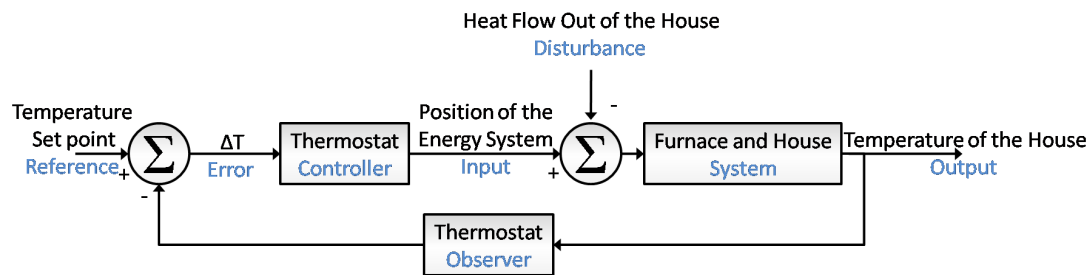
Figure 2.6 Block Diagram for Thermostat Controlled Heating

Thermostats used in residential heating and cooling systems have evolved from mechanical systems that measure temperature through the thermal expansion of metals, liquids, and gasses to electronic thermistors and resistance temperature devices (RTDs) (Haines 2006). Mechanical sensors operate with a continuous analog signal, while electronic sensors use digital signals. Sampling the temperature in intervals helps digital thermostats filter out noise and reduce the chance of requesting actuation when the true conditions do not dictate it.

2.2.1 Energy Conservation

Reducing the amount of energy a heating or cooling system consumes is a goal that benefits both the occupants of the residence (lower energy bills) and the energy providers (lower peak demands). Two major aspects of energy consumption in these systems that can be addressed are to increase energy conservation and to improve the energy efficiency. Meyers et al. (2009) determined that the average American house wastes 39 percent more energy than needed, with close to 23 percent involving the HVAC systems. They reviewed modern energy conservation techniques and believe the most amount of energy can be conserved by preventing heating and cooling an unoccupied rooms and houses and oversetting the thermostat.

Conventional heat transfer properties indicate smaller temperature differences between the indoor and outdoor environments require lower amounts of energy to maintain; therefore, lowering the thermostat set point during heating season and raising it during cooling season should reduce energy consumption. Vine (1986) examined several of the determinants associated with occupant's thermostat set points by analyzing self reported data. His findings suggested that individuals that understood the benefits of adjusting the set points (better educated individuals and occupants from household that have received an energy audit to be specific) reported lower levels of energy consumption than their counterparts. Lowering or raising the set point has energy benefits, but will obviously translate to lower levels of comfort. Research has been conducted in a wide variety of climates throughout the world and over several decades to determine settings that optimize comfort and energy conservation. Nassif et al. (2004)

used a genetic algorithm search to optimize the monthly set points for a building on the campus of École de technologie supérieure in Montreal, Canada. An evolutionary-programming technique was used by Fong et al. (2005) to find the set points for different weather conditions throughout a year in China.

Further energy conservation can be achieved by setting the comfort level in the house significantly lower during the nighttime and periods when the house is unoccupied. This practice is known as thermostat setback, and has been around for many years. Ingersoll and Huang (1985) investigated how much energy was saved using a combination of setbacks during the night and day in four major U.S. climate zones during the heating season. The base temperature set point was 21.1°C and setback to 15.6°C, 10°C, and -6.7°C , as well as, using a higher set point of 22.2°C. Table 2.5 shows the annual heating energy consumptions for multiple schemes of setback tests in the four climates. The energy consumption is listed in gigajoules and the percents relate the energy consumption of that strategy to the base case of an all-day 21.1°C set point.

Table 2.5 Annual Energy Savings for Single-Zone Setback Options for Tight Houses (Ingersoll and Huang 1985)

Setback Strategy ⟍ Climate Zone	Base case (21.1°C all Day)	Night setback (21.1°C setback to 15.6°C at night)	Night and day setback (21.1°C setback to 15.6°C at night and day)	High thermo-stat temperature (22.2°C all day)
Cool (MN)	84.87	81.29 (-4.2%)	75.75 (-10.7%)	81.29 (+7.2%)
Temperate (NY)	46.64	43.82 (-6.0%)	39.84 (-14.6%)	52.61 (+12.8%)
Hot-humid (TX)	16.04	14.43 (-10.0%)	12.76 (-20.5%)	17.54 (+21.6%)
Hot-arid (AZ)	12.33	10.57 (-14.3%)	9.62 (-22.0%)	13.81 (+30.6%)

They found the energy savings was dependent on the climate zone and characteristics of the house. Houses with looser construction and lower levels of insulation were classified as having "lower thermal integrity" and saw more relative energy savings using the setbacks than tight and well insulated houses. This does not suggest that looser construction and lower insulation will save more energy; rather, that if those conditions already exits, using setback will have more of an impact. The energy conserved in having the house float down from a base point to the setback point is usually equivalent to the energy require to reverse the process and return from the lower setback to the base levels; the energy is saved while the system operates at the lower setback point due to a lower temperature difference between the indoor and outdoor temperatures. The lower thermal integrity houses would reach the setback temperatures faster, and have a longer opportunity to operate at the lower demanding setback conditions, resulting in up to 22 percent energy savings in the case of the hot-arid climate with day and nighttime setbacks to 15.6°C from 21.1°C. Energy savings were still seen for the houses with tight construction and sufficient insulation, but the authors cautioned that using setbacks could be counterproductive because they shifted the peak load and degraded efficiency because of periods of overwork. Although energy can be saved using setbacks, most occupants would not find the gains enough to outweigh the uncomfortable period experienced while the temperature returns to the normal set point if they had to manually perform the setting change.

Programmable thermostats were designed to reap the benefits of thermostat setback while preventing daily periods of discomfort by scheduling the setback periods to end before the occupants would wake-up in the morning and return from work/school

and extended periods away from the house. The DOE's Residential Energy

Consumption Survey (EERE 2009) reported that 30 percent of American homes have

programmable thermostats; however, only 56 percent of those (17% of American

homes) utilize their setback programming potential. Irregular occupant schedules and

difficulty with the programming interface are two problems noted in explaining why

such a large percentage of programmable thermostats are not used properly.

Preliminary work at the Massachusetts Institute of Technology using the global

positioning system (GPS) features of mobile phones has been done to improve

scheduling issues with programmable thermostats (Gupta 2008). Instead of having a set

time for the thermostat to return setback temperatures to normal conditions, the return is

triggered by the occupant's distance from home and estimated arrival time. The

investigators observed up to 12.2 percent energy savings in their pilot study. An

improved interface for the programmable thermostat using a graphical user interface

(GUI) program on a personal computer has also been tested (Williams 2006). Occupants

were able to monitor their indoor conditions and electricity usage throughout the day.

This information guided users in their cooling system decisions and, with the adoption

of precooling to shift loads, energy and money were saved. Home occupancy can be

monitored to develop statistical models that predict when the house will be occupied in

the future, and need heating or cooling.

Recent work at the University of Virginia with self-programming thermostats has

yielded positive results (Gao 2009). These thermostats observe the occupancy patterns in

a home and automatically optimize the heating and cooling schedule based on statistical

occupancy. The occupant can set the level of occupancy that translates to an energy

system being activated by turning a comfort knob. An example would be if the house is occasionally occupied at 14:00 and the optimized schedule does not provide heating or cooling at that time. If the occupant wanted to make sure that the house would be comfortable at 14:00, in case one of those rare occasions occurred, they could adjust the comfort knob to have the system consider that level of occupancy worth controlling the comfort. The costs for this added comfort are reductions in the energy savings, but a balance can be tuned by the occupants to reach the best comfort / energy consumption ratio. In the most cost efficient mode, the test researchers reported 15 percent energy savings on top of the EnergyStar recommended setback schedule (EnergyStar 2010).

Hydronic heating systems can also be improved to reduce energy waste that occurs during low demand periods. Instead of keeping the hot water reservoir at a constant high temperature throughout the course of a day, a process that requires energy even if the water is not circulated for heating use, the reservoir temperature can be lowered during these observed periods when heating is not needed. Butcher et al. (2006) observed energy savings on the order of 25 percent when they adopted temperature reductions to fit with an annual load pattern model.

2.2.2 Improving Energy Efficiency

Energy conservation strategies save energy by reducing the benefits of the energy system (such as not providing optimal comfort at certain periods of the day); energy efficiency improvements are able to save energy and provide equal, if not greater, benefits. These efficiency gains can be reached by improving both the physical hardware and how the system operates.

Improving the performance of individual components in the heating and cooling system can improve energy efficiency by requiring less electricity and running in shorter intervals. For central forced air heating and cooling systems, energy can be saved by using a more efficient blower fan. Studies conducted at Lawrence Berkley National Laboratory have investigated several high efficiency motors used for blowers (Walker and Lutz 2005; Lutz et al. 2006)). Two prominent technologies are permanent split capacitor (PSC) single-phase induction and brushless permanent magnet (BPM) motors. Under field conditions, natural gas furnaces fitted with PSC motor driven blowers consumed 10 percent less electricity than the DOE test procedure results; BPM consumed 36 percent less electricity. Note that these percentages are only the electricity savings for the fan motors, actual energy savings would be less.

The heat source / sink used in heat pump and VCC cycles offer an area to improve the system efficiency. Lower outdoor temperatures for heat pump evaporator units translate to higher pressure ratios if the condenser coils are to deliver the same temperatures for heat exchange. Higher pressure ratios require more compressor work, and lower overall system efficiency. The ground around a house can be used as the heat source for heat pump systems and the heat sink for VCC cooling systems. These geothermal ground source heat pump (GSHP) systems can predominantly use the soil or water in the aquifer to exchange heat with depending on the size and demand of the system. Sanner et al. (2003) and Lund et al. (2003) evaluated the world utilization of geothermal heat pumps. In 2003 they reported only over one million worldwide units, but observed a 10 percent increase each year. Omer (2008) reviewed the current technology and configurations of GSHP and recommends them based on improved

energy efficiency and reductions to CO_2 emissions. Energy savings are seen in almost all systems; however, the high installation costs are still limiting widespread adoption.

The Center for Environmental Energy Engineering (CEEE) at the University of Maryland observed promising results using evaporative cooling in the condenser unit (Hwang et al. 2001). The experiment was performed in two environmentally controlled test chambers to control both the indoor and outdoor conditions a cooling system would see. The tube sizing and wheel speed were optimized to maximize the evaporative condenser's benefits, and a higher capacity, COP, and seasonal energy efficiency ratio (SEER) were seen compared to a standard air cooled unit.

Energy is often lost by systems overshooting their set points; overshoot occurs when the house continues to cool down below the set point after the system has been turned off. This is detrimental because it introduces a larger, unwanted temperature difference. Often this triggers a manual re-set of the temperature controls by the occupants in an effort to maintain comfort. Occupants even overset the thermostat setting, believing that the system will respond similarly to an automobile throttle. They believe the conditions will arrive at a comfortable position faster than simply setting it at that comfortable position. Use of proportional, integral, and/or derivative (P, I, and/or D) controllers has been shown to eliminate overshoot and save energy in simulations (Kolokptsa 2003) and environmental chambers testing (Kolokotsa et al. 2006) on the order of 20 percent. While these have been shown to work, applying improper gains often results in instability, and predictive modeling is needed to account for large disturbances such as elevated solar and human loading (Dounis 2009).

Multiple-stage furnaces and compressors are used to improve the efficiency of heating and cooling systems. A specific load can be met with the most efficiency by a particular capacity. The multi-stage systems are able to deliver different levels of capacity at the different stages. Lower loads might only require a little bit of heat, so the low setting on a multi-stage furnace might only combust the natural gas at a fraction of what it is capable of. In 2006 both the DOE and ASHRAE performed studies on residential two-stage furnaces with traditional fan motor technology; interestingly, each test arrived at a different conclusion. The Lawrence Berkley National Laboratory compared the two tests and results reported by other field tests (Lekov et al. 2006). When combining the reduction in fuel with the increase in electricity consumption in two-stage furnaces, the DOE test yielded a three percent reduction in energy. The ASHRAE test showed almost no difference in the energy consumption compared to a single-stage system in the same efficiency class. The reviews cited ASHRAE's better methodology for calculating the energy consumption as the reason for the discrepancy because the field tests also were unable to show energy savings. Two-stage furnaces with BPM blower fan motors are shown to improve the energy efficiency, so these results suggest savings is due primarily to the motor.

2.3 Multiple Sensor Control

2.3.1 Room Variations and Zoning

Another source of energy loss in residential heating and cooling systems is in large temperature differences between rooms; individual rooms or areas in a house can be several degrees cooler or warmer than the remainder of the house and even the area

surrounding the thermostat. Occupants can experience large periods of discomfort and again try to compensate by treating the thermostat like an "ON/OFF switch" by manually adjusting the set point to a temperature higher or lower than the comfort level desired. The system then heats or cools constantly until the occupant achieves localized comfort; consequently, other areas of the house become uncomfortable and an unstable cycle of overshooting the set points ensues. A solution that has been explored is to have multiple sensors distributed throughout the house so the controller will know about any large temperature differences. The ASHRAE Handbook (ASHRAE 2009) recommends the use of multi-zone control when a single thermostat is not able to properly characterize the house due to zone-to-zone temperature differences.

Simulations have been conducted that yield energy savings in central, single position systems that use multiple sensors to construct a more detailed environment. Lin et al. (2002) found savings in control strategies that averaged the conditions in the house so heating or cooling was not initiated if it would push a room further away from the set point. Though rare for residential use due to the price, multi-zoning and using a VAV system to deliver variable amounts of air can save energy by only providing heating or cooling to zones that need it. Oppenheim (1992) developed several multi-zone setback strategies and compared them to a single zone strategy with an 8-hour 12°F setback. He was able to see fuel savings of 12 percent with a multi-zone strategy using 22-hour setbacks in two of the zones, but saw six percent additional fuel consumption when the bedroom zone was set back 18 hours and the rest of the house only 12. An extensive comfort and outdoor condition analysis was not performed with this study. This analysis could show the sources for the unexpected results of increasing the fuel consumption.

Temple (2004) also showed that energy consumption increased slightly in a home installed with a zoned system because rooms that were originally uncomfortable from not receiving enough cooling energy, were provided with it. This cost the system more energy but provided more overall and uniform comfort.

Systems can also be zoned that are CAV by opening and closing the registers in the zones. Manually adjusting the registers would be a daunting task if variable loads and demands were always being imposed on the house. The Demand Response Enabling Technology Development (DRETD) group at the University California Berkeley has performed some preliminary work in the field of automating dampers to zone houses (Brown 2007). The research project divided a two-story home into four zones, and used an occupancy schedule to dictate the set points for individual zones during heating season. The original thermostat was located in the zone that would always report the lowest temperatures, so without the multi-zone system this house saw over heating in every other zone. This observation and the occupancy schedule are two important details that can explain the high 26 percent energy savings. Another factor that register automation systems need to be cautious of is restricting too much airflow. Walker (2003) determined that closing registers translates to increased energy usage by the fan. He warned that closing 60 percent of the registers could lead to frozen evaporator coils (not enough heat transfer) and other pressure related issues.

2.3.2 Wireless Sensor Network's Opportunity

Many articles in the ASHRAE Journal discussed using wireless technology to develop sensor networks for building monitoring and control applications. Wireless sensor networks are becoming easier to install and operate while decreasing in price and

operating power consumption (Wills 2004; Healy 2005). Questions about the cost effectiveness in retrofit and new construction applications and the reliability of wireless sensor networks are still being asked (Roth 2008).

Akyildiz et al. (2002; 2005) review current wireless technology trends and explain how sensor networks operate. A simple network is comprised of sensor nodes (motes) that can transmit and receive information, a gateway, and a server to store information collected by the network (sink). The motes contain sensors, a microprocessor, a radio transceiver, and a power supply. TinyOS (2009) is the standard operating system motes are programmed in. Most networks are set up as ad-hoc so that a preexisting routing infrastructure does not need to be in place. This allows for new sensors to join the network or ones to be removed (self healing mesh). Motes can also transmit their information through other motes by multi-hopping. Figure 2.7 shows a basic diagram to explain the different features found in wireless sensor network communication.
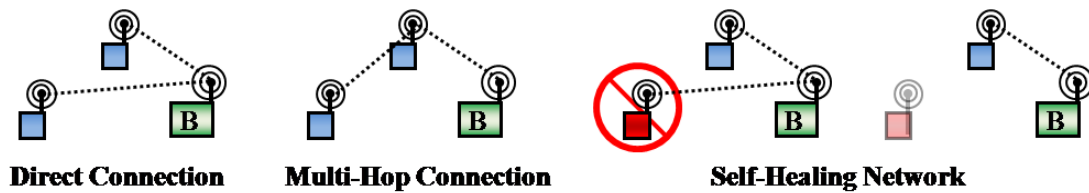
Figure 2.7 Wireless Sensor Network Communication

The Center for Environmental Design Reach at UC Berkeley conducted a study in a simulated office building with under floor air distribution (UFAD) (Wang 2002). Several single and multi-senor control strategies were developed to test different sensor locations. One simulation used two sensors (one located at foot level and one located at chest height) and showed both an eight percent energy savings and improved thermal comfort. The second, floor level sensor allowed the supply air temperature to be

28

optimized to reduce stratification. Placing only one sensor at non-standard height can also improve the thermal comfort with UFAD systems.

Research by the Center for the Built Environment (CBE) at UC Berkeley has yielded cooling system energy savings through control strategies that employed a wireless sensor network (Ota et al. 2008). The testing was performed on a single story residence with a central, two position cooling system in Pleasanton, California during the late summer. Three multi-sensor strategies, two of which used Fanger's PMV-PPD comfort metric, were compared to single-sensor strategies. Figure 2.8 presents a figure from the study showing the average energy consumption of each control strategy normalized by the cooling degree hours. The error bars estimate the range of energy consumption from periods where data was missing from the test.
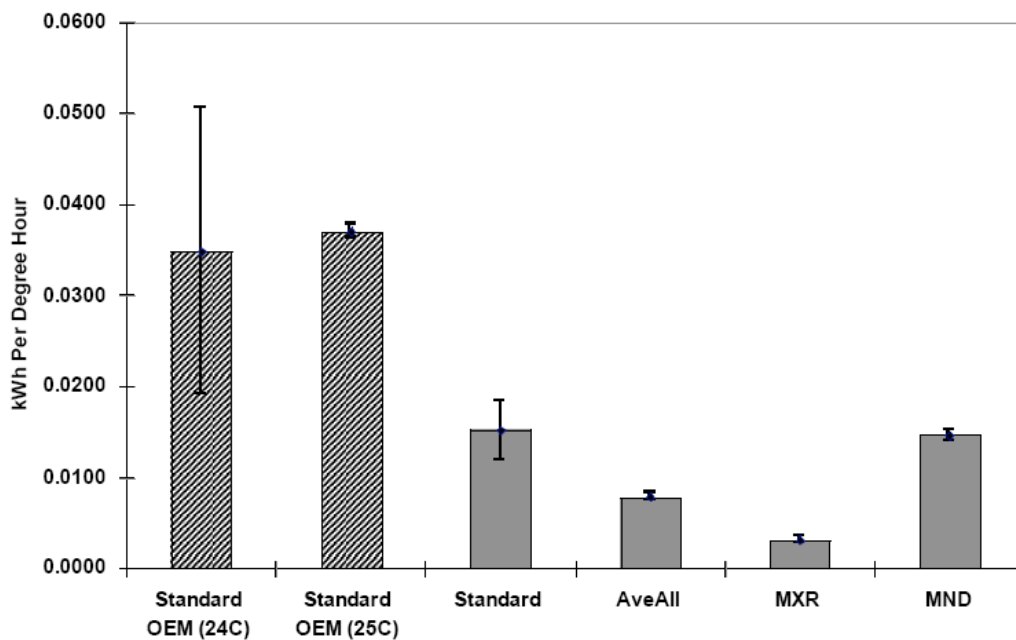
Figure 2.8 Normalized Average Energy Consumption (Ota et al. 2008)

These results show simultaneous comfort improvements and normalized energy savings of up to 79 percent. One can speculate that reported energy savings this large

could not be entirely due to these innovative control strategies. Several concerns that come to mind are the Standard OEM strategy used to benchmark the other strategies. The error bars for StandardOEM(24C) on Figure 2.8 show that there was a large amount of lost data. Figure 2.9from the study shows the temperature traces for each of the strategies on days with similar outdoor conditions.
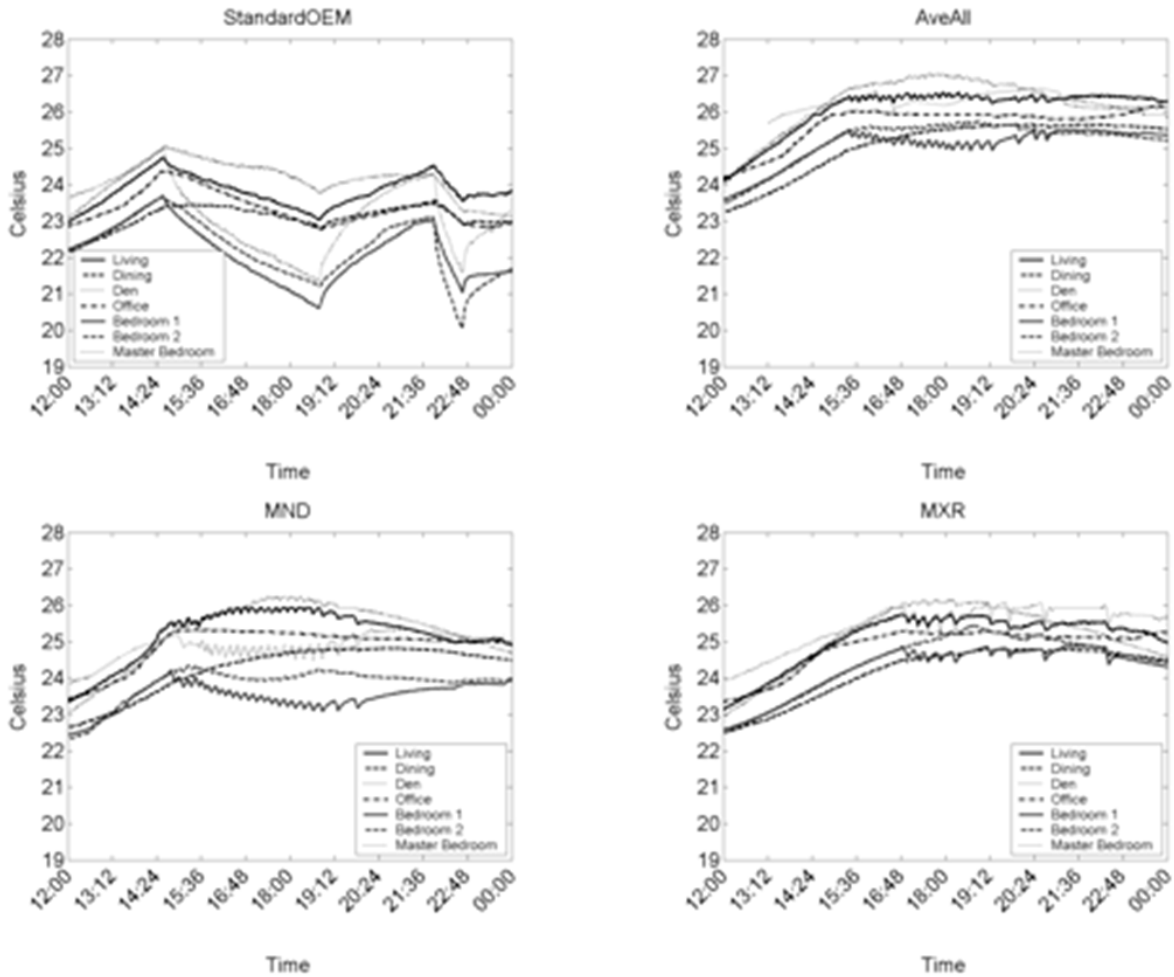
Figure 2.9 Daily Temperature Traces (Ota et al. 2008)

The StandardOEM strategy on this figure also behaved quite differently than the other strategies. It appears that StandardOEM kept the entire house at a much cooler temperature during the day and even one room reaches 20°C, at least 5°C cooler than the corresponding point on the other strategies' plots. These cooler conditions in the

StandardOEM would certainly translate to lower energy consumption in the warmer strategies. The small oscillations in the temperature after 14:30 in the plots for AveAll and MND suggests that the house stops floating and the conditions have reached a point where the control strategy thresholds are reached and begin actively controlling the house. The MXR plot does not exhibit this behavior until 16:45; if energy consumption is calculated over the course of the day or half day, these two hours can be significant. Section 3.4.4 of this thesis will investigate how even using the same strategy on days with similar outdoor conditions can start the main actuation period at different times in the day. The experiment was also only performed from August 11 to September 7in 2006, and smaller levels of data could translate to less statistically significant data.

Discrepancies also existed between the ASME IMECE Conference Paper (Ota et al. 2008) and main author's thesis (Ota 2007). The conference paper said that the benchmarking strategy was the StandardOEM strategy; specifically it reads, "The AveAll, MND, and MXR strategy reduce consumption by 48%, 4%, and 79%, compared to the StandardOEM strategy." The thesis presents the Standard strategy as the benchmark for energy consumption and reads, "The air-conditioning system consumes approximately 75% less energy when maximizing the number of rooms below a 10 PPD threshold [MXR] than compared to the Standard strategy." Figure 2.10 shows a plot of the normalized energy consumption and a table of the values found in the thesis. Using the values from the table to calculate the energy savings between the Standard and MXR strategies yields the 79 percent reported. Using the StandardOEM(24C) strategy yields 91 percent energy savings, so it appears that the conference paper had a misleading typographical error. Also the Standard strategy had a

daily temperature trace plot in neither the conference paper nor the thesis, and said that

the temperature profile was very similar to that of the AveAll(24C), a strategy that

showed 48 percent energy savings. More information about the benchmarking strategy is

needed for a reader to understand the results of the study.

	Standard OEM (24C)	Standard OEM (25C)	Standard (24C)	AveAll (24C)	MXR	MND
▣ Best Case	0.0192	0.0364	0.0120	0.0083	0.0036	0.0152
◆ Average	0.0349	0.0371	0.0153	0.0080	0.0032	0.0147
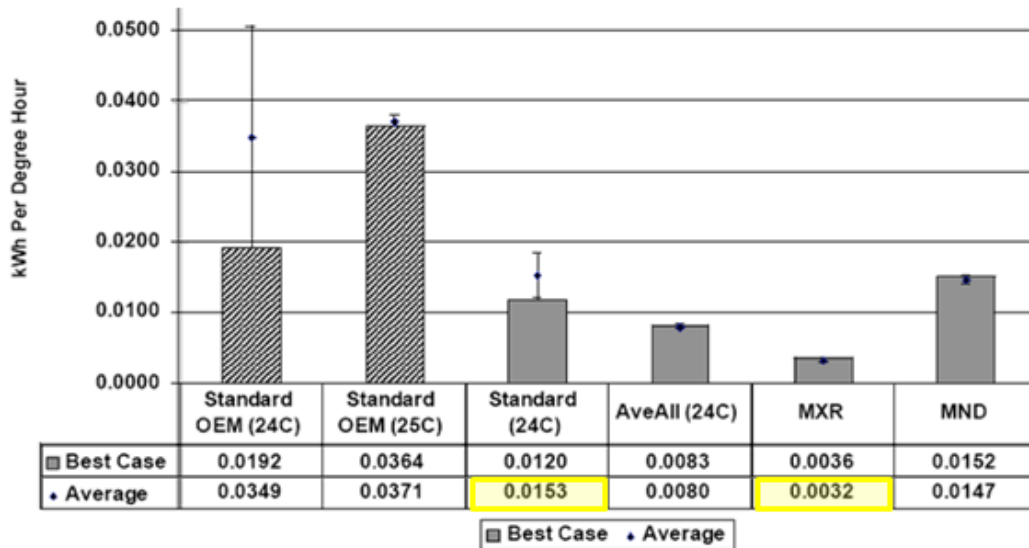
Figure 2.10 Normalized Average Energy Consumption (Ota 2007)

The authors may have been unable to demonstrate their understanding of these

concerns in the paper, and they may turn out to be insignificant compared to the driving

mechanisms. The research appears to show very promising results. Energy savings this

large could accelerate the adoption of wireless technology into building control and

monitoring, and if these strategies are applied on a large scale, they could bring about

significant reductions to the country's energy consumption.

2.2.3 Summary of Savings

Table 2.6 summarizes the energy conservation techniques found in the literature

pertaining to residential heating and cooling systems. Table 2.7 summarizes the latest in

energy efficiency technology.

Table 2.6 Residential Heating and Cooling Energy Conservation Techniques

Energy Conservation Technique	Investigative Authors	Benefits and Energy Savings
Set point education	Vine 1996	Lower energy consumption
Optimize temperature and comfort	House et al. 1991 Nassif et al. 2004 Fong et al. 2005	Optimal comfort and energy consumption
Thermostat setback	Ingersoll and Huang 1985	22% energy savings
Programmable thermostat with setback		Easier method to perform setback
GPS programmable thermostat with setback	Gupta 2008	12% energy savings
HVAC GUI	Williams 2006	Energy and money savings
Self programmable thermostat with setback	Gao 2009	15% energy savings and tuning
Hydraulic temperature setbacks	Butcher et al. 2006	25% energy savings

Table 2.7 Residential Heating and Cooling Energy Efficiency Techniques

Energy Efficiency Technique	Investigative Authors	Benefits and Energy Savings
Improved fan motor	Walker and Lurtz 2005 Lurtz et al. 2006	10-36% less electricity
GSHP	Sunner et al. 2003 Lund et al. 2003 Omer 2008	Energy savings and reduced CO_2 emissions
Evaporative cooled Condenser	Hwang et al. 2001	Increased capacity, COP, and SEER
PID thermostat control	Kolokotsa et al. 2006	20% energy savings
2-Stage furnace	DOE 2003 ASHRAE 2003	3% energy savings No significant savings
Multi-zone sensing	Lin et al. 2002	17% energy savings
Multi-zone with VAV	Oppenheim 1992 Temple 2004	12% energy savings Energy consumption increases but thermal comfort improved
Multi-zone with CAV and register control	Brown 2007	26% energy savings
UFAD with wireless sensors	Wan et al. 2002	8% energy savings and improved comfort
Distributed wireless sensing and innovative control algorithms	Ota et al. 2008	79% energy savings and thermal comfort improvements

2.4 Research Objectives

Residential heating and cooling amounts to a significant portion of the country's energy consumption, and small improvements can have large impacts if they are deployed throughout the country. After reviewing the literature, it appears that energy conservation techniques may be more limited by the habits and education of occupants, and not the technology. These projects have shown that any implemented technology should involve as little required interaction with the occupants as possible. Energy efficiency improvements can be run in series with these energy conservation techniques to further reduce the energy consumption; therefore, investigating the efficiency of heating and cooling systems will have a greater potential for impact.

The work presented by the CBE showed the highest energy saving results at 79 percent using distributed wireless sensors and innovative control algorithms employing the PPD-PMV thermal comfort model. The adoption of wireless sensor network technology in buildings is still in the beginning stages, and more research is needed to push the market further. This project can easily be adapted to a retrofit commercial product once energy savings are seen.

This thesis complimented the work done by the CBE by investigating how much energy was saved using similar WSNs and control strategies under different conditions and seasons. According to Weather Underground (2009), the site for this test (North Bethesda, Maryland) experienced an average of 214 more cooling degree days (CDD) calculated from 19°C during the last three years and higher relative humidity (RH) than Pleasanton, California. The control strategies were also deployed in the winter for use with a natural gas furnace for heating. The house used in this study had two stories and

data was collected from the beginning of June, 2009 to the end of August, 2009 as well as late November, 2009 to the end of January, 2010.

Two strategies from the CBE and three new strategies were compared in this new environment to see if their energy and comfort performance were statistically significantly different than conventional thermostat logic. Statistical tests were unable to show significant amounts of energy reductions in the different control strategies in the summer. A strategy that used thermal comfort instead of thermostat temperature logic was shown to require 36 percent more energy when comparisons were made using hot days and a 14:00-20:00 interval. The two CBE control strategies were unable to save energy; however, the MND strategy improved average comfort by 3 PPD and the MXR by 1 PPD. The control strategies used in winter heating experiment were neither able to show energy savings nor reduced the large temperature differences between the two floors. Varying the strategy set points was able to show that the energy consumption depended more on the outdoor conditions and set point than the particular strategy.

Chapter 3: Experiment Design, Setup, and Analysis Techniques

3.1 Introduction

Since the results of the experiments are heavily dependent on the test house, heating and cooling systems, and climate, a detailed description of each is provided in this chapter. Other parameters involving the test setup are explained as well including the control system, wireless sensor network, and control strategies. Several of the control strategies draw on the PMV and PPD metrics, and the calibration parameters play a significant role in determining what conditions are defined as comfortable. These parameters changed between the summer cooling and winter heating tests. Degree days are used to characterize the outdoor weather conditions, and duty cycles give a good measure of the energy consumption. Intervals were used to capture specific periods of interest and played a role in mitigating errors introduced by initial conditions. The statistical methods and uncertainty analysis are also explained in this chapter so only statistically justified conclusions are only drawn.

3.2 Test House Setup

3.2.1 House Parameters and HVAC systems

The house used in the heating and cooling experiments was constructed in 1987 and is located in North Bethesda, Maryland. There were two above ground stories with a walkout basement, seven main rooms including a 3.7 by 4.9 square meter (12x16 square feet) family room with a cathedral ceiling. The house had 178 square meters (1900 square feet) of floor space with an additional 98 square meters (1050 square feet) of

finished basement space. The house faced the northwest, had an attached garage on the north side, and a roofed deck attached off the back. Figure 3.1 provides a scaled version of the test house's floor plan and Figure 3.2 is a photograph taken of the front of the test house.
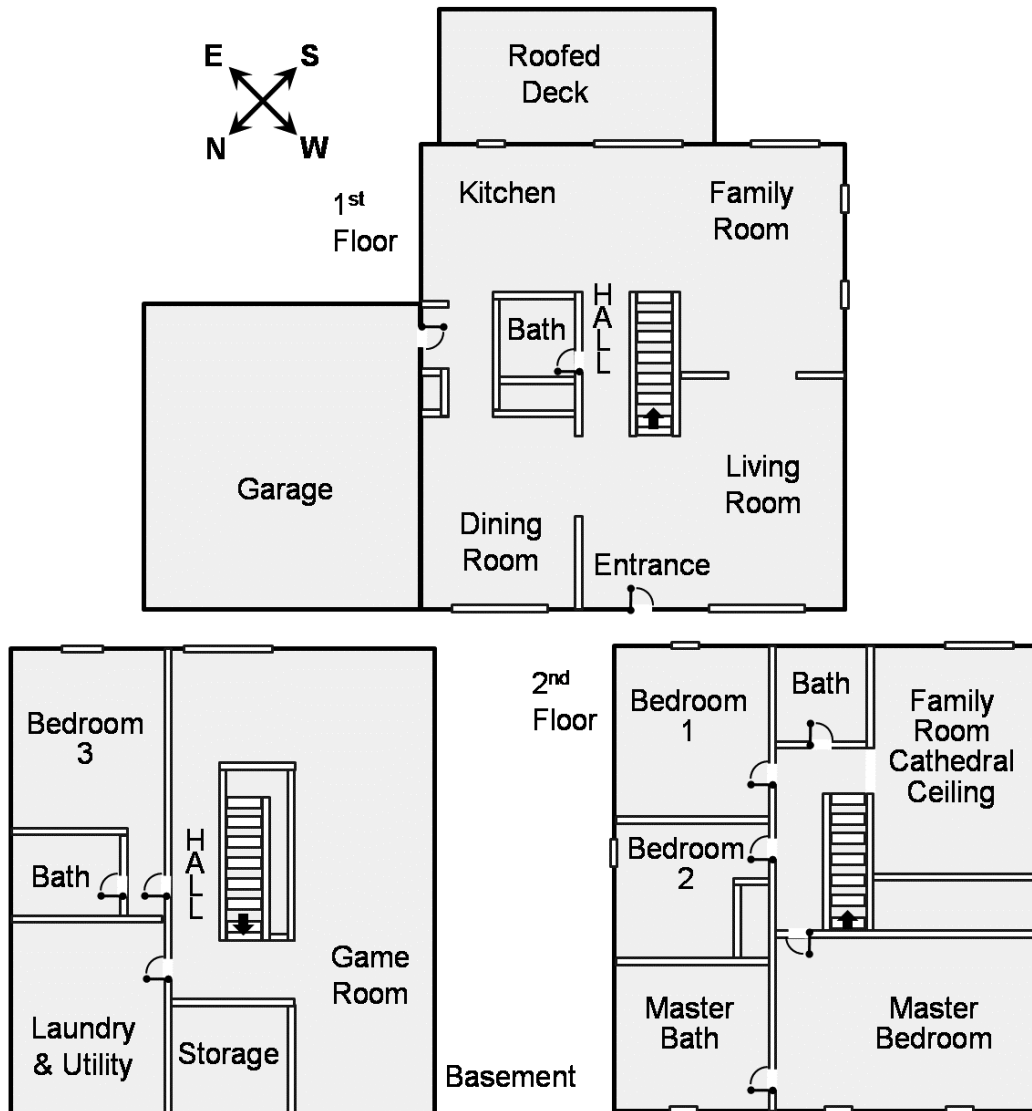
Figure 3.1 Test House Floor Plan

Figure 3.2 Photograph of the Test House (taken in March 2010)

The house was built with a wooden frame and drywall interior walls. The roof was covered in asphalt shingles and the attic had approximately 30.5 cm (12 inches) of loose-fill fiberglass insulation. The windows and sliding glass doors on the first and basement levels were double-paned, Argon filled, and had insulated PVC frames. The house was covered primarily with light grey aluminum siding and had a brick front facade.

There were several sources of shading throughout the course of the day for the house. Two trees are located in the front and a wooded area comprised of bamboo and trees is found in the back. Neighbor houses flank the house to the left and right 8.6 and 6.2 meters (28 and 20 feet), respectively. There was also a patch of large trees 30 meters to the west of the house that shaded in the late evening. Figure 3.3 shows the locations of the shading trees and neighbor houses and Figure 3.4 is a photograph of the wooded area behind the house.
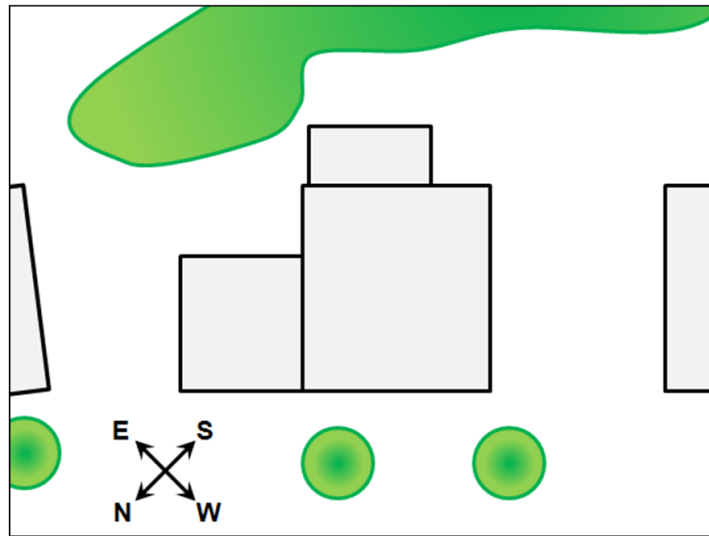
Figure 3.3 Shading Trees and Neighbor Houses

Figure 3.4 Photograph of the Shading on the Back Side of the House (taken in March 2010)

The house was cooled using a ten-year-old Carrier TECH2000SS 3.5 ton central air conditioning system with a SEER of 12. The heating furnace input was 100,000 BTU of natural gas with a nominal 80% efficiency. The furnace had existed since the construction of the house and the current efficiency is unknown. The systems were controlled using a Ritetemp 8030 programmable thermostat located in the first floor hallway.

3.2.2 Climate

The test house is located in Climate Zone 4 according to the DOE (Energy codes 2010). The region falls on the boundary between the Köppen defined humid subtropical and hot summer continental climates (Peel 2007). The average annual relative humidity is 67 percent, with a 73 percent average found in the summer months (Weatherunderground 2010). When calculated from 19°C (66.2°F), North Bethesda has averaged 750 annual cooling degree days over the past three years (1493 if calculated from 65°F). It has averaged 2037 annual heating degree days if calculated from a base of 15.5°C (4768 from 65°F; note calculating the degree day metric is discussed in section 3.4.2). The Environmental Sciences Services Administration (ESSA 1970) shows the historical average annual cooling and heating degree days for the entire United States in Figure 3.5 and Figure 3.6 respectively; these show how the numbers for North Bethesda, MD compare to the rest of the country.
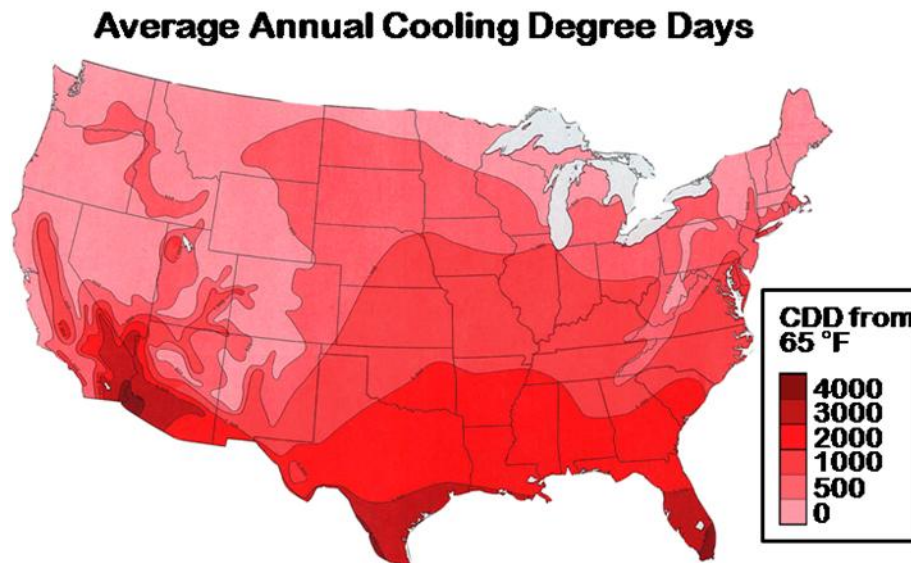
Figure 3.5 Average Cooling Degree Days for the USA (ESSA 1970)
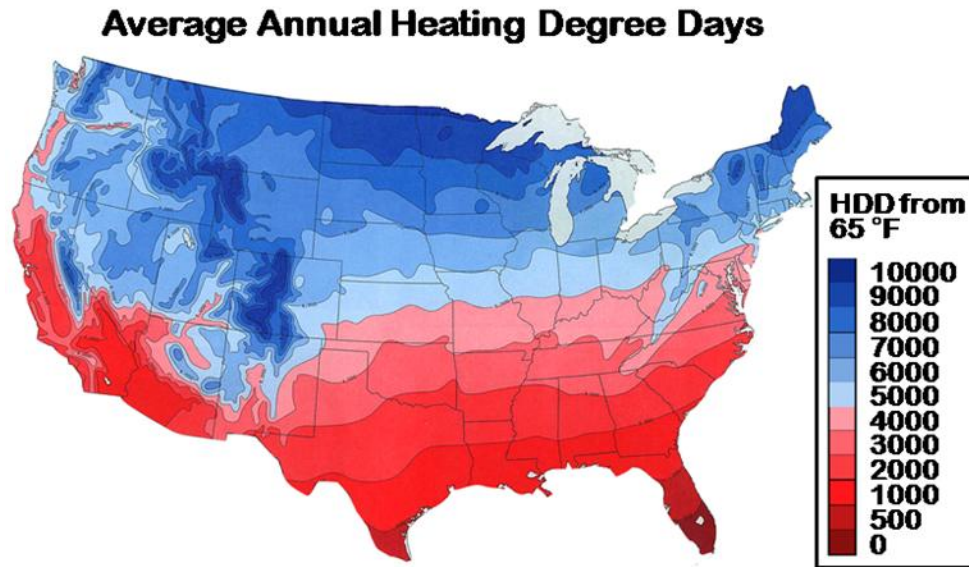
Figure 3.6 Average Heating Degree Days for the USA (ESSA 1970)

3.2.3 Wireless Sensor Network

The wireless sensor network was constructed using the Crossbow Starter and Professional Kits (See Appendix II). The network contained a Crossbow MIB520 basestation and eight (7 indoor and 1 outdoor) distributed wireless Crossbow sensor modules called motes. The basestation serves as the gateway between the WSN and the computer, and this connection is made through the universal serial bus port (USB). The motes are comprised of 2.4 GHz IRIS microprocessor and transceiver boards, MTS400 environmental sensor boards, and powered by two AA batteries. The IRIS microprocessor is a XM2110CA microcontroller with internal flash memory and an IEEE 802.15.4 compliant RF transceiver. The MTS400 sensor boards were developed at UC Berkeley and are integrated with four sensors: an ADXL202JE Dual-axis Accelerometer, an Intersema MS5534AM Barometric Pressure Sensor, a TAOS TSL2550D Ambient Light Sensor, and a Sensirion SHT11 Relative Humidity and

41

Temperature Sensor. Holes were drilled in the mote plastic housing to reduce the thermal lag the of temperature sensor. Figure 3.7 is a photograph of the Crossbow basestation and a sensor mote.
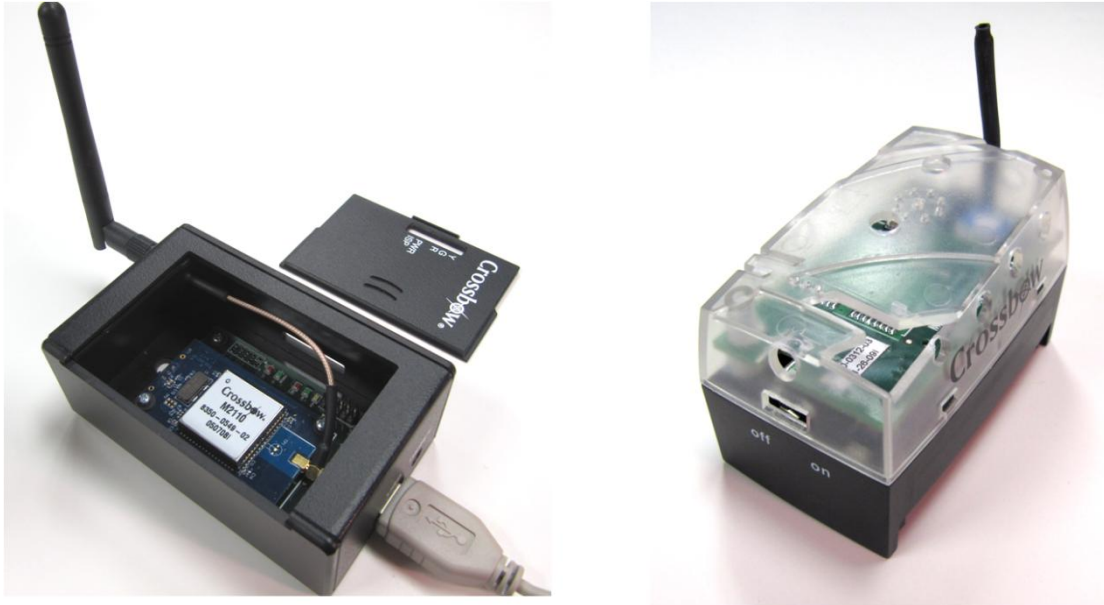
Figure 3.7 Photograph of Crossbow Wireless Basestation (left) and Mote (right)

The motes communicated over Crossbow's XMesh network protocol and ran on the TinyOS operating system. The XMesh network protocol created a self-healing mesh that allowed motes to multi-hop to expand the network's range and extended the motes' battery life. The motes were programmed to operate in low power mode, which kept them asleep for about six minutes, before awaking to transmit data. The motes could also have been awoken to receive and transmit another mote's data (multi-hopping). A more power efficient wireless network could have been developed, but the Crossbow technology was used because of the preexisting network protocol. A custom sensor network and protocol would be recommended if this project were to be considered as a marketable product.

The sensor network passed information through the basestation gateway using XServe in an Extensible Markup Language (XML) stream. The basestation was connected to a Dell Optiplex GX280 desktop computer located in the basement of the house. Figure 3.8 shows the scaled floor plan of the test house with the locations of the wireless motes (small radio image), the basestation (B), the AHU (AHU), and the outdoor condensing unit (C).
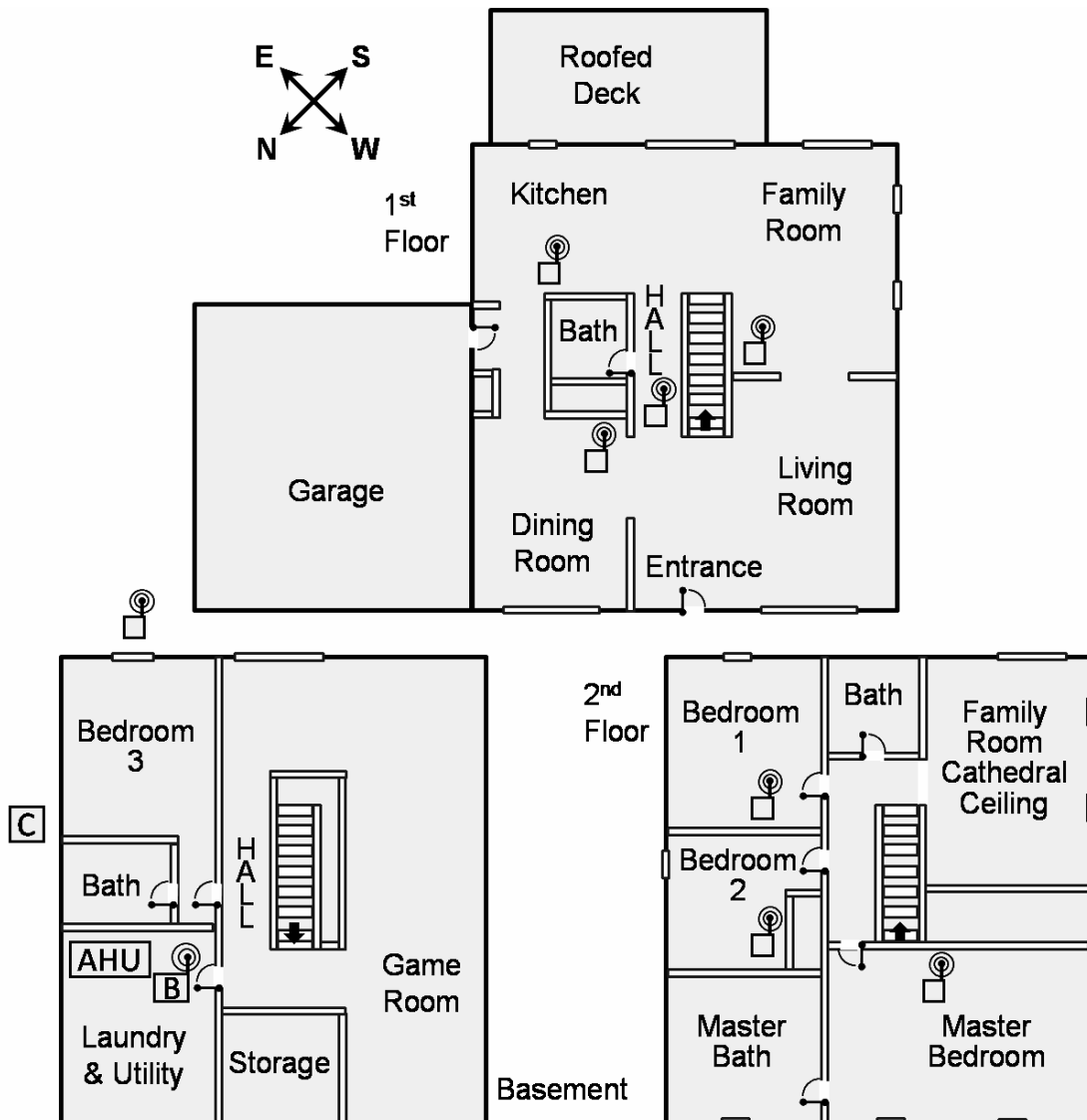
Figure 3.8. Wireless Sensor Locations.

The motes were attached to the walls at a height of about 1.2 meters (4 feet) off the ground. The locations chosen experienced neither direct sunlight nor significant airflow from registers and return vents. The basement floor was rarely occupied and all the dampers and registers on this floor were closed; therefore, no wireless motes were positioned in the basement. The outdoor mote's purpose was to provide very local outdoor temperature, humidity, and light data. It was installed underneath the deck, in a position that would never be exposed to direct sunlight and in front of a window to minimize the transmission resistance from the aluminum siding. The outdoor mote was also housed in a plastic container with several large holes to shield it from the elements. A photograph of the outdoor mote setup is shown in Figure 3.9.

Figure 3.9 Photograph of the Outdoor Mote in Plastic Housing (without the cover)

Each mote sent an XML packet containing its environmental data through the gateway where it was written to a file using executable programs in the Unix-like environment and command-line interface Cygwin. Figure 3.10 shows the command line interface of Cygwin with lines of code to change the directory, intercept the XML stream through the USB port, write the XML packet to a file, and package it into a form

that is compatible with the parser. Figure 3.11 shows the XML file Cygwin writes for

incoming mote data.
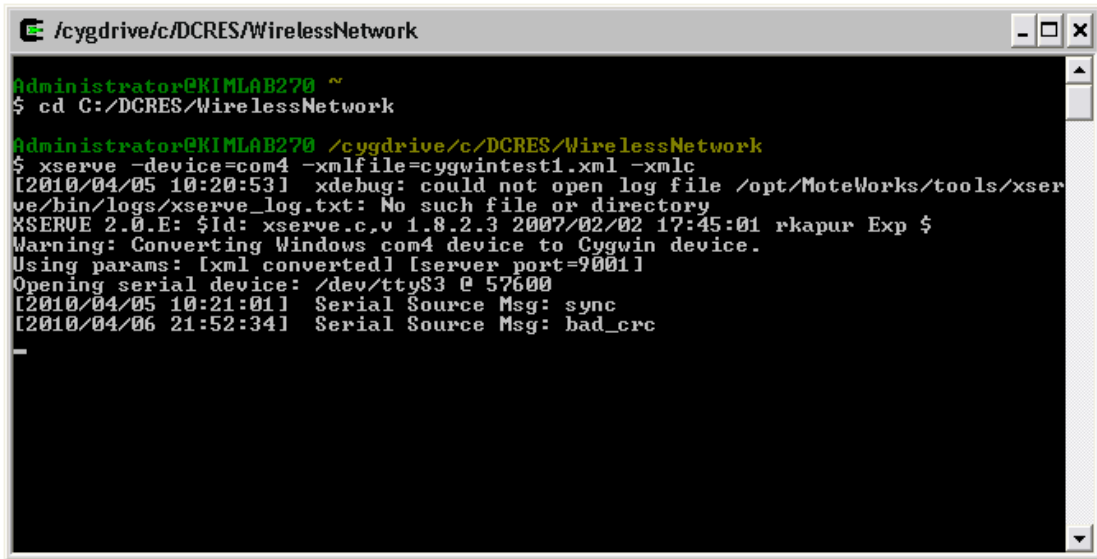
Figure 3.10 Cygwin Command Line Interface

Figure 3.11 Sensor XML Packet (unparsed)

3.2.4 Control System Setup

Many of the important tasks in the control system were performed in a Matlab program. The program constantly read in the XML file Cygwin wrote, and parsed the mote packets into engineering units. It saved the individual mote's environmental and performance data and calculated the PMV and PPD comfort metrics for every room. The code also ran the control strategies that determined if the heating or cooling system should be ON or OFF. Once the program determined the position for the energy system, it would send a 5V DC signal out of the output terminal of the parallel port. This signal would open or close the circuit of a solid state relay that served as a switch between the thermostat and the AHU circuit control board. The thermostat was set to 23.9°C (75°F) during the heating experiments so the signal would always be requesting the furnace and blower fan to be ON (unless the conditions ever reached above 23.9°C in the hallway). The same idea was employed in the summer for cooling using 18.3°C (65°F) as the thermostat set point. Since the solid state relays were installed as switches to intercept the signal lines between the thermostat and circuit control board, opening and closing the relay served as the controller, not the thermostat. These relays allowed the Matlab program to start or stop the gas furnace, blower fan, and condenser as needed. Figure 3.12 is a photograph of the AHU circuit control board with the relay switching lines intercepting the thermostat signal lines for the cooling control system setup. A simplified circuit diagram is also included to label the specific wires in the photograph. The black circles with a centered Y or G represent the input pin on the circuit board. Relay 1 is used to actuate the condenser and Relay 2 is used to actuate the blower fan.
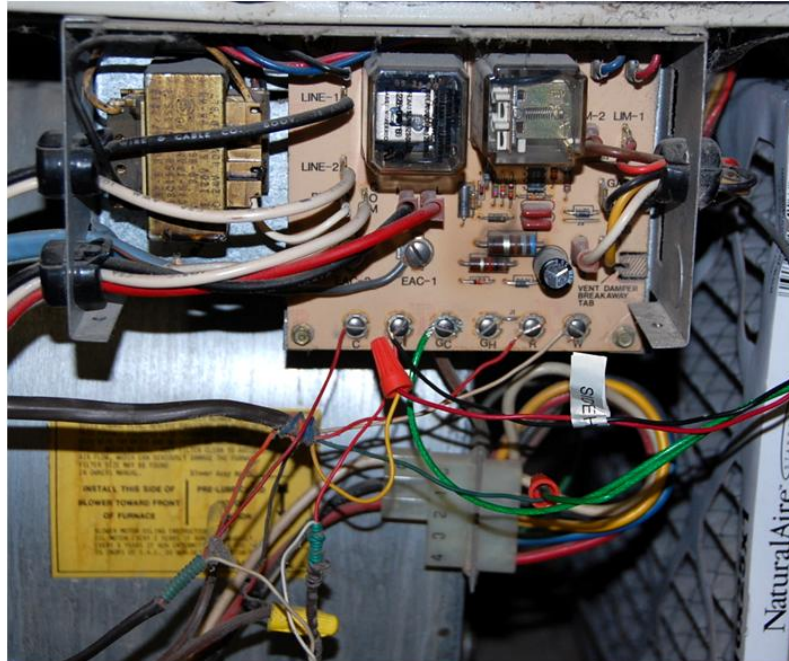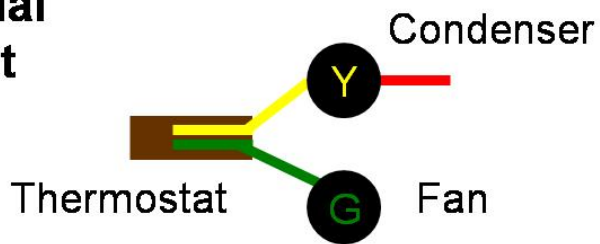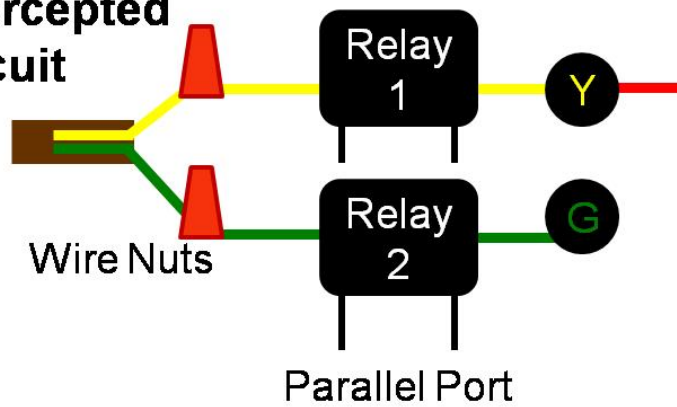
Figure 3.12 Photograph of the AHU Circuit Control Board with Intercepted Signal Lines and Simplified Circuit Diagram

Figure 3.13 is a photograph of the AHU and the system computer.

Figure 3.13 Photograph of the AHU and Control System Computer

The Matlab program ran continuously every day the system was in control. A particular control strategy would control the HVAC system for the entire day starting at midnight, and the strategy turn-over would occur automatically based on a predetermined schedule. In an attempt to conserve sensor battery life and reduce erroneous actuation due to sensor jitter, the Matlab program and control strategies made a decision to turn the energy systems ON or OFF every 10 minutes.

A different Matlab program was used for each of the experiments; lessons learned from the summer cooling test were used to improve the program for the winter heating testing. These improvements allowed the heating experiment to run relatively error free for two months. See Appendix 1 for the Matlab controlling program code.

The test computer was remotely operated using LogMeIn Professional (Logmein 2009). This allowed the test computer to be controlled from any computer with an

internet connection. LogMeIn ignition was also used with an iPhone to remotely control the test computer. This allowed the system to be carefully monitored throughout the entire duration of the experiments. System errors were recognized quickly and any necessary changes or resets were made almost immediately. Figure 3.14 schematically illustrates the entire control system. The red arrows symbolize the flow of information from the sensors al the way to actuating the HVAC system and providing heating or cooling.
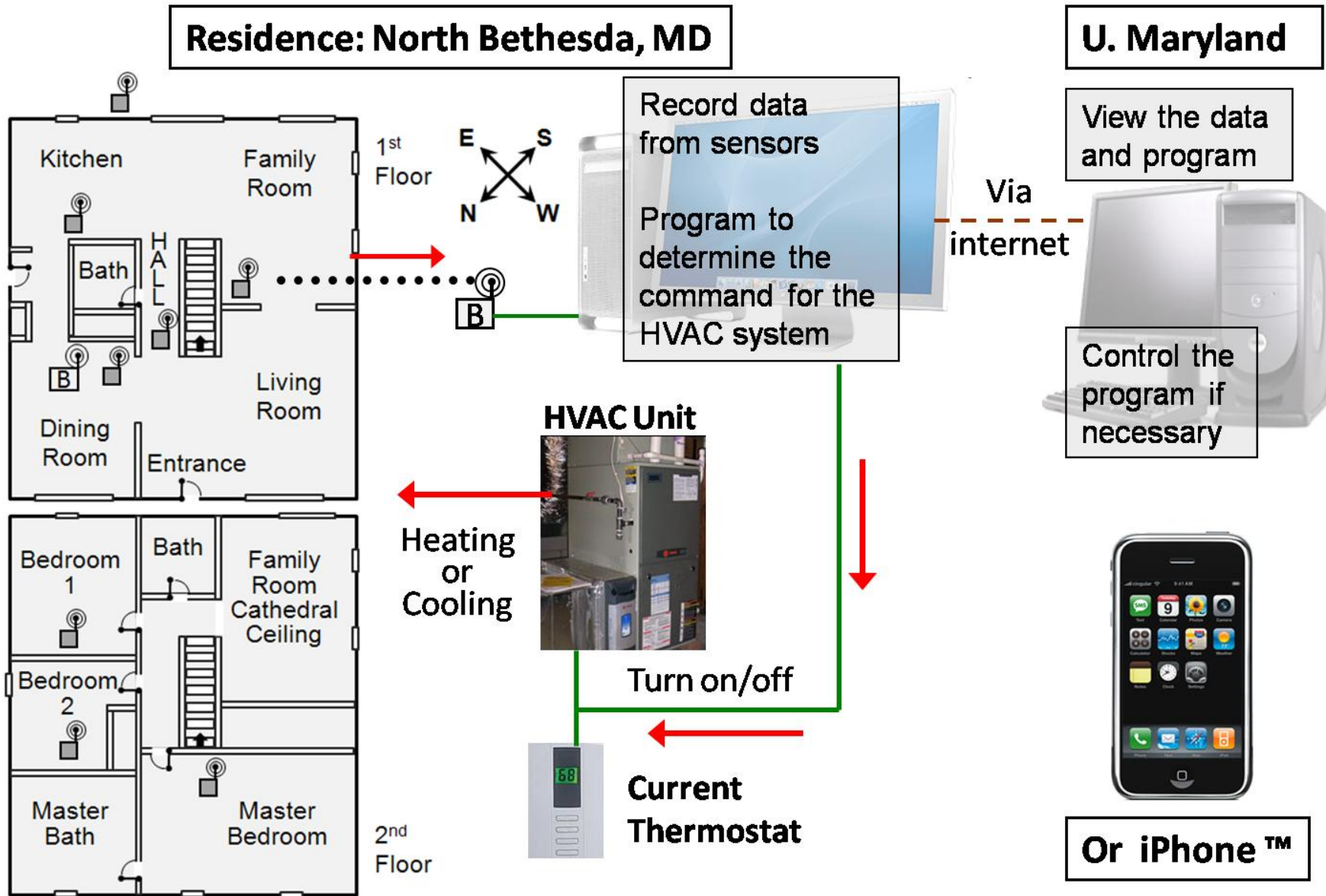
Figure 3.14 Control System Diagram

50

3.3 Control Strategies

3.3.1 Temperature Baseline

The control strategies were designed to mimic conventional, single-sensor thermostat logic or maintain comfort levels using multi-sensor thresholds. The 'Temperature Baseline' strategy controlled the heating and cooling systems with the same logic as a thermostat, and was implemented to benchmark the other strategies. During the summer cooling experiment, the strategy would turn ON if the temperature measured by the hallway mote ever rose above 25°C (77°F). It would continue to be ON, and not turn OFF, until the hallway temperature dropped below 24.5°C (76.1°F). This gave the strategy a 0.5°C (0.9°F) deadband.

There were several operations in place if the hallway mote signal was ever missed (packet loss) in the control interval. If the previous step had the system OFF, hallway mote packet loss would still keep the system OFF. If the previous step had the system ON, a control decision would be based on the dining room mote (closest to the hallway in location and reported conditions). If packet loss occurred subsequently, regardless of position, control would be based on the dining room mote, and continue until the hallway mote rejoined the network (this alternative procedure was only utilized on a few, rare occasions). Figure 3.15 is a diagram that presents the main control characteristics of the Temperature Baseline strategy with the summer set points. The values given are temperatures of the hallway in degrees Celsius.
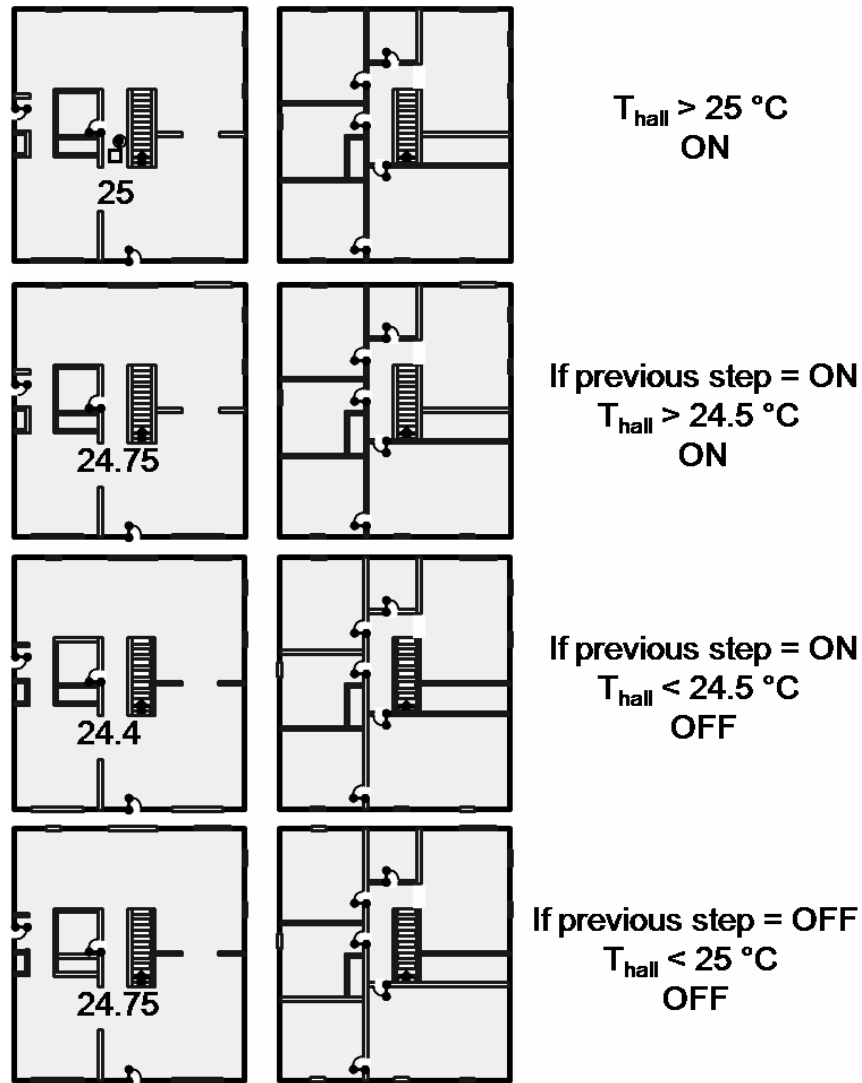
Figure 3.15 Temperature Baseline Control Diagram (summer cooling 25-24.5°C)

The winter heating versions of the Temperature Baseline strategy involved the same control logic, but multiple temperature set points were used to vary the comfort level. A 0.5°C deadband was used in every version, and the same alternative operations were used if the hallway mote experienced packet loss. The four set points tested were 19.5-20°C, 19-19.5°C, 18.5-19°C, 18-18.5°C (67.1-68°F, 66.2-67.1°F, 65.3-66.2°F, and 64.4-65.3°F). Figure 3.16 is the control diagram for the 19.5-20°C version of the heating Temperature Baseline.

52

T_{hall} < 19.5 °C
ON

If previous step = ON
T_{hall} < 20 °C
ON

If previous step = ON
T_{hall} > 20°C
OFF

If previous step = OFF
T_{hall} > 19.5 °C
OFF
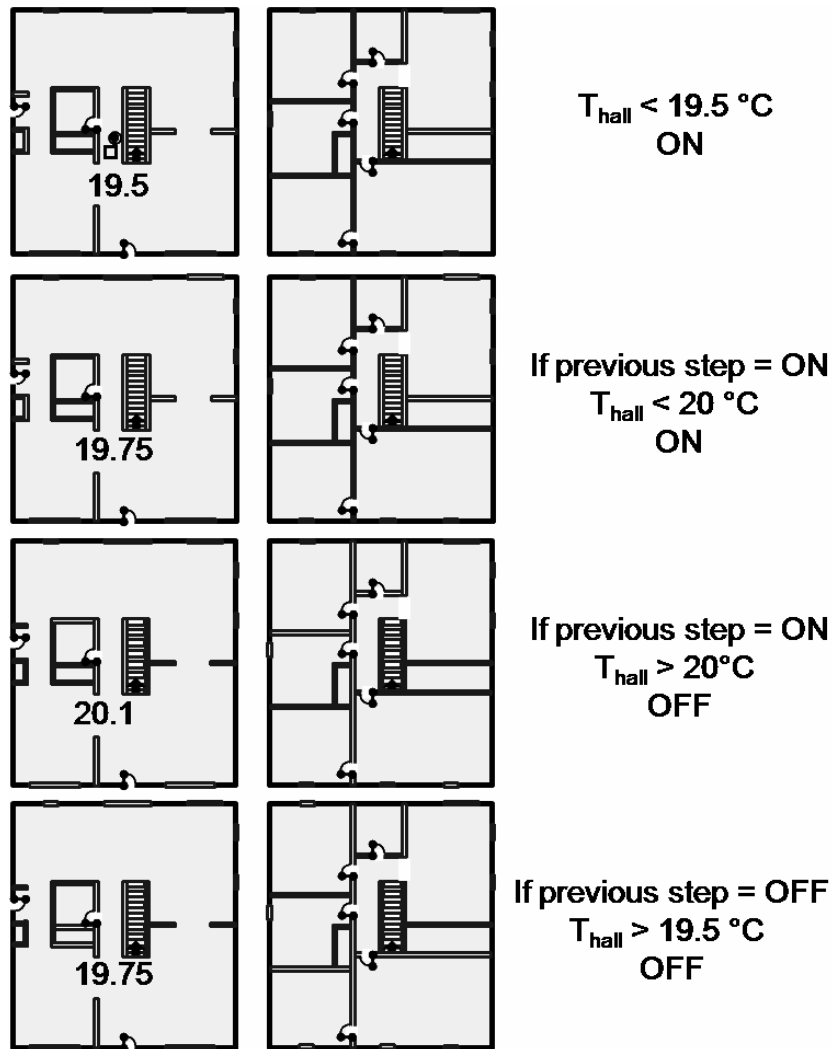
Figure 3.16 Temperature Baseline Control Diagram (winter heating 19.5-20°C)

3.3.2 Comfort Baseline

The 'Comfort Baseline' strategy was developed to see how a thermostat would behave if the controlling metric was thermal comfort instead of temperature. The strategy operated similarly to the Temperature Baseline strategy, but instead of using hallway temperatures of 25°C and 24.5°C as the thresholds, it used equivalent hallway comfort levels of 7.4 and 5.7 PPD. These PPD values were calculated using 25°C and 24.5°C, 50 percent relative humidity, and the parameters given in Table 3.1.

The same alternate plan from the Temperature Baseline strategy was used if the hallway mote ever experienced packet loss, but instead of temperature, the dining room PPD was used. Figure 3.17 is the control diagram for the Comfort Baseline. The values shown are hallway PPD.

$PPD_{hall} > 7.4$
ON

If previous step = ON
$PPD_{hall} > 5.7$
ON

If previous step = ON
$PPD_{hall} < 5.7$
OFF

If previous step = OFF
$PPD_{hall} < 7.4$
OFF
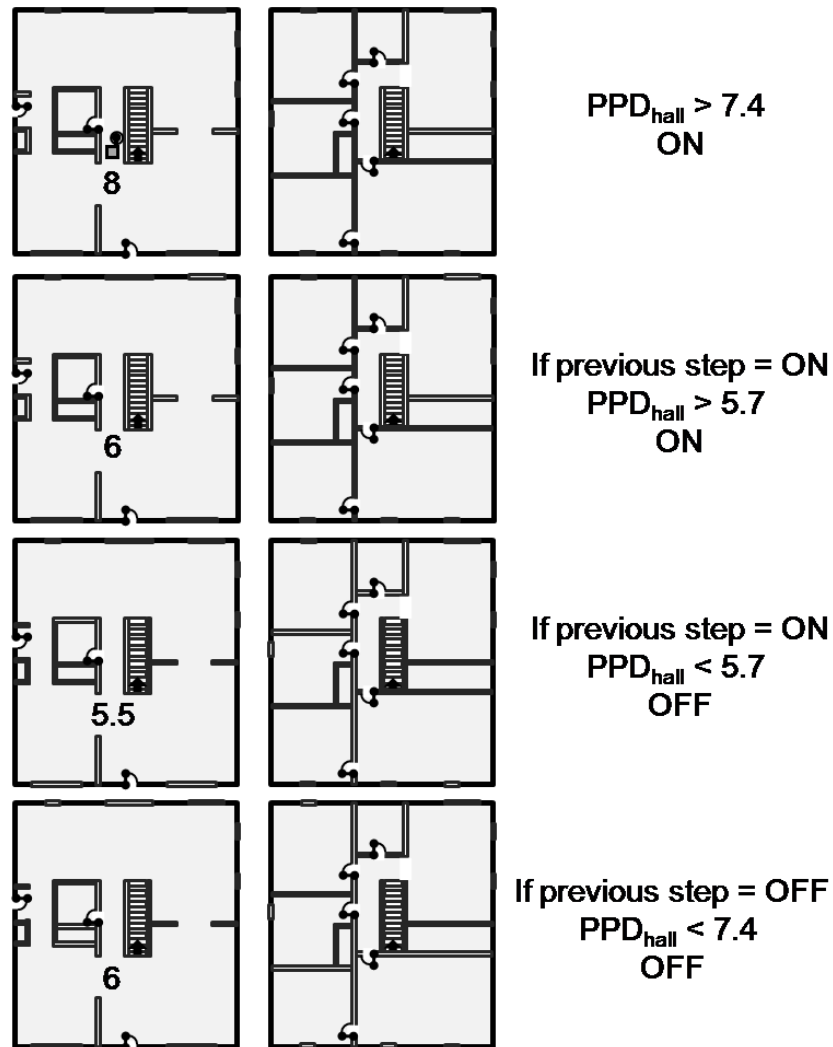
Figure 3.17 Comfort Baseline Control Diagram

3.3.3 PPD Average

The 'PPD Average' strategy was designed to improve large comfort differences between rooms. The PPD was calculated for each of the seven indoor rooms with wireless motes. These seven PPD values were averaged and compared to

54

the threshold value of 12 PPD (for the summer cooling experiment). The strategy turned the heating or cooling system ON if this mean PPD was above 12; otherwise, it turned/stayed OFF. There was not a packet loss alternative plan implemented in this strategy. If only six of the seven motes reported information, the average PPD value was only calculated based on those six rooms. Threshold average PPD values of 8, 10, and 12 were tested in the winter heating experiment.
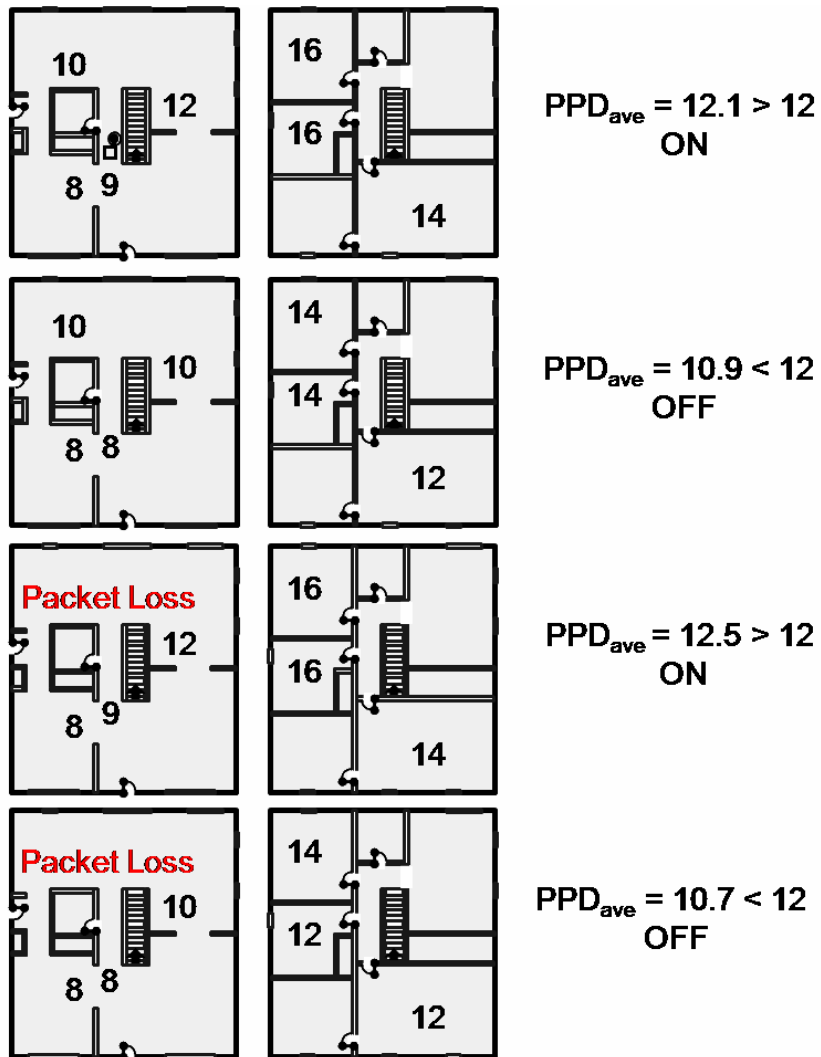
Figure 3.18 PPD Average Control Diagram (12 PPD threshold)

3.3.4 Minimizing the Probability for Dissatisfaction (MND)

Minimizing the Probability for Dissatisfaction (MND) was a strategy designed by the CBE and tested in Northern California (Ota 2008). MND minimized the total discomfort in the house by actuating the heating or cooling system if it predicted the comfort would benefit. The first step was to calculate the aggregate current PPD using the current conditions by summing up the PPD of every room. PPD values for each of the rooms were then calculated with a 0.25°C (0.45°F) temperature decrease for the summer cooling experiment and a 0.3°C (0.54°F) temperature increase for the winter heating experiment. These temperature differences represent the average temperature change the house experienced in 10 minutes with the energy system being ON. The PPD values calculated with the temperature differences were then summed up to calculate the aggregate future PPD. The strategy turned the system ON if the aggregate future PPD was lower than the aggregate current PPD. The strategy turned the system OFF if the opposite conditions existed and the aggregate future PPD was higher than the aggregate current PPD. This would occur when the temperature difference would push the rooms beyond the optimal comfort value of 5 PPD. A packet loss alternative plan was also not implemented with his strategy. Figure 3.19 shows the MND control diagram for the summer and a situation that would signal the cooling system to turn ON. The blue font represents future PPD values that correspond to a PPD decrease.
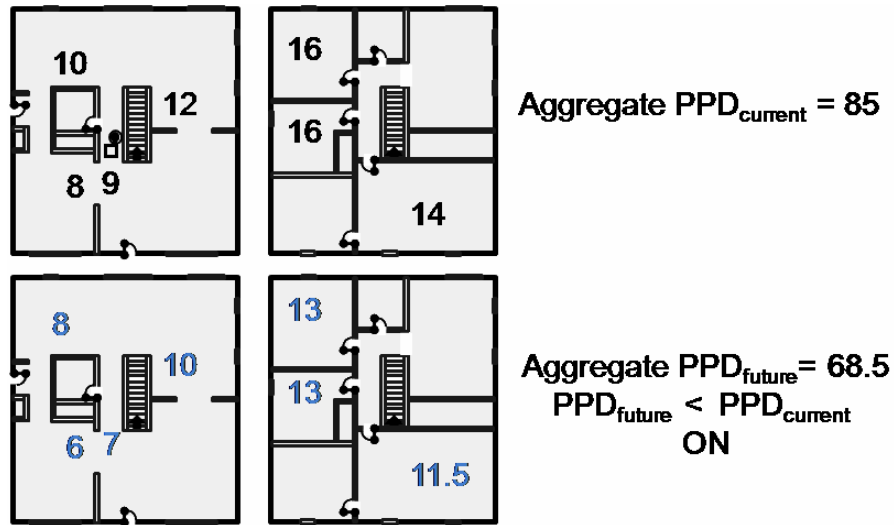
Figure 3.19 MND Control Diagram (-0.25°C future temperature difference = ON)

Figure 3.20 shows the control diagram for the MND strategy during the summer where the conditions would not initiate cooling. The blue font corresponds to PPD decreases, and the red font corresponds to PPD increases. For this case the first floor rooms were already at the optimal comfort level of 5 PPD, or less comfortable at 6 PPD due to the temperature being colder. The temperature decrease the cooling system would provide made these rooms more uncomfortable, so the aggregate PPD would increase if cooling was provided and the strategy elected to switch the cooling system OFF.

57
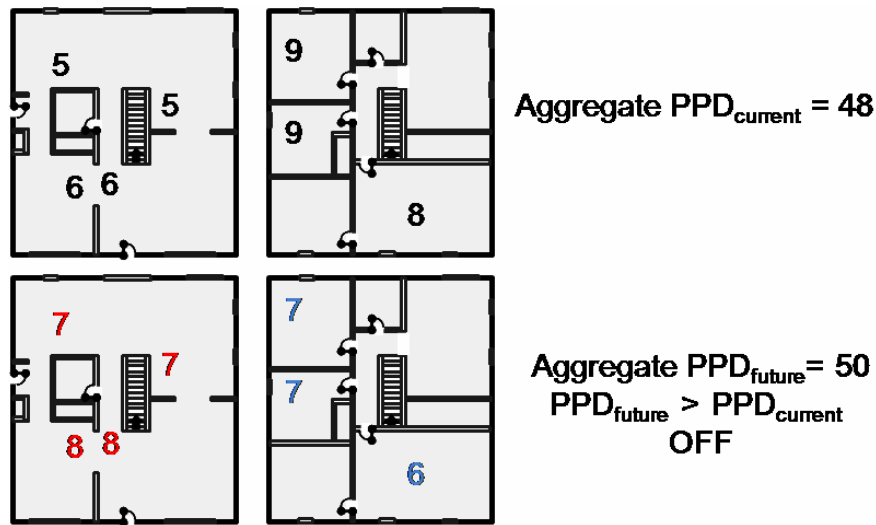
Figure 3.20 MND Control Diagram (-0.25°C future temperature difference = OFF)

3.3.5 Maximizing the Number of Rooms below a Threshold PPD (MXR)

Maximizing the Number of Rooms below a Threshold PPD (MXR) was also a strategy developed by the CBE. MXR maximized the number of rooms below a threshold comfort level of 12 PPD in the summer and 8, 10, and 12 PPD in the winter. The strategy first calculated the number of rooms with comfort levels below the threshold PPD using the current conditions; then it calculated the number of future rooms below the threshold PPD using the same -0.25°C and 0.3°C temperature differences explained previously. If the number of rooms below the threshold PPD would increase in the future by introducing the temperature difference, then the system would turn ON. The system would stay or turn OFF if the number of rooms below the threshold would remain constant or decrease with the proposed future temperature difference. An alternative plan was not needed if packet loss occurred because the present and future PPD values were only calculated using environmental information from reporting motes. The number of potential rooms below a threshold

58

was always the same regardless of being for the current or future calculation. It

should also be noted that this control strategy would be unstable in the summer if all

of the room PPD values were so high from being warmer than the optimal conditions

that the 0.25°C future temperature decrease would not be able to bring any below the

threshold. This issue was alleviated by having the system turn the cooling on if the

average current PPD was ever above 20 PPD. The same plan was implemented for

the winter heating experiment. Figure 3.21 shows the control diagram for MXR with

conditions that would turn the system ON in the summer with a threshold of 12 PPD,

and Figure 3.22 shows situations that turn the system OFF. The blue font represents

future PPD values that correspond to a PPD decrease, and the red font corresponds to

PPD increases.
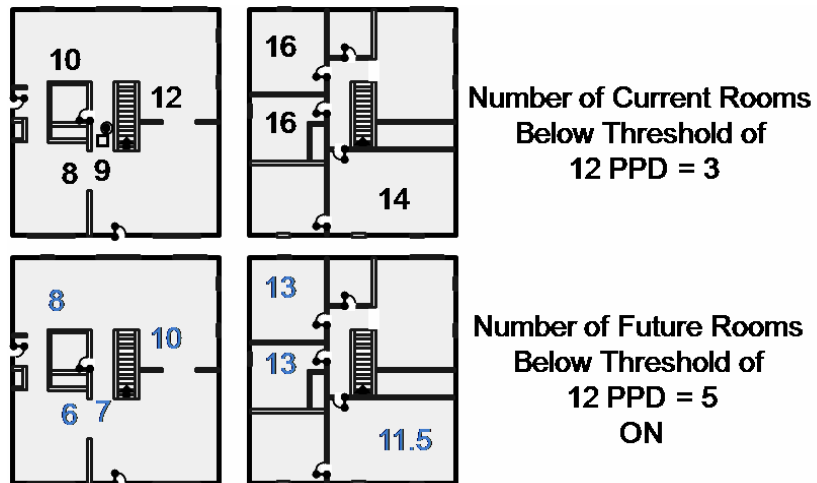
Figure 3.21 MXR Control Diagram (-0.25°C future temperature difference with threshold of 12 PPD = ON
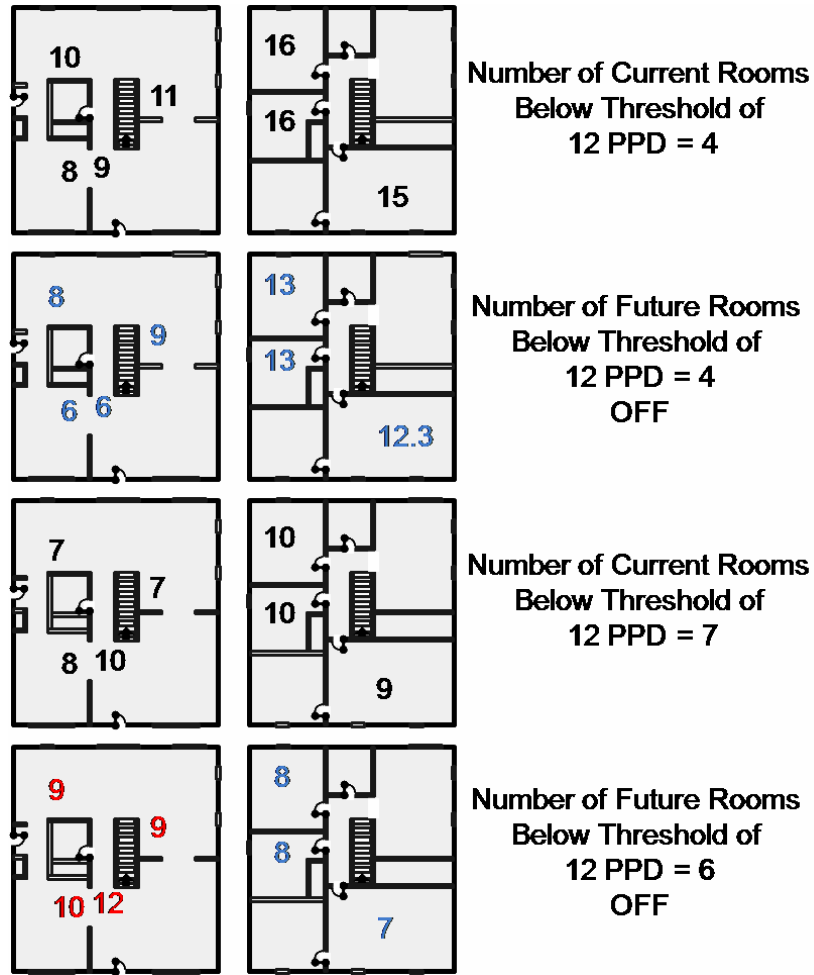
Figure 3.22 MXR Control Diagram (-0.25°C future temperature difference with threshold of 12 PPD = OFF

3.4 Test Metrics and Data Analysis

3.4.1 Thermal Comfort

The PMV and PPD thermal comfort metrics were used in several of the control strategies. These needed to be calibrated properly to have the strategies control the house within the occupant's desired comfort limits. Section 2.1.1 explained how thermal comfort was calculated and listed the physical parameters involved. The air temperature and relative humidity input values to the PMV-PPD model were directly from the wireless sensor network data. Table 3.1 gives the

60

recommended parameter values to be used in summer cooling experiments from

ASHRAE Standard 55 (2004, note that 0.1 m/s was found from another source, and

the mistake was not noticed until the experiment was completed).

Table 3.1 Parameters Contributing to the PMV and PPD (summer calibration)

Parameter	Value	Units	Equivalency
Clothing Insulation Level	0.5	clo	Light slacks and short sleeves or blouse
Occupant Metabolic Activity	1.2	met	Relaxed standing
Mean Radiant Temperature	Sensor Temperature	°C	
Air Speed	0.1 (0.15)	m/s	

       ASHRAE Standard 55 also recommends parameter values for winter heating

experiments. The optimal comfort provided using these recommendations was labeled

as "too warm" by the occupants of the test house. The clothing insulation level of 0.9

clo was increased to 1.05 clo, effectively shifting the optimal thermal comfort level to

a slightly lower temperature. The occupants agreed that this small shift made the

optimal comfort true to its name. The shifted clothing level and the rest of the

recommended parameter values for heating are shown in Table 3.2.

Table 3.2 Parameters Contributing to the PMV and PPD (winter calibration)

Parameter	Value	Units	Equivalency
Clothing Insulation Level	1.05 (0.9)	clo	sweater, long sleeve shirt, heavy slacks
Occupant Metabolic Activity	1.2	met	Relaxed standing
Mean Radiant Temperature	Sensor Temperature	°C	
Air Speed	0.25	m/s	

3.4.2 Degree Days

Seasonal outdoor conditions are characterized using the degree day metric, and they can also play a role in normalizing energy consumption in homes. Totalized degree days capture the entire season or year by summing the number of degrees a daily average outdoor temperature is above or below a base temperature for every day being evaluated. This average temperature is traditionally the average between the daily high and low temperature. Cooling degree days (CDD) are often calculated using 19°C (66.2°F) and heating degree days (HDD) are calculated using 15.5°C (59.9°F). An outdoor average of these base temperatures should correspond to the point where no energy input is required by the home cooling or heating system, in the respective seasons, throughout the course of the day. Average temperatures below 19°C in summer and above 15.5°C in winter do not correspond to negative degree days; rather the value will only be zero. Equation 5 and Equation 6 show how annual CDD and HDD are calculated.

$$CDD_{annual} = \sum_{Day=1}^{365} \left(\frac{\left(T_{high}(Day) - T_{low}(Day)\right)}{2} - 19 \text{ °C} \right) \tag{5}$$

$$HDD_{annual} = \sum_{Day=1}^{365} \left(15.5 \text{ °C} - \frac{\left(T_{high}(Day) - T_{low}(Day)\right)}{2} \right) \tag{6}$$

Degree intervals are a modified version of the degree day. Instead of summing days over entire seasons, the calculation is confined to a much smaller interval on the order of hours to a single day. Degree intervals calculate the average outdoor temperature over the interval by averaging every outdoor temperature measurement made in the interval. This method makes the length of time the temperature was at a

certain value more important than only averaging the high and low temperatures would. The same base temperatures are used to remain consistent if intervals are extended to entire days. Equation 7 and Equation 8 show how cooling degree intervals (CDI) and heating degree intervals (HDI) are calculated from the interval start to finish.

$$CDI = \frac{\sum_{t=14:00}^{20:00} T_{outdoor}(t)}{time\ steps} - 19\ °C \tag{7}$$

$$HDI = 15.5°C - \frac{\sum_{t=0:00}^{8:00} T_{outdoor}(t)}{time\ steps} \tag{8}$$

An example calculation using Equation 5 is illustrated in Table 3.3.

Table 3.3 CDI Example Data

Time	$T_{outdoor}$ [°C]
14:00	22
14:10	22.5
14:20	23
14:30	23.5
14:40	24
14:50	23.5
15:00	23

$$CDI = \frac{22 + 22.5 + 23 + 23.5 + 24 + 23.5 + 23}{7}°C - 19°C = 4.1$$

3.4.3 Duty Cycles

The energy performance of the strategy was quantified by the duty cycle. The duty cycle was chosen to remove any difficulty involving power and gas meters. The experiment by the CBE experienced periods where power consumption was not reported by the wireless meter (Ota 2008). The duty cycle is a method that should

63

accurately capture the energy consumption without relying on additional components. One element that is lost in using the duty cycle instead of the component power is the brief peak amount of energy needed to start up the compressor but the 10 minute interval used to prevent a strategy from cycling at too high of a frequency reduces the spike's effect. The definition of duty cycle can be explained using the following example given in Figure 3.23. In the plot the Y-axis represents the position of the system, and the X-axis represents the time step.
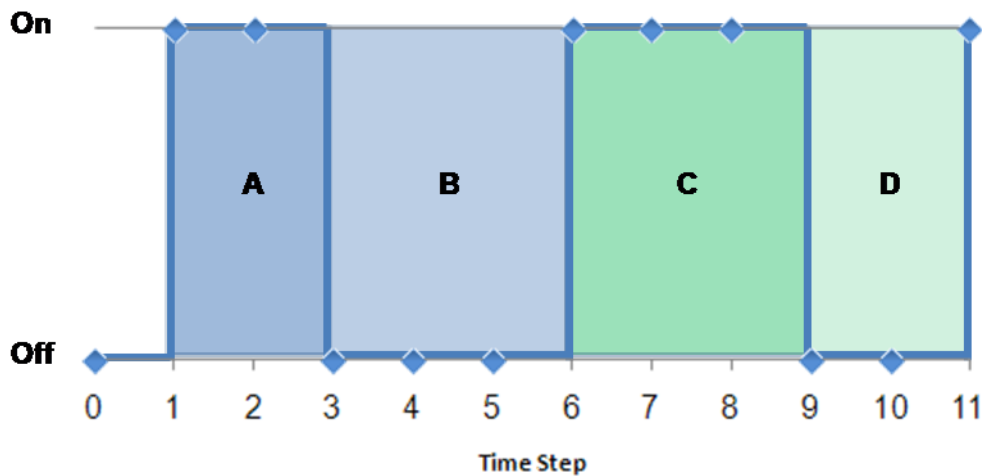
Figure 3.23 Duty Cycle Example Plot

An individual duty cycle pulse is the time that the system is ON. The first pulse in the plot is the dark blue shaded area lasting from time step 1 to 3 (*A*). The second pulse that occurs in the plot is the dark green shaded area lasting from time step 6 to 9 (*C*). A duty cycle period is comprised of the duty cycle pulse and the time the system is OFF. There are two duty cycle periods shown in the plot, the blue shaded area lasting from time step 1 to 6 (*A* and *B*) and the green shaded area lasting from 6 to 11 (*C* and *D*). Both of these duty cycle periods last five time steps (6-1=5 and 11-6=5). The duty cycle is the fraction of the pulse to the period. For the first

period the duty cycle would be 2/5, and for the second period the duty cycle would be

3/5. A duty cycle can be found for the entire plot from time steps 1 to 11 by

combining all the pulses, combining all the periods, and dividing. The total plot's

duty cycle would be 5/10.

The outdoor conditions can also be integrated into the energy consumption by

normalizing the duty cycle by dividing it by the CDD or CDI. Since hotter days in the

summer and colder days in the winter will consume more energy to maintain a

comfort level than more moderate conditions, normalized duty cycles (NDC) were

used to balance out this difference. High energy consumption divided by a high

degree day or interval would compare to lower energy consumption divided by a

lower degree day or interval. Normalizing the duty cycle should make comparing the

energy consumption of individual strategies more about the actual strategy's ON/OFF

properties than the outdoor conditions.

3.4.4 Intervals and Data Shifting

The initial conditions had a large impact on how the strategy behaves. Figure

3.24 shows the temperature plots of two days where the MXR strategy was exposed to

different initial conditions. The data worth noting are the empty circle outdoor

temperature data points, the blue triangles that correspond to the power position of the

AC system (triangles at the top of the chart signify that the system was ON for that 10

minute interval and triangles at the bottom indicate the system was OFF), and the

black line with crosses showing the average PPD on the secondary axis.
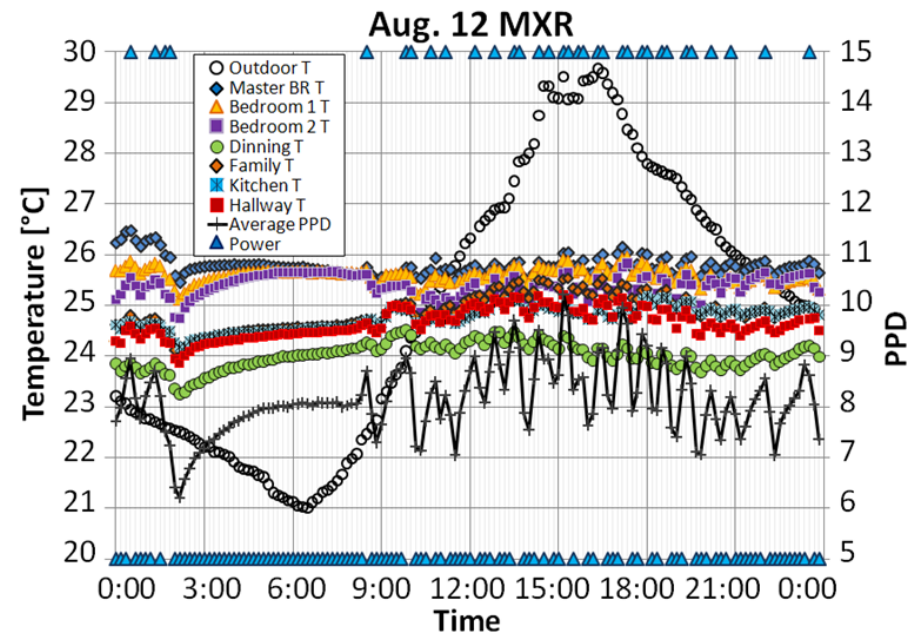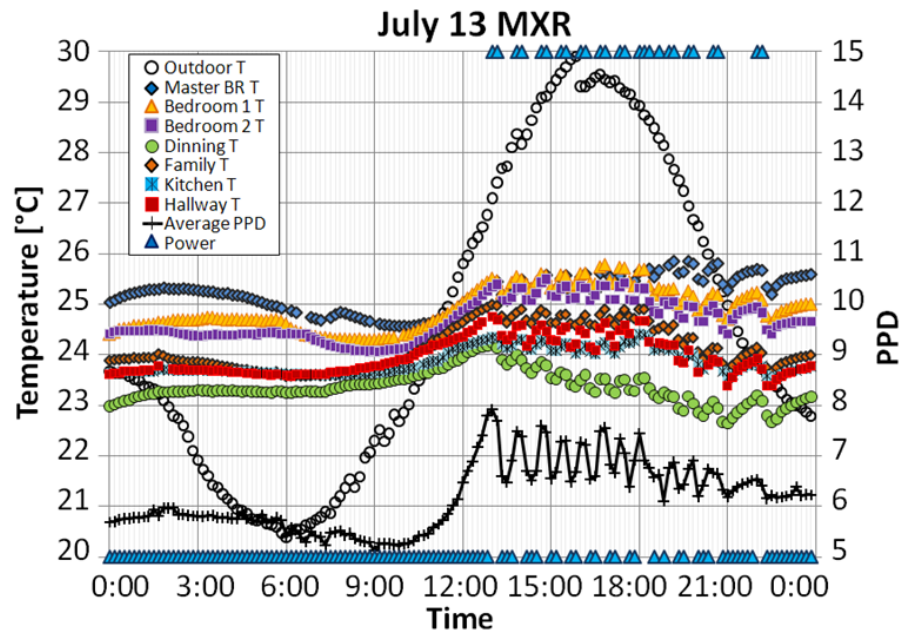
Figure 3.24 Temperature Plots Showing the Initial Condition's Impact on the MXR Strategy

The blue triangles show the position of the cooling system, and these triangles indicate that the cooling system did not turn ON until about 13:00 on July 13, 2009. On August 12, 2009 the cooling system turned ON briefly in the early morning (0:30 and 1:20) and then stated the main period of actuation around 10:00, resulting in a higher daily duty cycle. The outdoor temperatures for both days shown were very close throughout the entire day, so it was not the source of the different actuation start times. On July 13 the average comfort level beginning at 0:00 was at 5.7 PPD and on August 12 the average comfort level began at 7.8 PPD. This discrepancy in the starting comfort levels appears to be the main cause for different actuation times between the two days.

Misleading conclusions are drawn if the strategy is evaluated without considering the initial conditions; therefore, analysis was performed on intervals where the starting and ending conditions were approximately the same. This was usually met after the first actuation cycle completed. For days with high outdoor temperatures (average CDD of 6.1) during the summer testing, this interval began at approximately 14:00 and maintained a high frequency of cycles until about 20:00. A smaller, more inclusive interval that was evaluated for days with at least warm outdoor temperatures (average CDD of 5.5) occurred between 16:00 and 19:00.

An interval was also used in the winter heating experiment to remove the solar loading variable. This interval started after the first actuation cycle after 0:00 and ended at 8:00.

Figure 3.25 is a plot of the outdoor and indoor temperatures from September 1 to 3 2009 used to determine the time delay between the outdoor and indoor conditions.
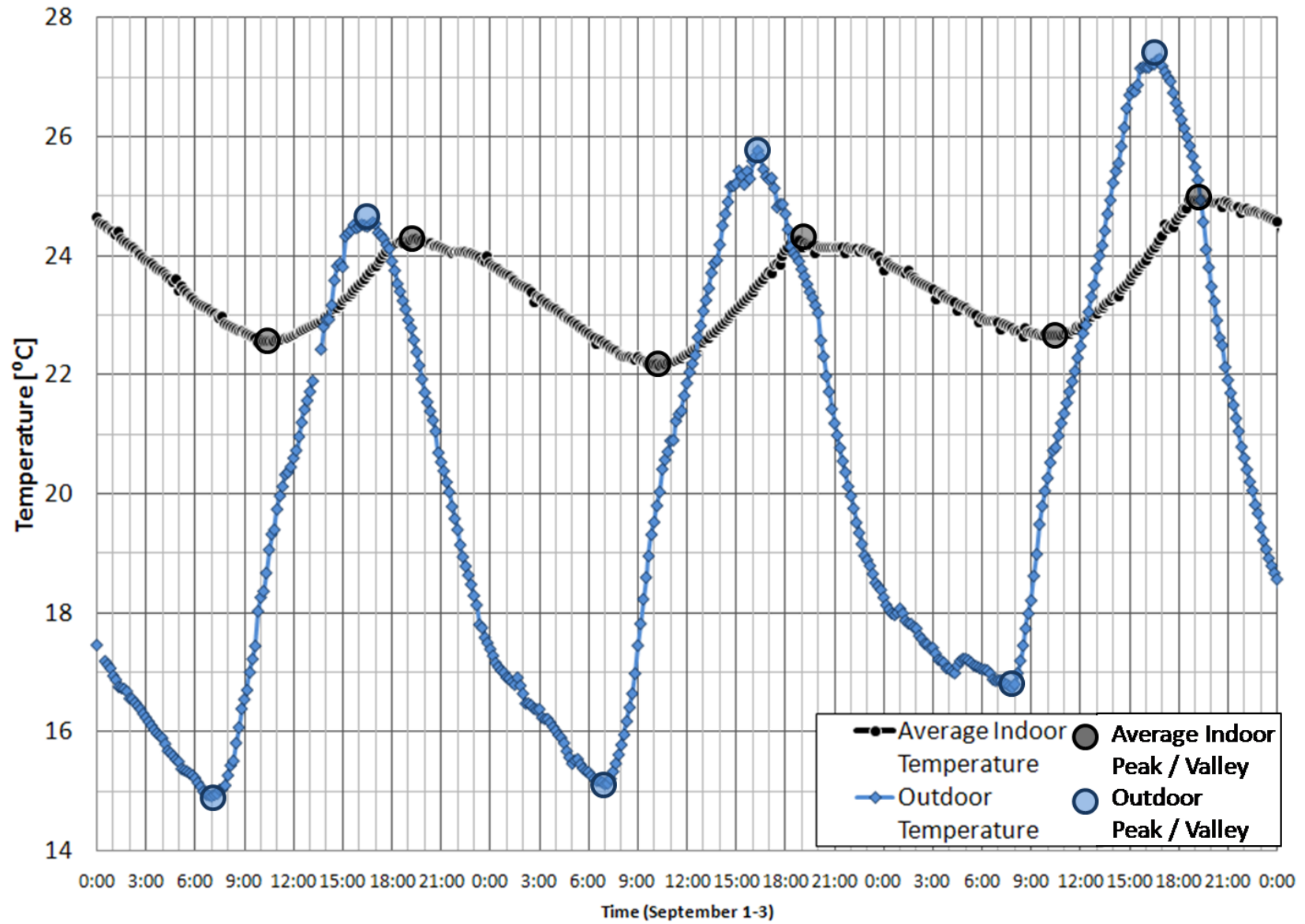
Figure 3.25 Determining the Time Delay with a Floating House Indoor and Outdoor Temperatures (Sept. 1-3 2009)

During this period from September 1 to 3 2009 the AC was disabled and the house floated with the outdoors conditions. The times of the daily maximum (peaks) and minimum (valleys) temperatures are listed in Table 3.4.

Table 3.4 Time Delay Calculation

Peak / Valley	Average Indoor Temperature Time	Outdoor Temperature Time	Delay [hours]
Sept. 1 minimum	7:00	10:15	3.25
Sept. 1 maximum	16:30	19:30	3
Sept. 2 minimum	7:00	10:15	3.25
Sept. 2 maximum	16:30	19:00	2.5
Sept. 3 minimum	7:30	10:30	3.25
Sept. 3 maximum	16:30	19:15	2.75

The average delay between the outdoor and indoor temperatures is three hours. The results suggest that a change in the outdoor conditions will not influence the indoor conditions for about three hours. A three-hour shift in the outdoor temperatures was implemented when calculating the CDI and HDI (a CDI calculated from 11:00 to 17:00 was used to normalize the duty cycle from 14:00 to 20:00).

3.4.5 Statistical and Uncertainty Analysis

A statistical analysis was performed to see if there was a significant difference between the normalized duty cycles of the Temperature Baseline and the other strategies. This was done using the Student's T-Test for two samples with an assumed unequal variance and a 95 percent confidence interval (Walpole 2007). A T-Test is designed to see if two samples are from the same population. If the energy consumption of the Temperature Baseline and another strategy are not shown to be

69

from the same population, then the statistical conclusion could be that the energy

consumptions are different.

This test was performed by calculating the daily or interval normalized duty

cycles for every day and finding the average and variance within the individual

strategies' sample populations. The T-statistic was calculated using Equation 9 and

the degrees of freedom were calculated using the Welch-Statterthwaite equation

(Equation 10). The variance is represented by s^2 and the number of days on the

strategy sample population is n.

$$T_{Strategy\ X} = \frac{\overline{NDC}_{Temp\ Baseline} - \overline{NDC}_{Strategy\ X}}{\sqrt{\frac{s^2_{Temp\ Baseline}}{n_{Temp\ Baseline}} + \frac{s^2_{Strategy\ X}}{n_{Strategy\ X}}}} \qquad (9)$$

$$v_{Strategy\ X} = \frac{\left(\frac{s^2_{Temp\ Baseline}}{n_{Temp\ Baseline}} + \frac{s^2_{Strategy\ X}}{n_{Strategy\ X}}\right)^2}{\frac{\left(\frac{s^2_{Temp\ Baseline}}{n_{Temp\ Baseline}}\right)^2}{\left(n_{Temp\ Baseline} - 1\right)} + \frac{\left(\frac{s^2_{Strategy\ X}}{n_{Strategy\ X}}\right)^2}{\left(n_{Strategy\ X} - 1\right)}} \qquad (10)$$

The T-statistic and degrees of freedom were used to find the probability of

obtaining that T-statistic (P-value) given a Student-T normal distribution. The

statistical conclusion was reached with a hypothesis test. To see if a particular

strategy consumed more or less energy than the Temperature Baseline, the null

hypothesis that the two sample populations were from the same population was

tested. If the P-value was lower than 0.05, the null hypothesis could be rejected, and

the conclusion would be that the samples are from different populations. For this

specific case the strategy tested against the Temperature Baseline would be shown to

consume a different amount of energy, and the conclusion is made with 95 percent confidence. If the P-vale is higher than 0.05, the null hypothesis cannot be rejected, and no statistical conclusions can be drawn.

Uncertainty can be found in several of the measurements and calculations. The Sensirion SHT 11 relative humidity and temperature sensor used on the MTS400 sensor board of the wireless motes is rated at ±3.5 percent relative humidity and ±0.5°C. A calibration test was performed to evaluate the accuracy of the motes in the middle of the summer cooling experiment, and before the winter heat experiment began. The calibration experiment consisted of placing all of the motes in a Styrofoam container and monitoring their measurements. Figure 3.26 shows a plot of the temperatures from the motes during the calibration experiment.
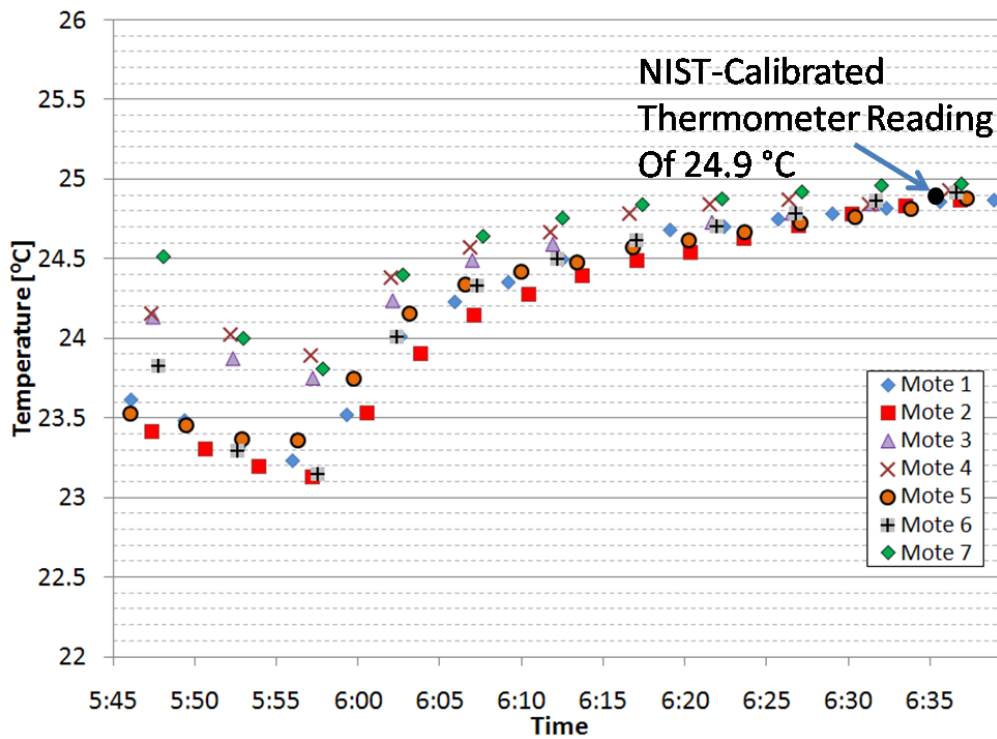
Figure 3.26 Mote Sensor Calibration Test (temperature)

The motes were moved from their locations in the house and placed into the container at around 5:55. Once the initial temperatures of the motes leveled out and the air in the container reached equilibrium, all the motes were reporting within ±0.07°C of the temperature measured by a NIST-calibrated glass tube thermometer (24.9°C). Figure 3.27 shows the calibration test results in measuring the relative humidity. The motes all measured the same relative humidity within a range of 2.5 percent.
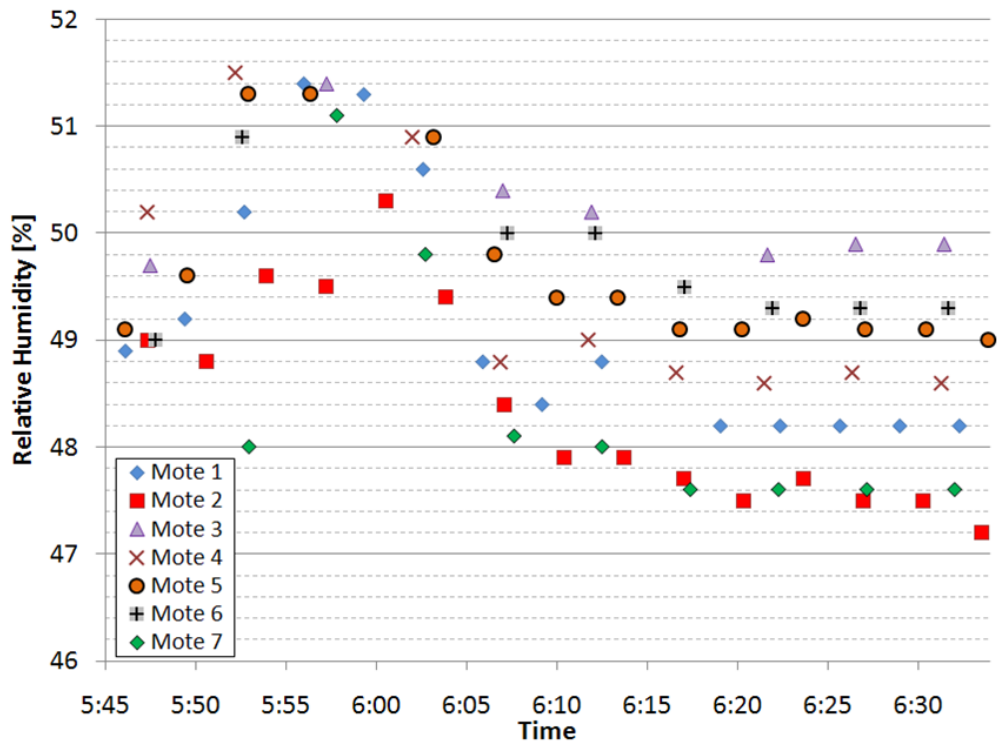
Figure 3.27 Mote Sensor Calibration Test (relative humidity)

The uncertainty of the motes environmental measurements will introduce an uncertainty in the PPD values. Since PPD is non-linear with respect to temperature and relative humidity, this uncertainly is investigated at two predicted percents: optimal conditions (5 PPD) and slightly less comfortable 10 PPD. A ±3.5 percent

relative humidity and ±0.5°C uncertainty propagates to a ±0.64 PPD at 5 PPD. At 10

PPD adding the 3.5 percent relative humidity and 0.5°C propagates to a +4.4 PPD;

subtracting only brings the uncertainty to -2.99 PPD. If the uncertainties of ±2.5

percent and ±0.07°C from the calibration experiment are used, the uncertainty in PPD

is reduced. At 5 PPD the uncertainty lowers to ±0.08 PPD, and at 10 PPD it lowers to

+1.4 PPD and −1.1PPD. These values reflect the uncertainty of the measurements

with respect to the other sensors and actual value. The sensors will probably continue

to over or under-predict the measurements compared to the actual value at the same

rate and over the entire experiment duration; therefore, the significance of the

uncertainty reduces because the consistency of the measurements is more important

in running the control strategies.

When using the intervals to calculate the NDC of each day uncertainty will

arise because the duty cycle period at the beginning and end of the interval can be

affected. If a duty cycle period starts before and continues through the interval start

point at 14:00, that individual duty cycle can change dramatically (have a shorter ON

time) and have a noticeable effect on the total interval duty cycle. Since this also

happens at the end of the interval the effect can balance out because the end of the

interval can remove some of the system OFF time. Figure 3.28 shows an example that

exhibits two different interval duty cycles if the interval is only shifted one time step.
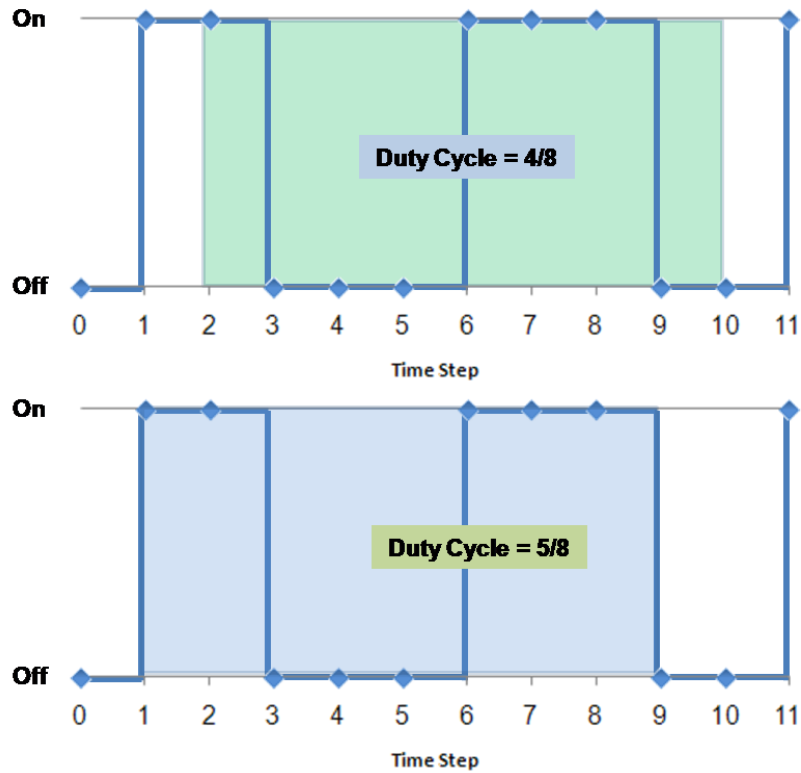
Figure 3.28 Duty Cycle Interval Uncertainty Example

The uncertainly introduced by choosing the interval to begin and end at exact times is mitigated by actively shifting the start and end time a few time steps. This shift is made to avoid cutting a duty cycle period into pieces with the interval. The NDC for each strategy is then expressed as the average of the individual daily NDC and the uncertainty is given as the standard deviation within the strategy.

Chapter 4: Summer Cooling Results and System Performance

4.1 Introduction

An experiment was performed in the summer to evaluate the performance of the cooling control strategies and control system. The setup explained in chapter 3 was installed in early June 2009, and the system began collecting the data used in the analysis in the middle of the month. Data collection involving the control strategies continued until the last day of August. Due to an uncharacteristically mild summer (668 CDD compared to the 791 CDD average for the 2 previous years) many cooler days occurred and were not considered in the analysis; the cut-off daily duty cycle was 0.042, or one hour of ON time throughout the entire day. Hardware malfunctions and software issues also removed a few days from the analysis. In total, 44 days were used to evaluate the five control strategies, 27 days meet the criteria to be evaluated on the 14:00-20:00 interval, and 38 days (including the 27 from the other interval) were fit to be included in the 16:00-19:00 interval.

The outdoor mote measured a temperature range from a low of 6.7°C (44.1°F) to a high of 34.1°C (93.4°F) and averaged 22.5°C (72.5°F) during the evaluation period. The outdoor relative humidity varied from 29 to 95 percent and averaged 73 percent. During the test the average indoor temperature (an average of all 7 rooms) reached a low of 21.1°C (70.0°F), high of 26.4°C (79.5°F), and averaged 24.8°C (76.6°F). The average indoor relative humidity ranged from 41.2 to 61.8 percent and averaged 51.1 percent.

The particular strategies were evaluated in detail and explained using plots from typical days where they were in control. The temperatures, comfort levels, and actuation times were examined to determine how well the strategy performs in the eyes of an occupant, and to set the stage for a proper analysis of the energy consumption. The energy consumption was normalized by the CDD or CDI and tested for statistical significance. Every strategy was compared to the Temperature Baseline control strategy to see if it outperformed a traditional, single sensor thermostat. Comfort improvements are seen with the multi-sensor strategies, but the energy consumption were not observed to significantly change.

4.2 Control Strategies

4.2.1 Temperature Baseline

The Temperature Baseline strategy was designed to behave like a conventional thermostat. The hallway temperature set point was 25°C with a 0.5°C deadband. Figure 4.1 shows a plot of a typical day controlled with the Temperature Baseline strategy. In the plot the empty circles represent the outdoor temperature data points, the other colored shapes are temperatures in various rooms throughout the house. The blue triangles correspond to the power position of the AC system (triangles at the top = ON, bottom = OFF), and the black line with crosses shows the average PPD on the secondary axis. The two straight black lines show the 25°C and 24.5°C thresholds that govern the control. Figure 4.2 shows a plot of the individual rooms' PPD values for the same typical Temperature Baseline control day.
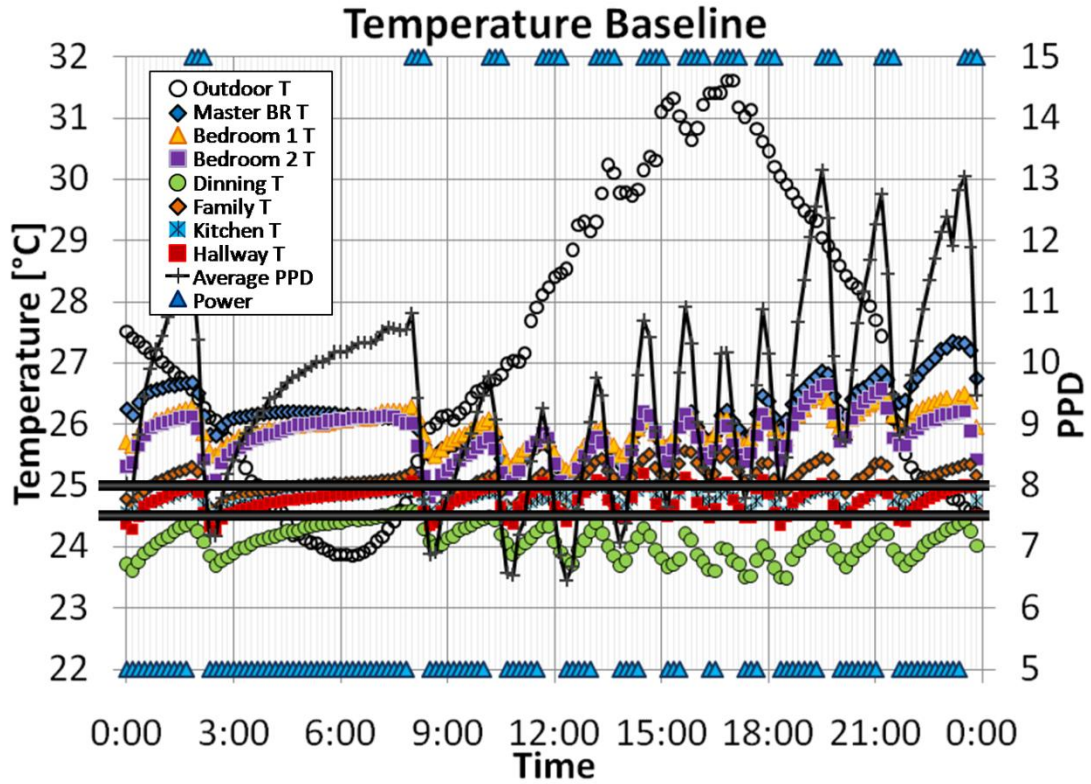
Figure 4.1 Temperature Baseline Temperature Plot
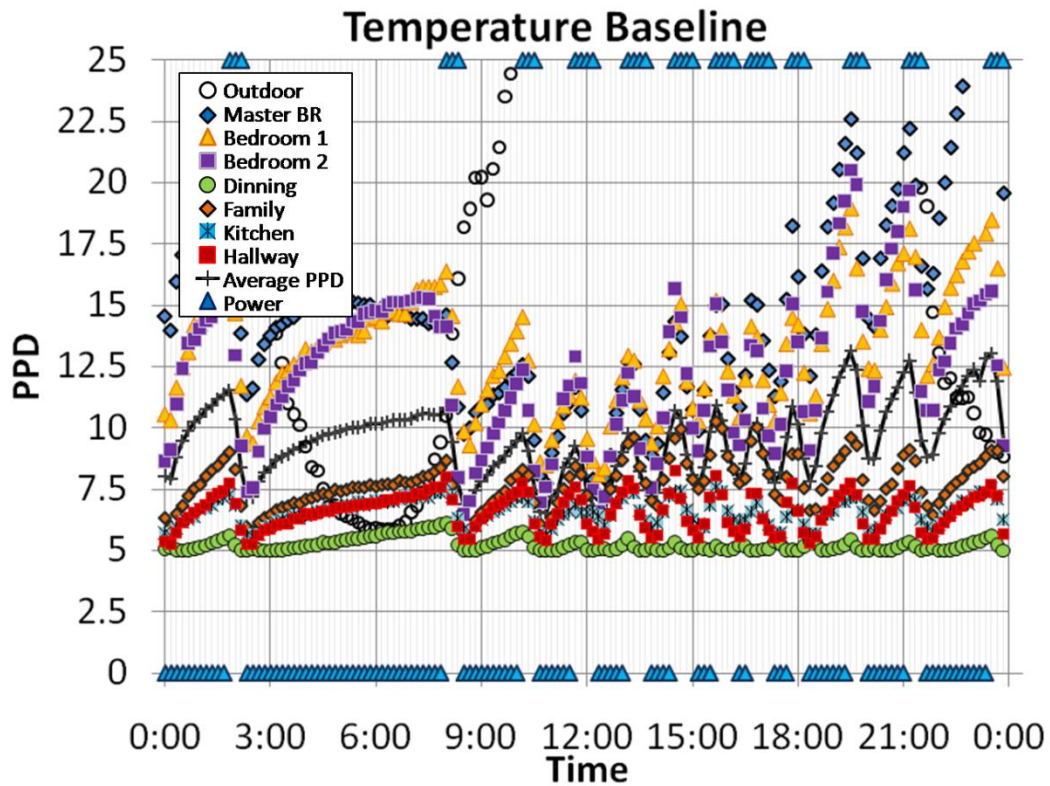
Figure 4.2 Temperature Baseline Comfort Plot

77

The Temperature Baseline strategy controlled the AC by usually turning ON for 20–40 minutes then OFF for 30–50 minutes. The red squares on Figure 4.1 show the hallway temperature and the ON and OFF time can be explained by following the temperature across the threshold lines. For this particular day, the dining room was kept the most comfortable, and the master bedroom saw the least comfortable conditions. All three upstairs rooms experienced PPD of 18 percent or higher in the evening. The longer duty cycle periods and low duty cycles that occurred after 18:00 are responsible for these high PPD values. The hallway temperature was not changing as much as the upstairs rooms, and like a traditional thermostat, that information was not used by the control strategy to provide comfort. The long duty cycle pulse time and period may not be seen in all thermostats. The large deadband, thermal lag of the sensors, and decision interval all contributed to this phenomenon; however, the strategy still performed well enough to be used as the benchmarking strategy.

4.2.2 Comfort Baseline

The Comfort Baseline strategy was a thermostat that used thermal comfort instead of temperature as the control metric. The strategy used 7.4 and 5.7 PPD as the set points. Figure 4.3 shows the temperature plot for a typical day where the Comfort Baseline was controlling the AC. Figure 4.4 plots the thermal comfort for all the rooms on the typical Comfort Baseline day.
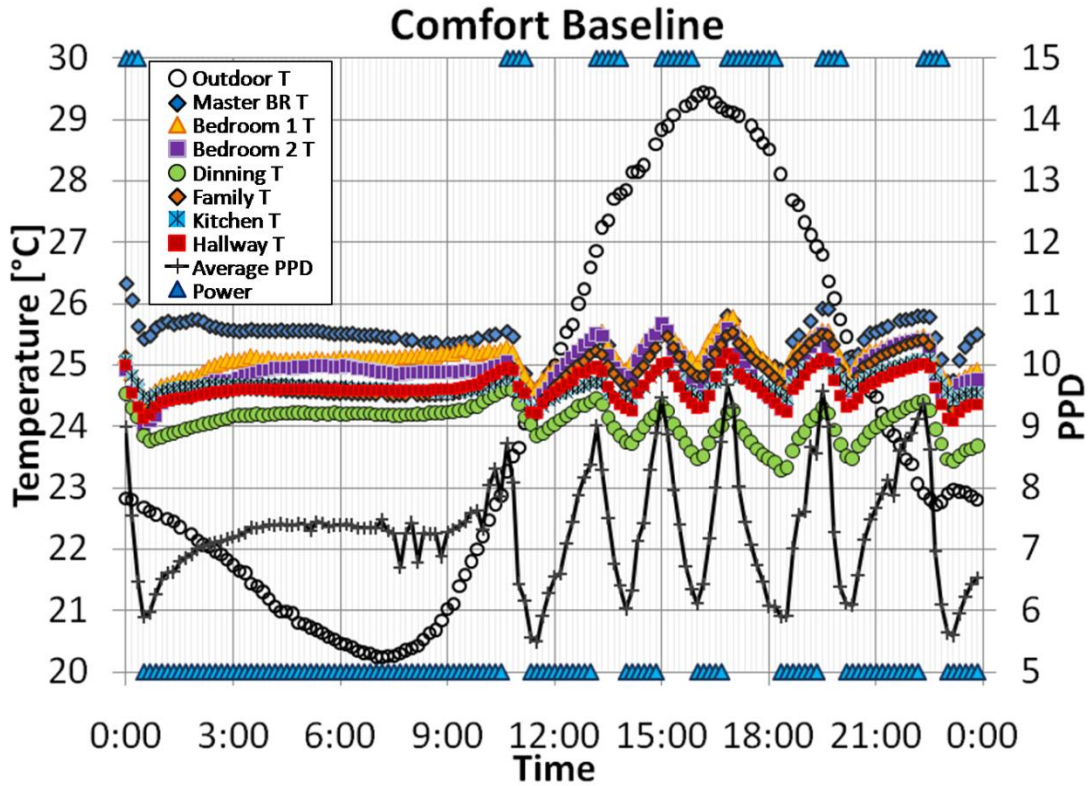
Figure 4.3 Comfort Baseline Temperature Plot
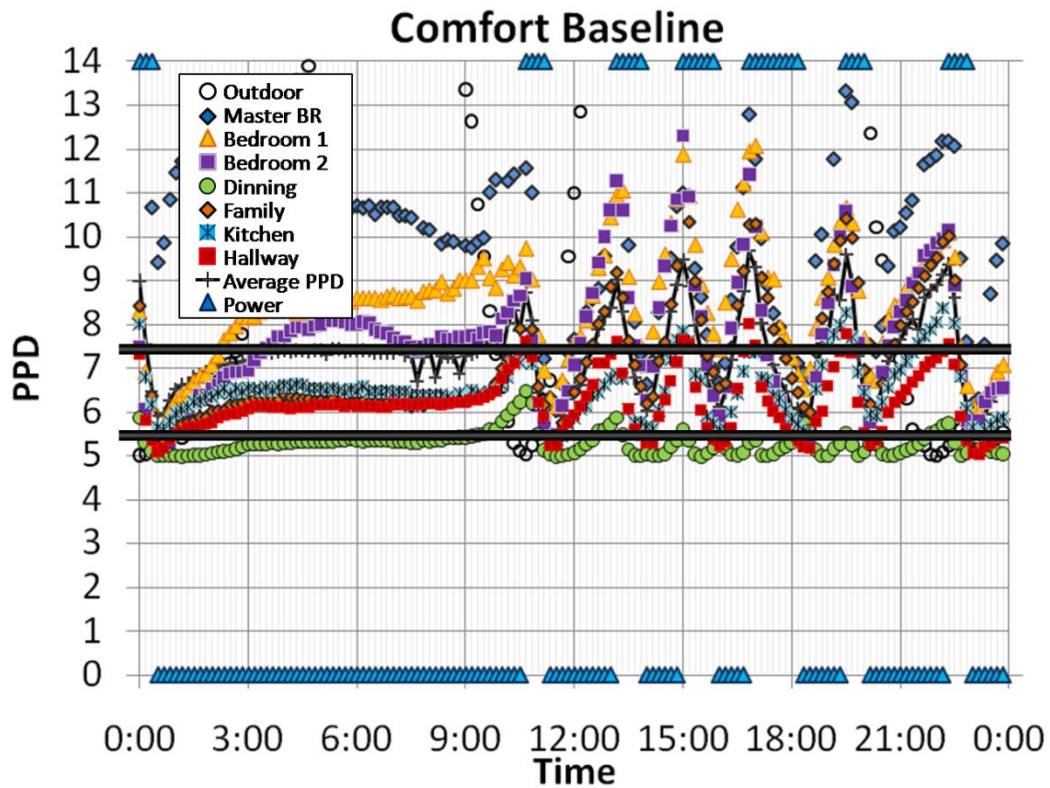
Figure 4.4 Comfort Baseline Comfort Plot

The Comfort Baseline strategy behaved similarly to the Temperature Baseline. It controlled the AC with 30-40 minute periods in the ON position followed by 40-50 minutes with the system OFF. The red squares in Figure 4.4 represent the hallway PPD and show how the power positions are determined. Like the Temperature Baseline, the dining room was the most comfortable and the master bedroom was the least comfortable. The upstairs rooms do not experience as high a PPD as what was seen with the Temperature Baseline. This can be explained by the longer pulse period in the duty cycle. It cools down the upstairs rooms enough so that they do not have the time to rise to the temperatures that show larger discomfort.

4.2.3 PPD Average

The PPD average control strategy averaged all the rooms' PPD values and compared that average to the threshold of 12 PPD. If the average PPD is higher than 12, the cooling system is turned ON; if the average is lower than 12, the system is turned OFF. Figure 4.5 is a temperature plot from a typical day being controlled by the PPD Average strategy. Figure 4.6 shows the individual PPD values for each room during the same typical day. The straight black line at 12 PPD shows the threshold PPD value, and the average PPD line in the plot can be used to see how the power positions are determined.
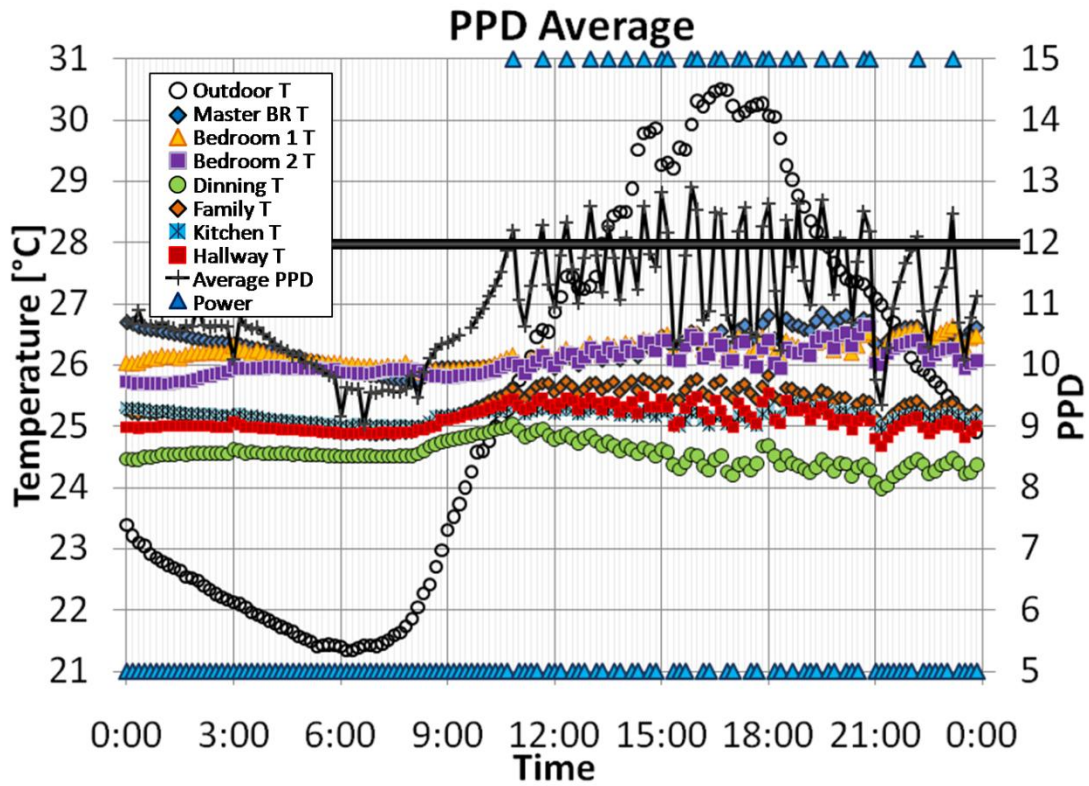
Figure 4.5 PPD Average Temperature Plot
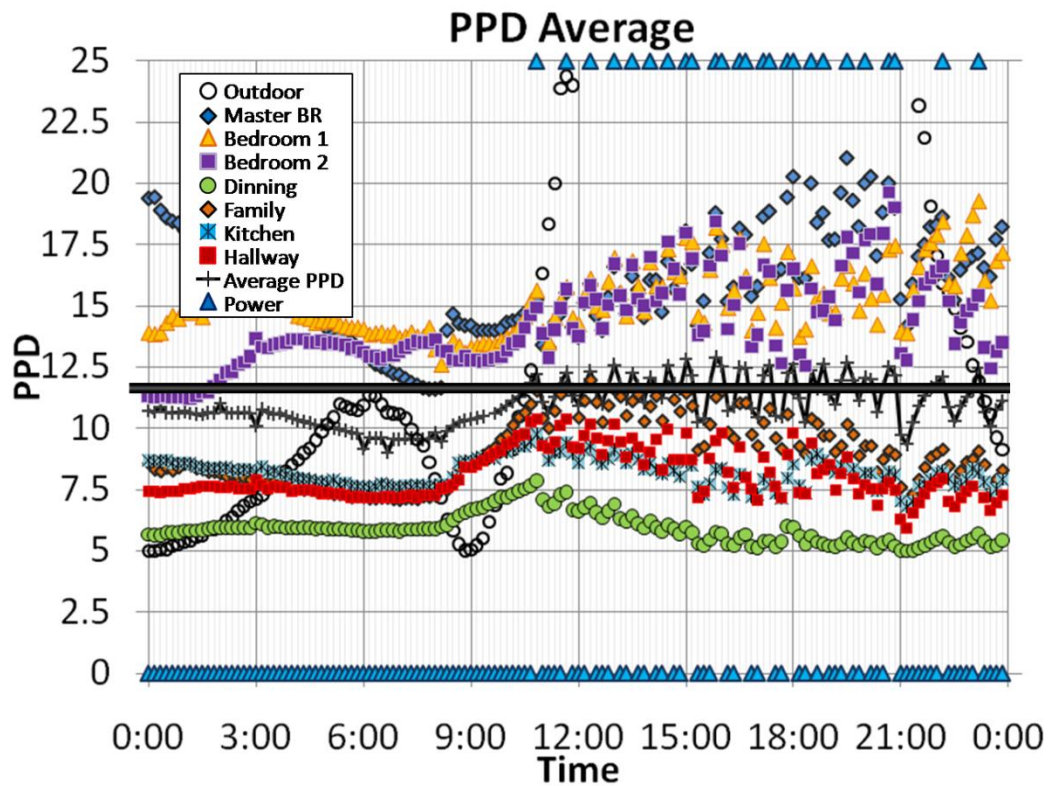
Figure 4.6 PPD Average Comfort Plot

81

The PPD average strategy experienced smaller duty cycle periods than the two Baseline strategies. These usually consisted of 10-20 minutes ON and 20-30 minutes OFF. The average PPD value used to control the system was between the lower PPD downstairs rooms and the higher PPD upstairs rooms. The dining room was the most comfortable room, and the master bedroom experienced the greatest discomfort. The shorter duty cycle frequency made the rooms have a more constant comfort level throughout the day. The large comfort swings that were observed in the two baseline strategies were not seen with the PPD Average strategy. The upstairs rooms reached comfort levels over 18 PPD in the evening; however, it appears that if the threshold PPD value was lowered (or one downstairs room was removed), this can be avoided. Accounting for packet loss was important with this strategy. If a room that was previously one of the most comfortable or uncomfortable failed to report, the average PPD value could be skewed several PPD, causing the average PPD to cross the threshold when it would not have had all the motes reported.

4.2.4 MND

The Minimizing the Probability for Dissatisfaction (MND) strategy controlled the cooling system by comparing the current discomfort in the house to the predicted discomfort found if the cooling system was triggered. Figure 4.7 shows the temperature plot of a typical day where the MND strategy was controlling the cooling system. Figure 4.8 shows the comfort plot for the typical MND day.
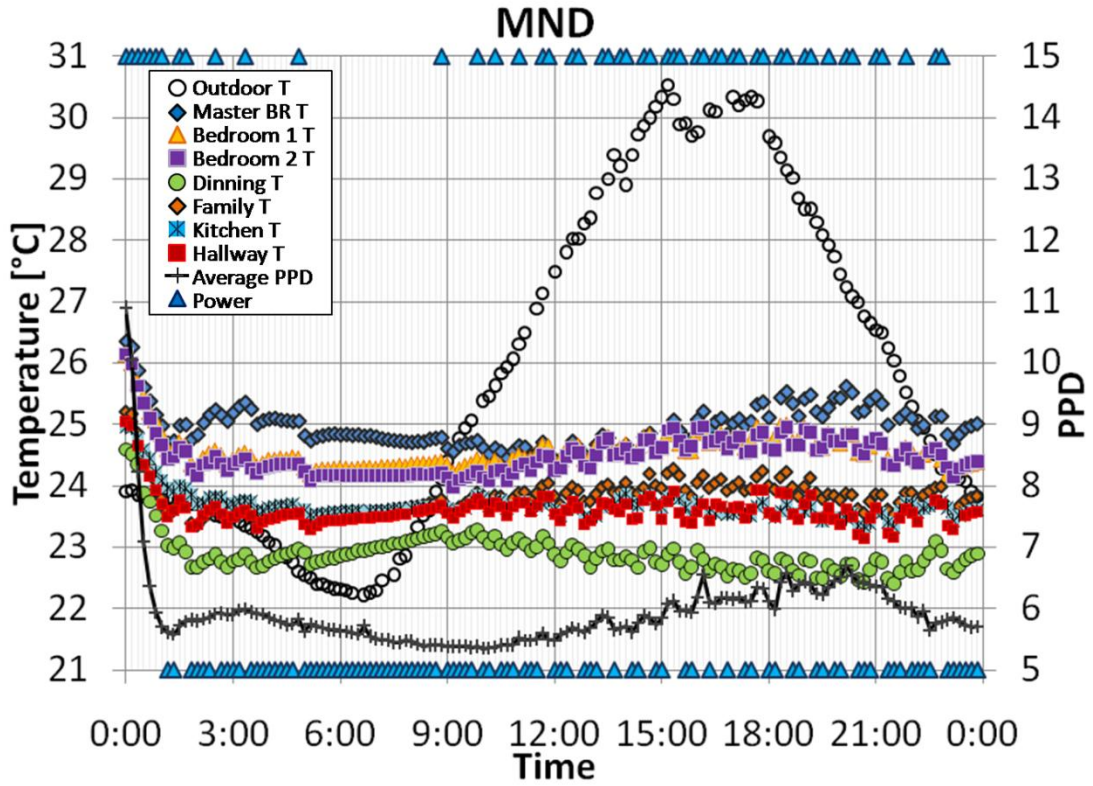
**Figure 4.7 MND Temperature Plot**
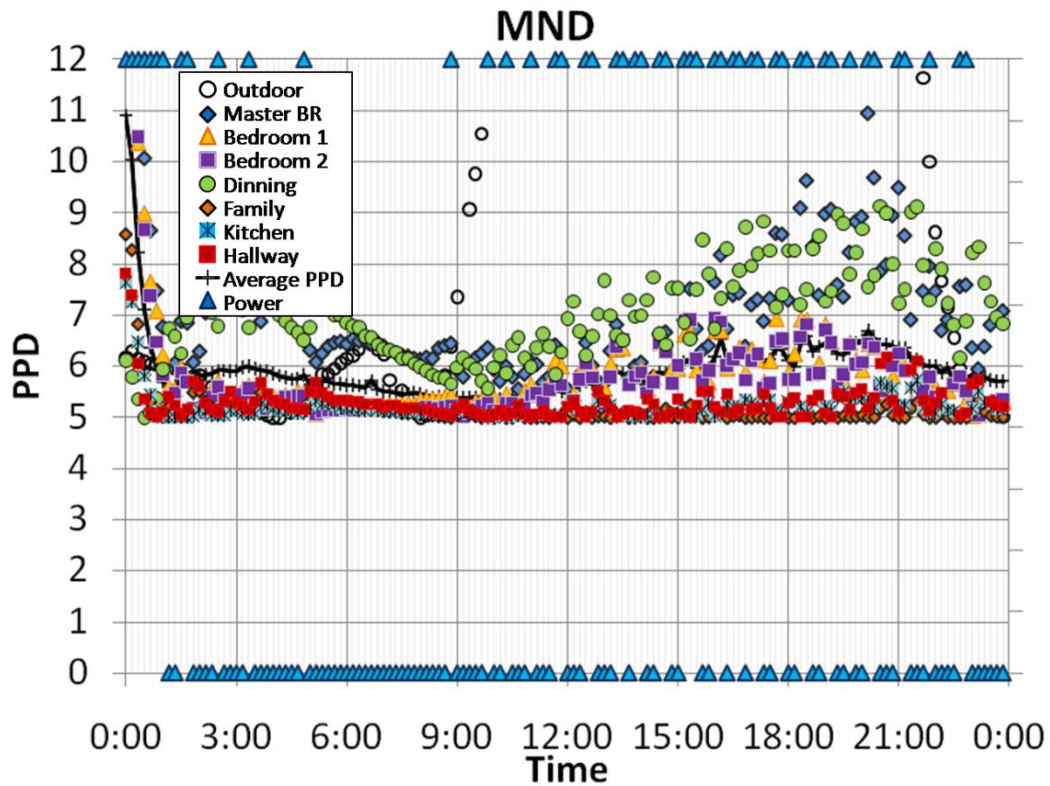
Figure 4.8 MND Comfort Plot

83

The MND strategy cooled the house quite differently than the other strategies. Instead of actuating about a threshold, the strategy drove the house down to the most comfortable conditions, and operated at the bottom of the PPD-PMV curve. In all the previous cases, when the strategy turned the cooling OFF, keeping it ON would have improved the houses comfort more. The MND only calls for the system to be OFF if cooling will reduce the comfort. This made a lot of the rooms very comfortable; five were kept under a PPD of 7 for the majority of the day. Several of the rooms were constantly around 5 PPD, and would be considered the most comfortable rooms. The master bedroom and the dining room alternated throughout the day for the highest level of discomfort. An interesting observation is that this discomfort in the dining room is not from warmer conditions (the reason for every previous discomfort value); rather, the discomfort came from being too cold. The hallway even experienced discomfort from colder than optimum conditions at a few points in the day.

4.2.5 MXR

The Maximizing the Number of Rooms below a Threshold PPD (MXR) strategy controlled the AC by comparing the number of rooms below a threshold PPD value of 12 PPD at the current and predicted future conditions. Figure 4.9 is the temperature plot of a typical day controlled by the MXR strategy. Figure 4.10 is a plot of the comfort for the typical MXR day and Figure 4.11is the comfort plot viewed on the 12:00-midnight interval.
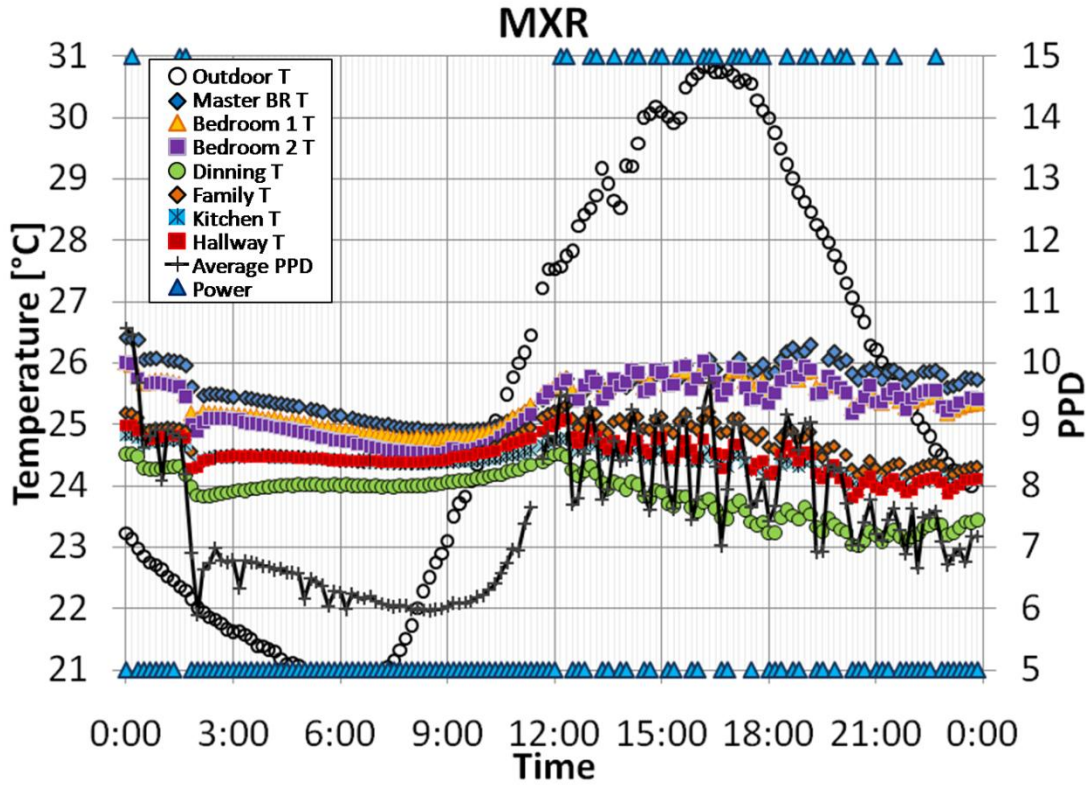
Figure 4.9 MXR Temperature Plot
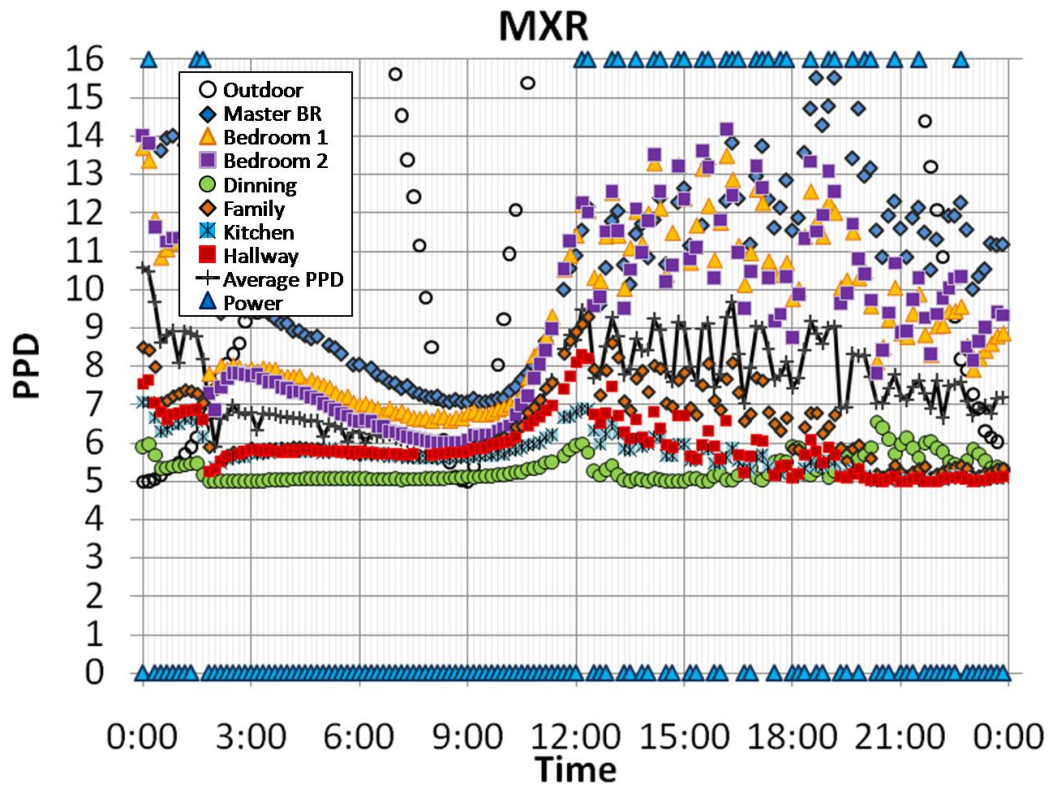
Figure 4.10 MXR Comfort Plot

85
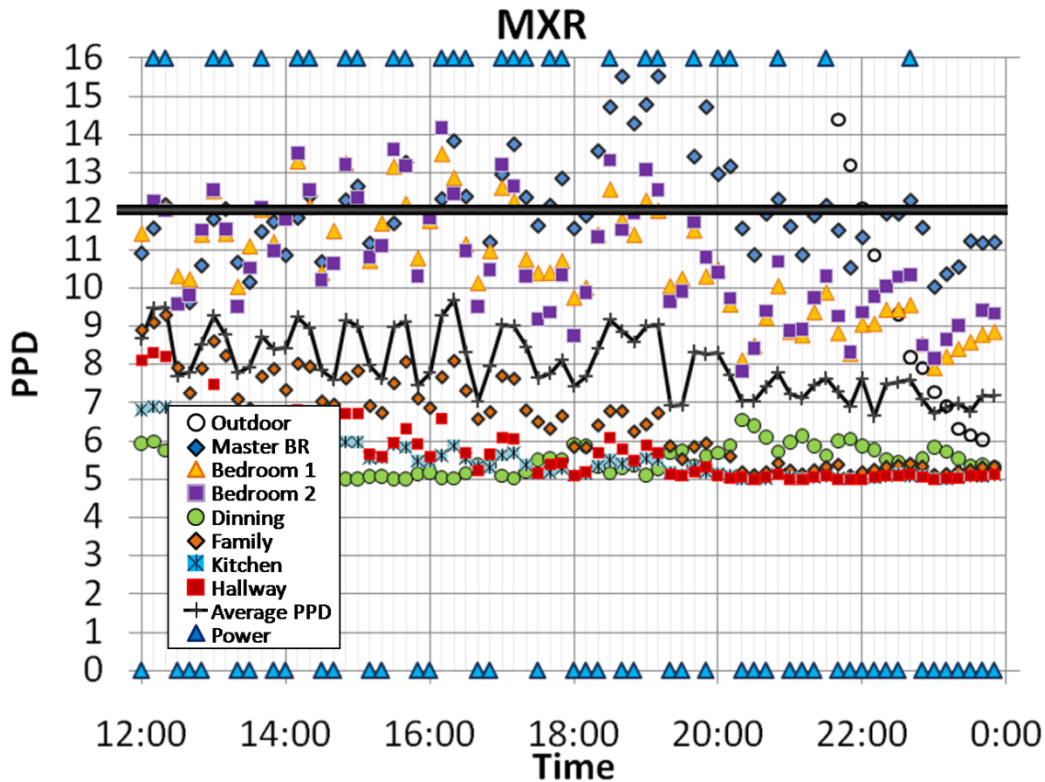
Figure 4.11 MXR Comfort Plot (zoomed)

The MXR strategy did not keep the house comfortable with a set pattern in the ON and OFF times, and the duty cycle periods would vary in length. The three upstairs rooms were responsible for triggering all of the system position changes. There would be times when all three, two, or one room had PPDs higher than 12, and there were even periods where all the rooms were below 12 PPD. Figure 4.11 shows how these rooms jumped about around threshold value. This sporadic movement about the threshold by all three of these rooms can explain why a pattern did not develop. This property of the control strategy was beneficial because it was more adapt to responding to sudden changes in conditions. All four of the downstairs rooms were right around the optimal PPD for significant portions of the day. The dining room saw cooler than optimal conditions, but not at the level seen in the MND

86

strategy. The master bedroom and bedroom 1 alternated being the least comfortable

room.

4.2.6 Average Temperature and Thermal Comfort

Table 4.1lists the average indoor temperature the strategies controlled the

house to when observing the entire day and the main interval of actuation from 12:00

to 20:00.

Table 4.1 Average Indoor Temperature by Strategy

Strategy	*Temperature Baseline*	*Comfort Baseline*	*PPD Average*	*MND*	*MXR*
0:00-23:50 (Full Day)					
Average Temperature [°C]	24.81	25.15	25.14	23.86	24.58
Standard Deviation [°C]	0.65	0.35	0.57	0.31	0.71
12:00-20:00 (Main Actuation)					
Average Temperature [°C]	25.00	25.14	25.46	23.94	24.76
Standard Deviation [°C]	0.44	0.28	0.41	0.14	0.37

The average temperatures calculated over the entire day for each strategy had

several low temperatures from the morning inherent to the calculation; therefore, the

average from the main actuation interval yielded more definitive results. When only

looking at the main actuation interval, the PPD average strategy kept the house the

warmest, while the MND kept the house the coolest. These results were expected

after reviewing the typical days in the previous sections. Higher standard deviations

in the temperature mean that the temperatures fluctuated more. It is logical for the

Temperature Baseline to have the largest standard deviation because it controlled the

house with large temperature swings. The MXR strategy had the largest standard

deviation when considering the full day interval because of a few cooler morning temperatures.

Figure 4.12 shows the average PMV of every strategy over the course of the summer cooling experiment. PMV is shown to capture the observation that the MND strategy averages a slightly cooler than optimal comfort over daily intervals. Figure 4.13 shows the average PPD of the control strategies from the summer experiment. The values for the intervals shown are only calculated from data from days that meet the criteria to be classified by that interval (similar starting conditions).

The average PMV and PPD plots show that the MND strategy kept the house at the most comfortable level. The PPD Average and MXR strategies used the same threshold of 12 PPD, but the MXR strategy averaged better levels of comfort. The Temperature and Comfort Baseline strategies also had very similar thresholds, but the Comfort Baseline averaged a lower PPD. Figure 4.14 plots the average PPD of each strategy throughout the course of an entire day.
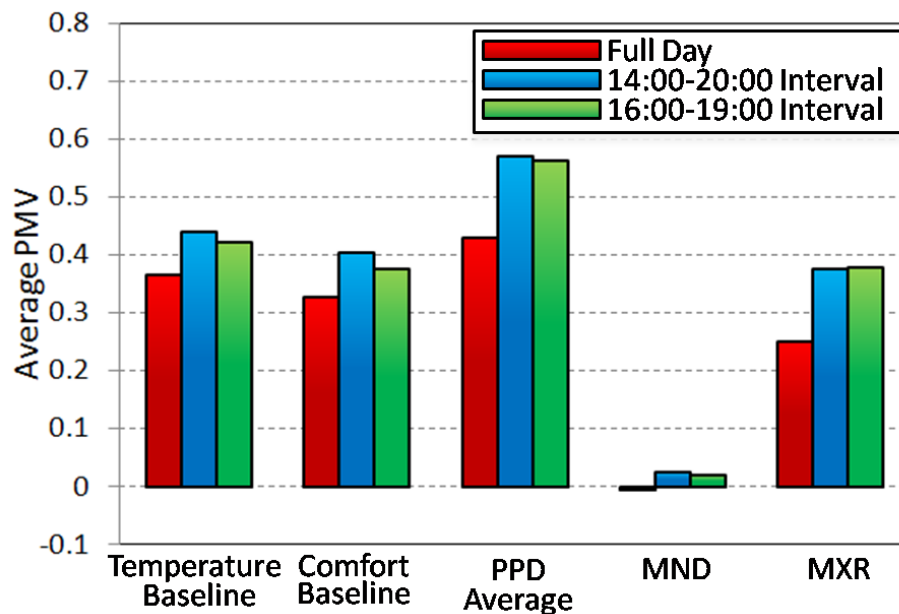

**Figure 4.12 Average PMV**
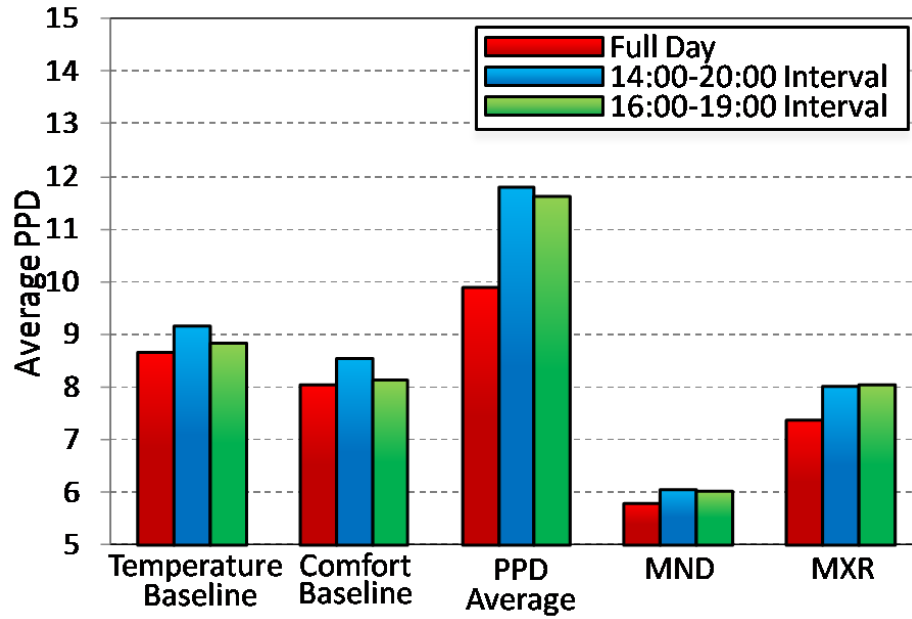
Figure 4.13 Average PPD
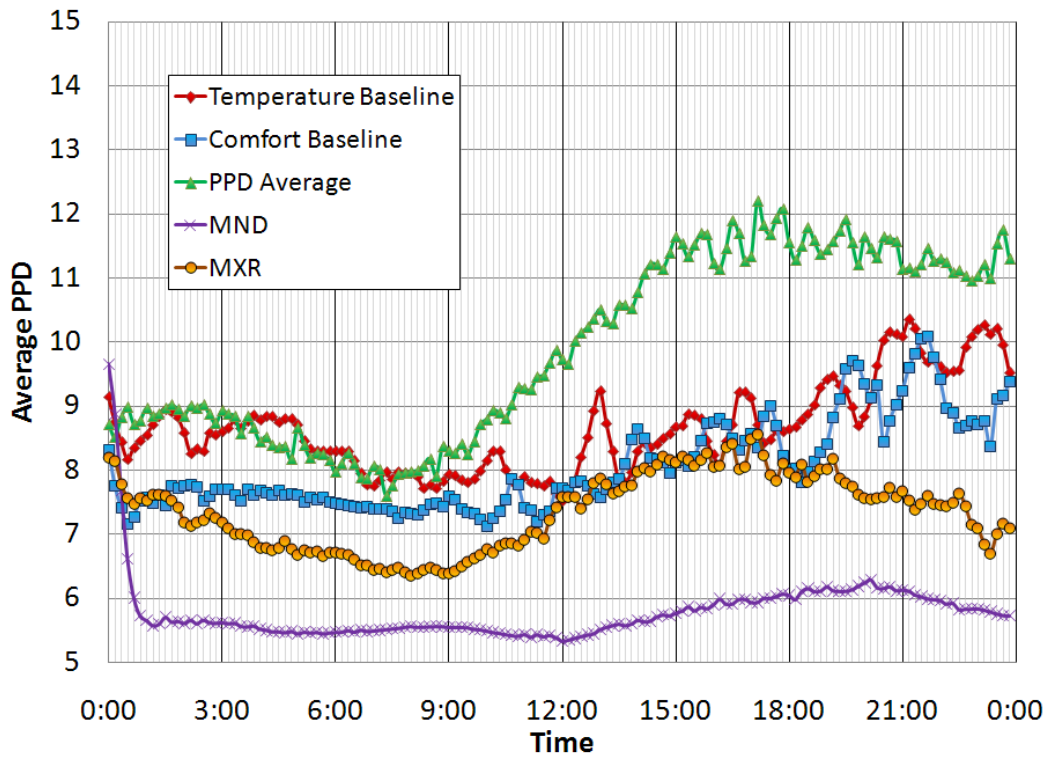
Figure 4.14 Average PPD over the Entire Day

Observing the average PPD over the course of the day is able to give more

information than the average over the interval. The Temperature and Comfort

Baseline strategies' average comfort trends show that discomfort is minimal in the morning (6:00-10:00) and continues to increase into the evening. The PPD average strategy is more comfortable in the morning because the thermal loads on the house are the lowest, and the outdoor air and previous day's cooling are keeping the house cool. Once the temperatures rises outside, the comfort declines indoors until it reaches the point where actuation is required to maintain the average threshold PPD. The MXR strategy behaves similarly in the morning, but the actuation will occur earlier in the day because of the upstairs rooms crossing the threshold. This results in a lower PPD trend throughout the afternoon. The evening starts to see an increase in comfort, because the upstairs rooms are still relevant in the control. This trend is more desirable than the reducing in comfort trends observed with the Baseline strategies. The MND comfort trend shows how it quickly cooled the house to get to the most comfortable level, and then maintained that level throughout the entire day.

4.3 Energy Consumption

4.3.1 Daily Distribution and Start Time

There were 44 days tested that yielded worthwhile data in the summer cooling experiment. Figure 4.15 shows the fraction of days the system was ON to the total number of days at a particular time step. A fraction value of 0.5 at 13:40 indicates that 22 of the 44 days had the system ON at 13:40. The average outdoor temperature calculated over the entire test period is also shown to give a reference to when the highest and lowest temperature are usually observed in the day.
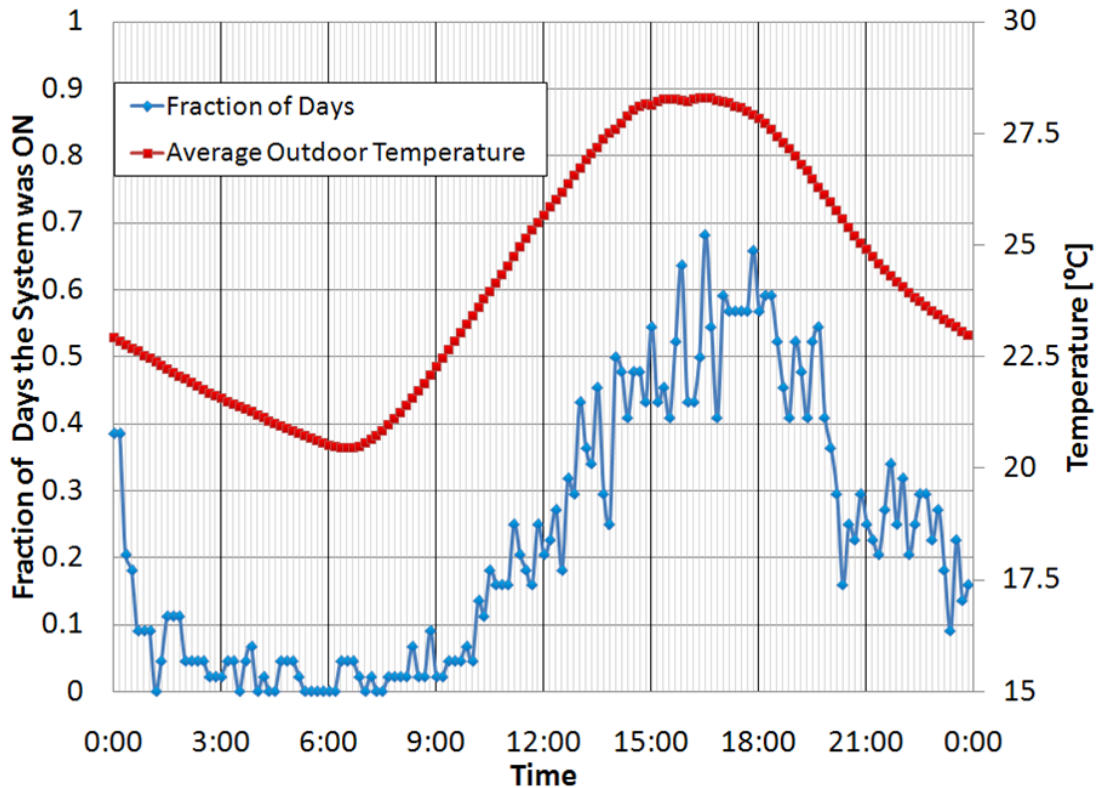
Figure 4.15 Fraction of Days the System was ON and Seasonal Average Outdoor Temperature

The fraction plot shows that the majority of the days had the system ON during the individual time steps between 15:00 and 19:00. This observation agrees with the average outdoor temperature being at its highest point around this time. Even though the beginning and end of the day experienced the same average conditions, the fraction of ON times were different. The first time step had close to 40 percent of the days with the system ON, while the last time step had 16 percent. This occurred because the strategy turn-over occurred at midnight, and several strategies called for cooling when the previous day would have continued to keep the system OFF. This can be seen in the MND plots in section 4.2.5.

Figure 4.16 shows the average starting time for each of the control strategies considered after 9:00. The primary axis and blue solid bars show the strategies'

average PPD at that set starting point. The secondary axis and red striped bars show the average time when a strategy would begin cooling the house using the AC. Figure 4.15 can be used to find the average outdoor temperatures at the start times given in Figure 4.16.
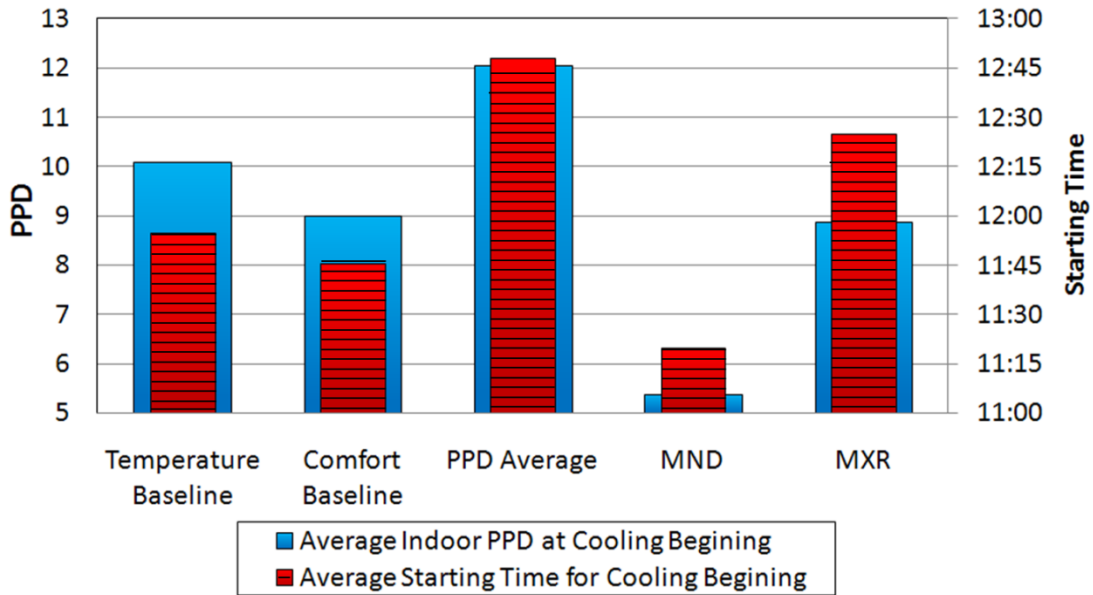
Figure 4.16 Average Strategy Starting Time and Indoor PPD

The start time plot shows that the MND strategy came on the earliest and at the lowest average indoor PPD. The minimizing discomfort driving mechanism of this strategy is the cause for the strategy to turn the system ON at this point, a point that is usually right after when the indoor conditions go from being a little too cool to the optimal conditions. The Temperature and Comfort Baselines and MXR strategy came ON with similar PPD values. MXR came ON a little bit later than the Baselines, but these were still earlier than the PPD Average starting time.

4.3.2 Duty Cycles

The duty cycle metric was used to quantify the energy consumption of the
control strategies during the cooling experiment. Figure 4.17 shows the average duty
cycle for each strategy on the three intervals. The error bars represent the 95 percent
confidence interval found using the standard deviation between the NDC of the
individual days in a strategy.
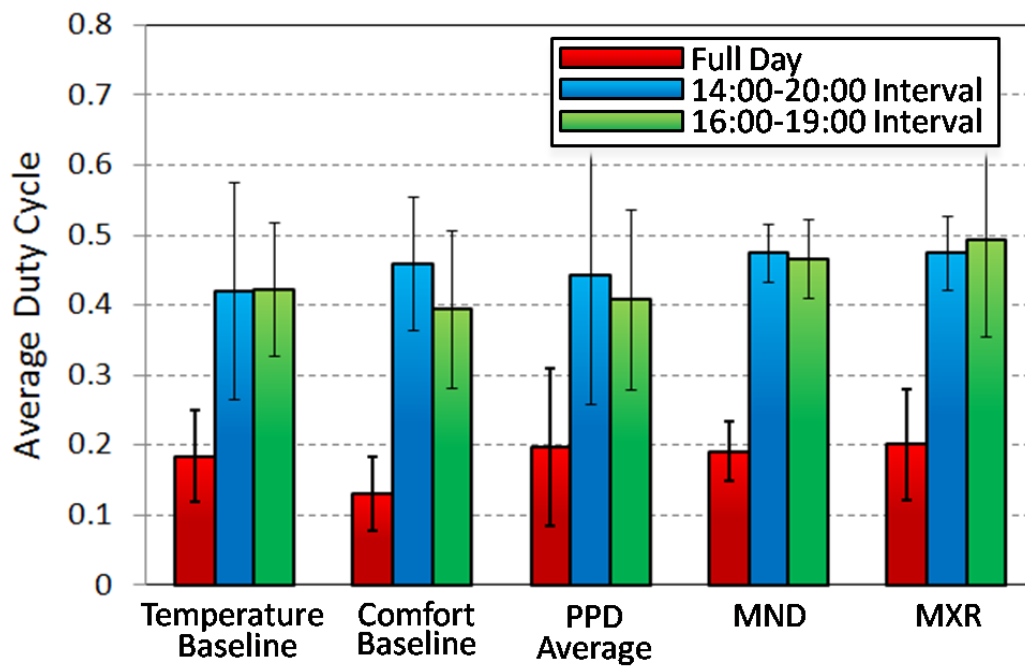
Figure 4.17 Average Duty Cycle

The average duty cycle plot shows that the strategies have very similar
average energy consumption levels; however, the large error bars show the wide
range of daily values that were used to arrive at that average. The 95 percent
confidence level for several of the strategies measured on the intervals is at least 50
perfect of the duty cycle value. Normalizing these duty cycles with CDD and CDI
will bring this large range down. Figure 4.18 shows the average normalized duty

cycle for each strategy evaluated over each of the intervals. The error bars represent

the 95 percent confidence interval of the data from each strategy.
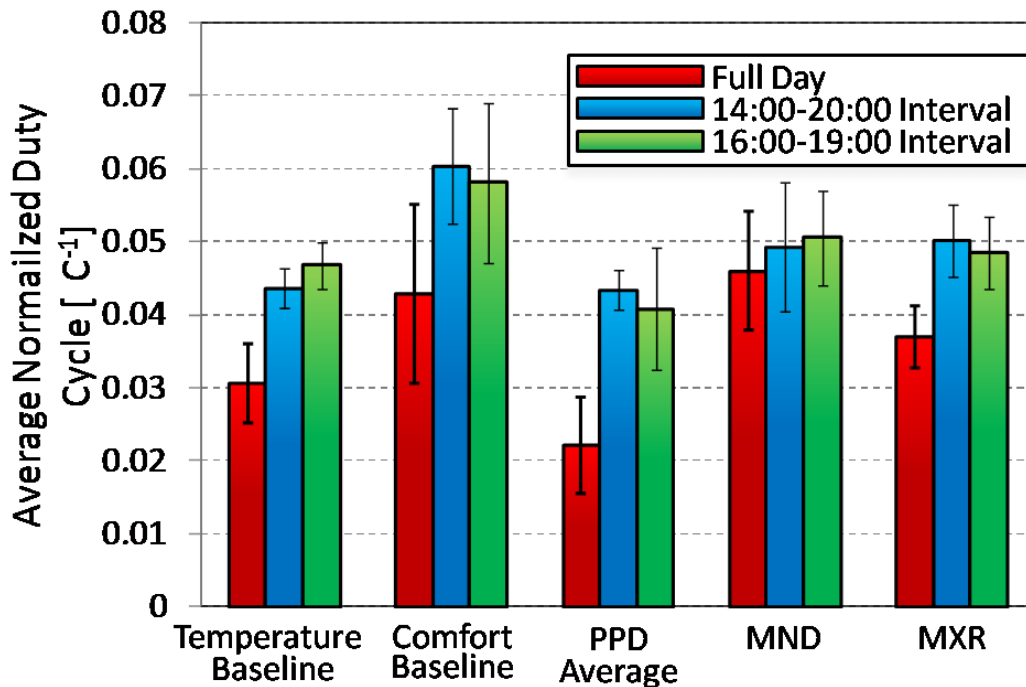
Figure 4.18 Average Normalized Duty Cycle

The normalized duty cycle plot gives the best representation of the individual

strategies' energy consumption. The full day interval will show how the strategy

behaved over the entire course of the day, but it should be noted that the results can

be skewed by the initial conditions. The trends deduced from Figure 4.14 are also

reflected in the average energy consumption of each strategy when considering the

entire day. The MND strategy has the highest NDC on the full day interval because it

controlled the house to be as close to the most comfortable conditions all day; the

PPD Average strategy was the opposite and had the lowest energy consumption over

the entire day because a significant part of the day was spent allowing the house to

warm up to the threshold PPD where the control was based.

The 14:00-20:00 and 16:00-19:00 intervals show data where the varied initial conditions effect had dampened out. The Comfort Baseline strategy averaged the highest energy consumption over the two intervals, and the PPD average consumed the least. The 95 percent confidence level has a lower range than the average duty cycles' interval from Figure 4.17, but it is still; large enough to suggest that the order of energy consumption between the strategies can change. Before the conclusions can be drawn with regards to the energy consumption of the control strategies, a statistical analysis is needed to determine how significant the results are.

4.3.3 Statistical Analysis

The Student's T-Test for two samples with an assumed unequal variance was used to compare the normalized duty cycles of the strategies to the benchmark Temperature Baseline strategy. The test was performed with an alpha value of 0.025 to achieve a level of 95 percent confidence in the conclusion. The hypothesis tested was that the particular strategy has a different average normalized duty cycle than the Temperature Baseline. Having a strategy be more or less energy efficient than the Baseline would be determined if the difference was shown to be significant and then from its position with respect to the Baseline (if strategy A was shown to be statistically different and had a lower average NDC than the Baseline, the conclusion would be that A is more energy efficient than the Baseline). Table 4.2 shows the results of the T-Test when the strategies are evaluated using the full day interval.

Table 4.2 T-Test of Normalized Duty Cycles Compared to the Temperature Baseline Strategy (full day interval)

Strategy	Days Tested	Average Normalized Duty Cycle	Variance	T-Calc	P-value	Reject Null Hypothesis
Temperature Baseline	9	0.031	0.000053	NA	NA	NA
Comfort Baseline	6	0.033	0.000182	2.36	0.68	**Fail**
PPD Average	10	0.022	0.000088	2.11	0.04	**Pass**
MND	6	0.046	0.000054	2.45	0.01	**Pass**
MXR	13	0.037	0.000048	2.11	0.06	**Fail**

The statistical test yields that the average normalized duty cycles of the PPD Average and MND strategies are significantly different than the Temperature Baseline average NDC. The PPD average strategy has a lower NDC than the Baseline, so the NDC improved by 29 percent. The MND average was higher, so the NDC declined in performance by 48 percent. As mentioned before, the results from the full day interval tests were misleading because of the initial conditions effect, and conclusions should not be drawn from them. Table 4.3 shows the results of the T-Test for the days that qualified for the 14:00-20:00 interval.

Table 4.3 T-Test of Normalized Duty Cycles Compared to the Temperature Baseline Strategy (14:00-20:00 interval)

Strategy	Days Tested	Average Normalized Duty Cycle	Variance	T-Calc	P-value	Reject Null Hypothesis
Temperature Baseline	4	0.044	0.000006	NA	NA	NA
Comfort Baseline	5	0.060	0.000062	2.57	0.01	**Pass**
PPD Average	5	0.047	0.000008	2.36	0.09	**Fail**
MND	2	0.049	0.000032	12.71	0.40	**Fail**
MXR	9	0.050	0.000043	2.20	0.02	**Pass**

The T-Test for the average normalized duty cycles on the 14:00-20:00 interval produced two strategies that were statistically different than the Temperature Baseline. The Comfort Baseline strategy was shown to be less energy efficient than the Temperature Baseline. The NDC for the Comfort Baseline increased by 36 percent compared to the Temperature Baseline. The plot in Figure 4.4 showed that the duty cycle pulse time was usually 10 minutes larger than the Temperature Baseline, and can explain why the NDC would be larger. The MXR strategy was also shown to be statistically less efficient with its NDC being 13 percent higher than the Temperature Baseline. This can be explained by the observation that the MXR strategy used more energy to improve the comfort in the evening than the Baseline did letting the house get more uncomfortable. Statistical conclusions could not be reached for the PPD Average and MND strategies. Table 4.4 shows the results of the statistical test on the shorter 16:00-19:00 interval.

Table 4.4 T-Test of Normalized Duty Cycles Compared to the Temperature Baseline Strategy (16:00-19:00 interval)

Strategy	Days Tested	Average Normalized Duty Cycle	Variance	T-Calc	P-value	Reject Null Hypothesis
Temperature Baseline	8	0.047	0.000016	NA	NA	NA
Comfort Baseline	6	0.058	0.000141	2.45	0.07	Fail
PPD Average	9	0.041	0.000125	2.23	0.16	Fail
MND	4	0.051	0.000034	2.57	0.30	Fail
MXR	11	0.049	0.000054	2.12	0.52	Fail

None of the control strategies' normalized duty cycles were shown to be statistically different than the Temperature Baseline. The variance was too high in the Comfort Baseline (a strategy that appears to use more energy) and PPD Average

(a strategy that appears to use less energy) populations for a statistical significant conclusion to be drawn. Figure 4.15 shows that the 16:00-19:00 interval experiences the highest percentage of ON time and outdoor temperatures, and when coupled with these statistical results, it appears that it does not matter what strategy is used during this high demand time in the day.

Since there was not a large difference between the amounts of energy used in each strategy, plotting the normalized duty cycle verses the average PMV can show how much comfort was provided using that energy. The NDC are plotted against average PMV for individual days in the 14:00-20:00 interval in Figure 4.19. Figure 4.20 plots the days on the 16:00-19:00 interval. The trend line is calculated using every day's data on the interval, and the equation is also shown.
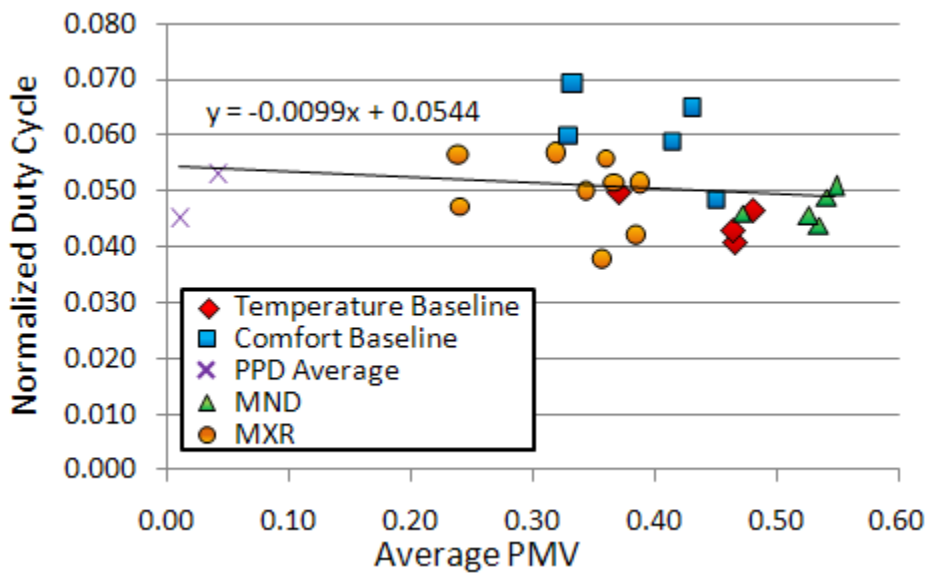

Figure 4.19 Normalized Duty Cycle verses Average PMV (14:00-20:00 interval)
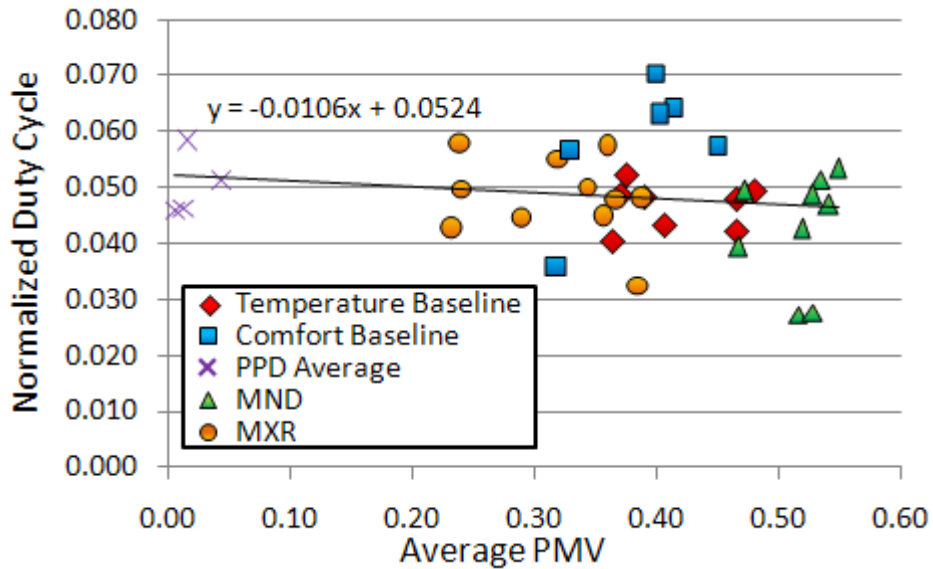
Figure 4.20 Normalized Duty Cycle verses Average PMV (16:00-19:00 interval)

The negative slope in the trend line is expected because it should require more energy to maintain a lower level of discomfort and less energy to keep the house at a warmer, more uncomfortable level. Since every strategy tired to maintain a set level of comfort the data points from the same strategy clumped into regions. In the 14:00-20:00 interval four out of the five Comfort Baseline data points had NDC higher than the trend line. This suggests that the strategy required more energy to provide comfort very similar to the other strategies and agrees with the statistical test. On the 14:00-20:00 interval the statistical test also showed that the MXR strategy consumed more energy than the Temperature Baseline, and Figure 4.19 shows that is due to the MXR strategy controlling at lower average PMV.

Two plots were generated for each interval to show the importance of normalizing the duty cycle to properly compare the energy consumption between the strategies. The daily duty cycles are plotted verses the average outdoor temperature

for the 14:00-20:00 interval in Figure 4.21and 16:00-19:00 interval in Figure 4.22.

Figure 4.23 shows how the normalized duty cycle changes with the average outdoor

temperature and Figure 4.24 plots the days from the 16:00-19:00 interval.
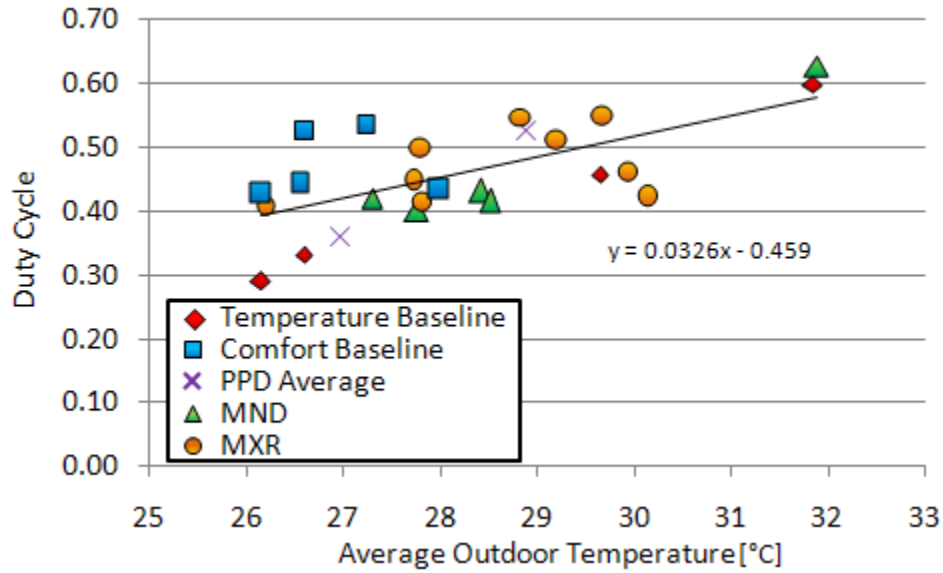
Figure 4.21 Duty Cycle verses Outdoor Temperature (14:00-20:00 interval)
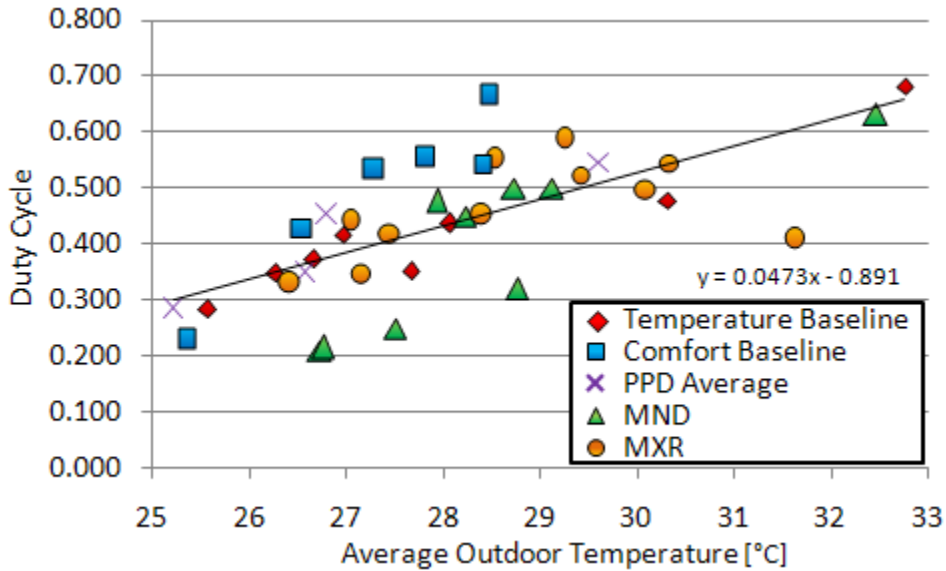
Figure 4.22 Duty Cycle verses Outdoor Temperature (16:00-19:00 interval)
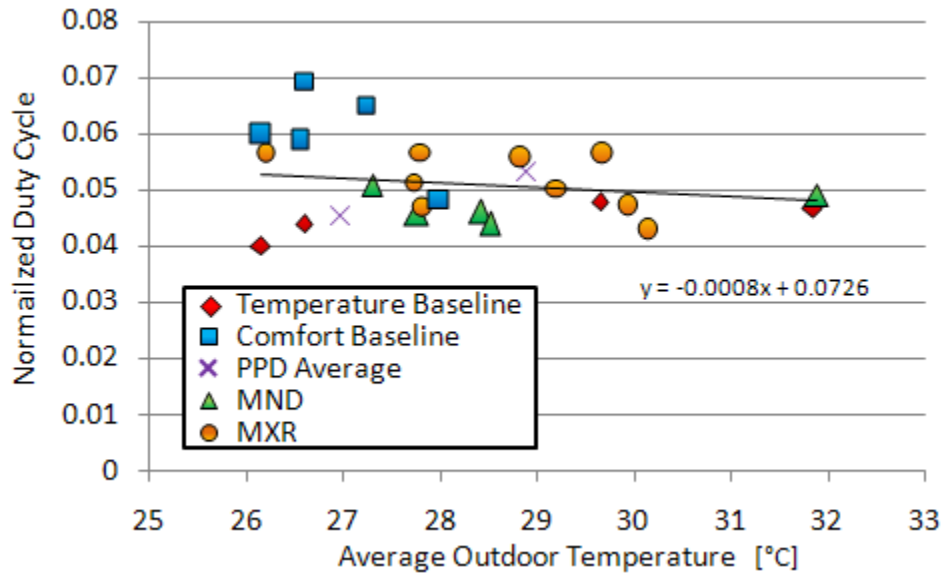
Figure 4.23 Normalized Duty Cycle verses Outdoor Temperature (14:00-20:00 interval using 19°C base)
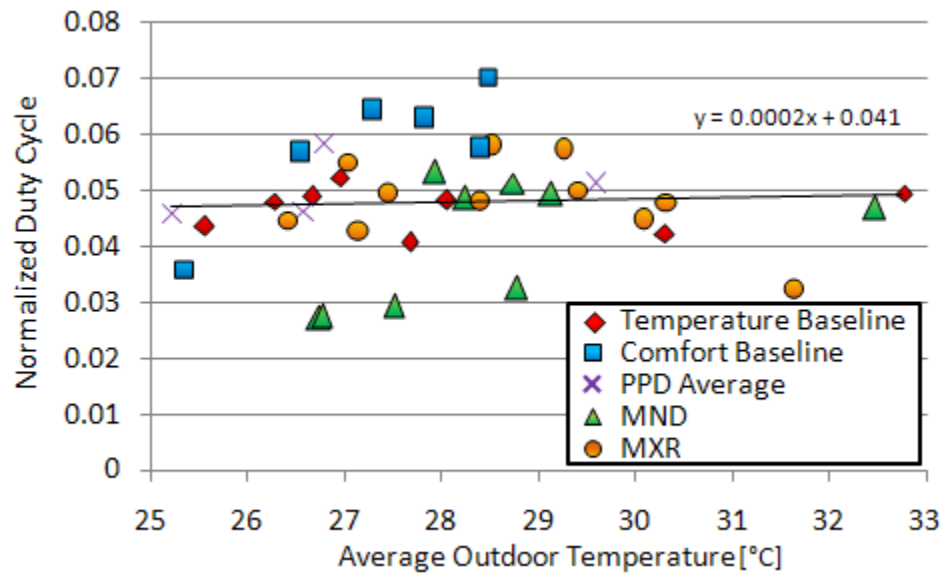
Figure 4.24 Normalized Duty Cycle verses Outdoor Temperature (16:00-19:00 interval using 19°C base)

The positive slope in the trend line of duty cycle verses the average outdoor temperature is expected because higher outdoor temperatures impose a higher thermal load on the house, thus requiring more energy. Higher outdoor temperatures would also reduce the efficiency of the compressor, and the system would compensate for it

by being ON longer and increasing the duty cycle. When the normalized duty cycle is plotted against the average outdoor temperature it is shown that the base of 19°C was chosen quite well to balance the loads and efficiency differences. Figure 4.21and Figure 4.22 show that the higher outdoor temperatures required more energy than the lower outdoor temperatures, but Figure 4.23 and Figure 4.24 show that when 19°C is used to normalize the duty cycle, the normalized values can be compared for all outdoor temperatures. The very small slopes in the normalized duty cycle trend lines shows how 19°C was a good choice for normalizing the duty cycle.

4.4 Discussion

The control strategies were shown to control the cooling system in different ways. The Temperature Baseline strategy controlled the AC with large temperature and comfort swings because of the large 0.5°C deadband, thermal lag of the sensors, and decision interval. The average comfort was close to 9 PPD for all three intervals, and was usually kept between 7 and 10 PPD, until the evening when the average comfort would start to diminish. This occurred because the upstairs rooms continued to need cooling to maintain comfortable levels. The upstairs rarely received the cooling in the evening because the hallway stayed below the threshold temperature for long periods.

The Comfort Baseline experienced the same large temperature and comfort swings as the Temperature Baseline strategy because it also had a large deadband and thermal lag in the hallway sensor. Having the PPD actuate the control instead of temperature made the duty cycle pulse usually increase by 10 minutes. Since the PPD thresholds for the Comfort Baseline were calculated using the Temperature Baseline

temperatures, this additional pulse length must be a result of the relative humidity. The average relative humidity during the Temperature Baseline control was 51.6 percent and the average was 50.4 during the Comfort Baseline. This suggests that more of the Comfort Baseline's energy went to condensing the water vapor in the air than the Temperature Baseline energy did, but since the difference is within the sensor's measurement error a strong conclusion is not made. This additional amount of cooling energy at the end of the ON cycle also was not as beneficial to the rest of the house as the energy at the start of an ON cycle. This resulted in the Comfort Baseline outperforming the Temperature Baseline in the comfort categories, but it paid for it with extra energy. The extra energy did not translate to a longer OFF time in the duty cycle period, so the normalized duty cycle ended up being larger than the Temperature Baseline's.

The threshold PPD for the PPD Average strategy was set too high to be able to make direct comparisons to the other strategies. Figure 4.13 and Figure 4.14 show that the average PPD was higher for this strategy and Figure 4.16 shows that it starts actively controlling the latest in the day. This is why the T-Test on the full day interval showed that the strategy improved the system by 29 percent (note that the validity of the full day data is questioned). When the interval was shortened, the statistical tests were unable to show that it consumed any less energy, and the conclusion that it is not superior to the Temperature baseline is reached.

The MND strategy was interesting because it kept the house constantly the most comfortable. The full interval statistical test showed that it consumed more energy that the Temperature baseline; however, Figure 4.7 and Figure 4.14 show that

this was due to it having to cool significantly at the start of its control time to reach the comfort level where it operates. Once it was at this comfort level, the strategy consumed about the same amount of energy as the other, less comfortable strategies. This can be seen in how the statistical tests over the intervals failed to show its energy consumption was statistically different from the Temperature Baseline. One issue that comes to mind with the MND strategy is how it controls with a high frequency of actuation. This may degrade the efficiency of the compressor over time, but a solution would be to increase the decision interval time to match what he compressor can handle sustainably.

The MXR strategy was driven primarily by the three upstairs rooms because when the system would turn over at midnight, they were the rooms that were the closest to the 12 PPD threshold. This became an advantage in the evening because the upstairs was able to request cooling for the house when it needed it, where the hallway control of the Baseline strategies was insufficient. This meant that the comfort actually improved in the evening, instead of declining like the Baseline strategies. The result is also going to be more useful to the occupants because more time is spent in the upstairs bedrooms in the evening.

The main problem with the statistical analysis is the small sample sizes. More statistical conclusions could be drawn with more data, but in the end it appeared that there were not large enough temperature overshoots in the Temperature Baseline to produce noticeable, additional energy consumption. The original thermostat was positioned in a sufficient location to control the house with that particular sized cooling system and summer load profile. It would be beneficial to test these control

strategies in a house that has a thermostat location that needs improvement, and also on an under, and over sized cooling system.

4.5 Conclusion

Energy savings might have been found in other similar studies, but the multi-sensor control strategies developed by the CBE and in this study were unable to improve the energy efficiency of a central AC system over traditional thermostat logic in this summer cooling system experiment. Using thermal comfort as the threshold metric of a single sensor thermostat was shown to increase the energy consumption of a system by 36 percent when evaluated on the 14:00-20:00 interval, and it was determined that this was a result of the relative humidity in the PPD calculation. Averaging the comfort of the rooms (PPD Average) may be mistakenly recognized for having superior energy performance. It was shown however, this was due to controlling the house at a higher level of discomfort and errors introduced by the initial conditions. The MND strategy might be the most desirable because it produces the best level of comfort (3 PPD average improvement over the Temperature Baseline) while approximately consuming the same amounts of energy as the other strategies. The MXR strategy also improved the comfort of the upstairs rooms compared to the Baseline strategies during the evening at a small energy price. The statistical analysis was limited by the low number of data points, because entire days would only correspond to one point. Further testing could improve the confidence in the conclusions, or find new phenomenon that explain the current level of statistical insignificance between the strategies.

Chapter 5: Winter Heating Results and System Performance

5.1 Introduction

An experiment was performed in the winter to evaluate the performance of the heating control strategies and control system. The setup explained in chapter 3 was used, and data collection began at the start of December 2009. Data collection continued until the last day of January 2010 with a brief interruption in late December. High winds on several days introduced significant amounts of infiltration and these days were not considered in the analysis. The days were not considered if the average wind speed measured by a local weather station (MC3648) was above 2.5 km/h (1.6 mph) or if a significant portion of the wind gusts were above 8 km/h (5 mph). Software issues also removed a day from the analysis. In total, 45 days were used to evaluate the four control strategies over the entire day and nighttime interval. The heating system experienced significant periods where it was turned ON because the outdoor temperatures were always colder than the indoor temperatures. This yielded very uniform data, and transient periods due to fluctuating outdoor conditions and changing between strategies were very small.

The outdoor mote measured a temperature range from a low of -6.2°C (20.9°F) to a high of 17.8°C (64.0°F) and averaged 2.9°C (37.3°F) during the evaluation period. The outdoor relative humidity varied from 24 to 95 percent and averaged 67 percent. During the winter test the average indoor temperature reached a low of 18.2°C (64.7°F), high of 25.4°C (77.7°F), and averaged 20.4°C (68.8°F). The average indoor relative humidity ranged from 19.7 to 46.2 percent and averaged 29.4 percent.

The particular strategies were evaluated in detail and explained using plots from typical days where they were in control. The temperature and comfort set points and thresholds for several of the strategies were varied to generate more equivalent comfort data between the strategies. This allowed the PPD Average strategy using a threshold of 8, 10, and 12 PPD to be evaluated by comparing it to equivalent set points using the Baseline strategy. The energy consumption is normalized by the HDD or HDI and compared against the comfort levels achieved and used as set points and thresholds. The Baseline strategy served as the only single-sensor strategy to benchmark the performance of the other, multi-sensor strategies. The Baseline strategy outperformed all the multi-sensor strategies when the proper set points were used. This was due primarily to fact that warmer air is lighter and is found primarily in the upstairs, resulting in a large temperature difference between the floors.

5.2 Control Strategies

5.2.1 Temperature Baseline

The Temperature Baseline strategy was designed to behave like a conventional thermostat. The hallway temperature set points used were 19.5, 19, 18.5, and 18°C with a 0.5°C deadband. Figure 5.1 shows a plot of a typical day controlled with the Temperature Baseline strategy with a19.5-20°C set point. In the plot the empty circles represent the outdoor temperature data points, the other colored shapes are temperatures in various rooms throughout the house. The blue triangles correspond to the power position of the AC system (triangles at the top = ON, bottom = OFF), and the black line with crosses shows the average PPD on the secondary axis. The thresholds that governed the control change depended on what set point was used

(instead of always being at a particular level as was seen in the summer cooling experiment); to avoid confusion, the black threshold lines are not shown on the plots in this chapter. Figure 5.2 shows a plot of the individual rooms' PPD values for the same typical Temperature Baseline control day. Also note that the dining room mote malfunctioned and was removed from the system at the beginning of the testing.
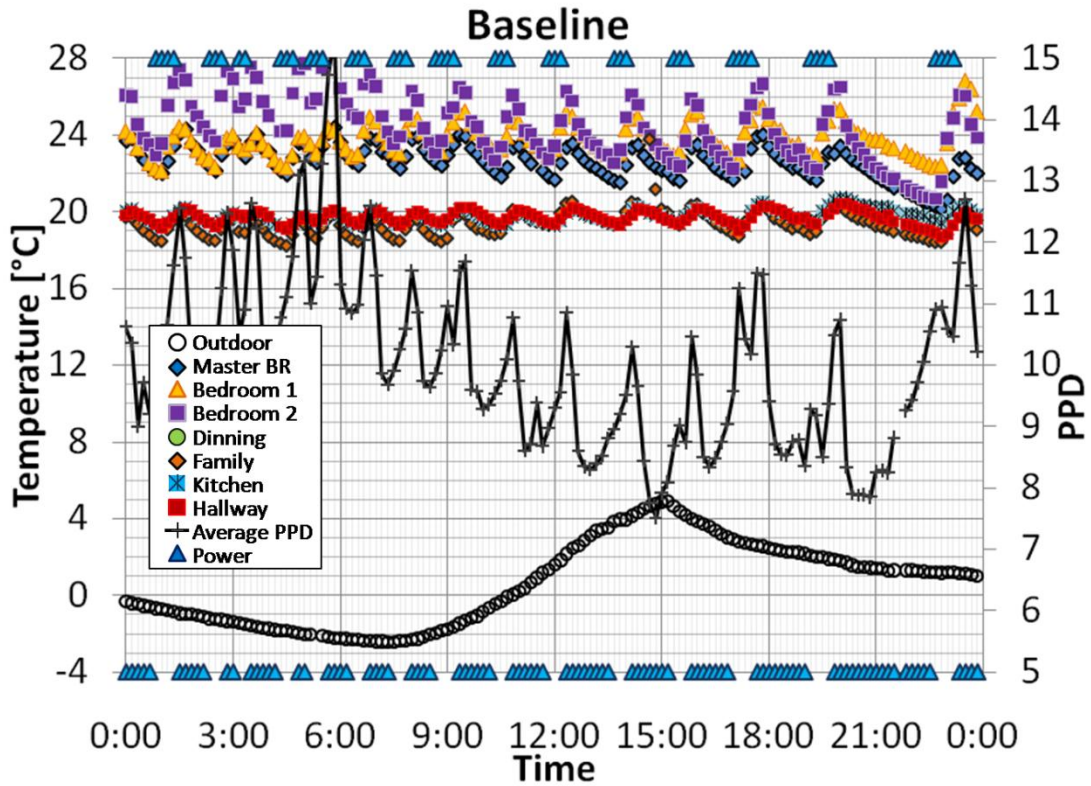
**Figure 5.1 Temperature Baseline Temperature Plot**
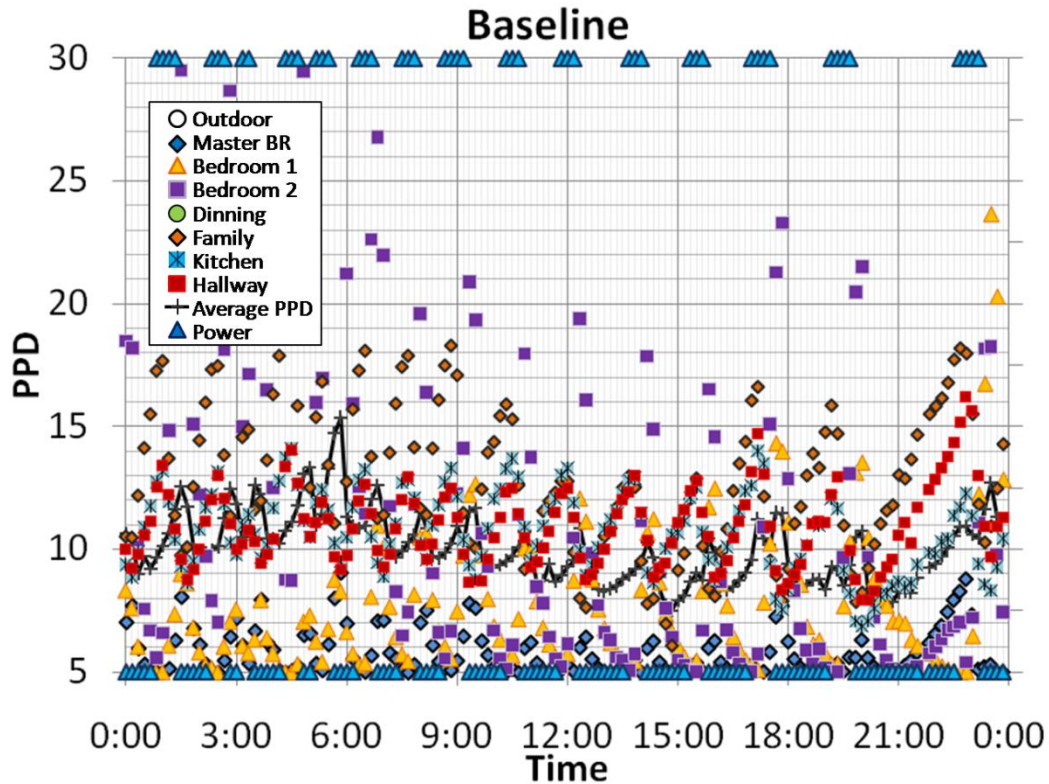
Figure 5.2 Temperature Baseline Comfort Plot

The Temperature Baseline strategy controlled the heating by usually turning ON for 20–40 minutes then OFF for 40–70 minutes. The red squares on Figure 5.1 show the hallway temperature and the ON and OFF time can be explained by following the temperature across the threshold temperatures of 19.5°C and 20°C. For this particular day the comfort level varied significantly. Bedroom 1 and 2 both experienced intervals where they were the most or least comfortable room. The least comfortable conditions were measured by the upstairs bedrooms being too warm. This even occurred during the night, when the occupants would be sleeping. Changing the set point level shifted the comfort of the downstairs, but even at the lowest 18-18.5°C set point the upstairs rooms experienced discomfort from receiving too much warm air. The strategy performed well enough to be used as the benchmarking strategy.

5.2.2 PPD Average

The PPD average control strategy averaged all the rooms' PPD values and compared that average to the threshold of 8, 10, or 12 PPD. If the average PPD is higher than the threshold, the heating system is turned ON; if the average is lower than the threshold, the system is turned OFF. Figure 5.3 is a temperature plot from a typical day being controlled by the PPD Average strategy with a threshold of 8 PPD. The average PPD was calculated using the average PMV value to get a true average of the houses comfort. It was also observed that if the average PPD was calculated by averaging the room PPD values, having rooms be too warm actually drove the strategy to want to heat even more. Figure 5.4 shows the individual PPD values for each room during the same typical day.
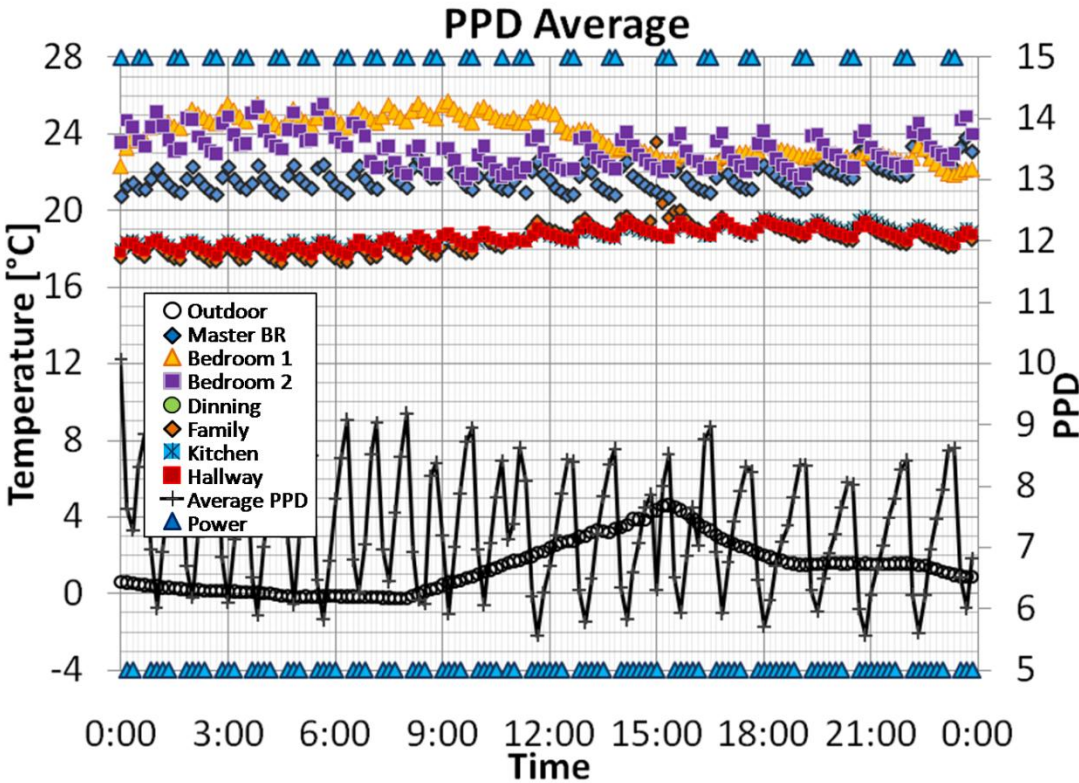

Figure 5.3 PPD Average Temperature Plot

110
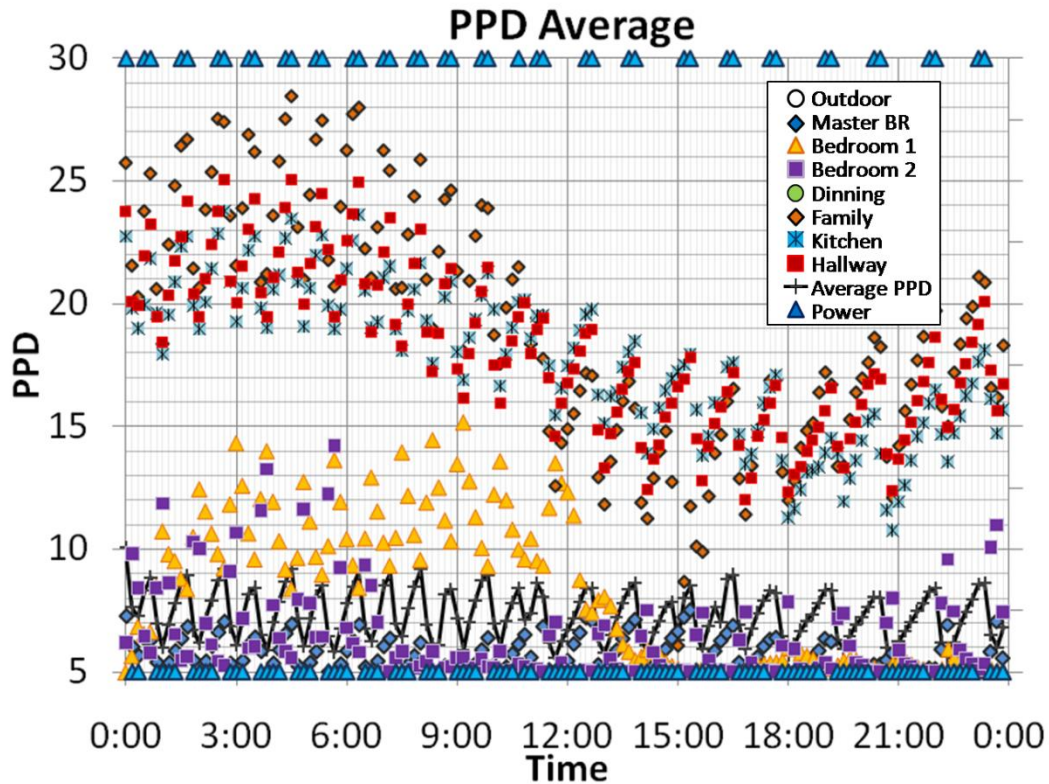
Figure 5.4 PPD Average Comfort Plot

The PPD average strategy experienced smaller duty cycle periods than the

Baseline strategies. These usually consisted of 20 minutes ON and 30-40 minutes

OFF. The average PPD value used to control the system was between the higher PPD

downstairs rooms and the lower PPD upstairs rooms. The master bedroom was the

most comfortable room, and the family room experienced the greatest discomfort.

The shorter duty cycle frequency made the rooms have a more constant comfort level

throughout the day. The large comfort swing that was observed in the Baseline

strategy was not seen with the PPD Average strategy. The downstairs rooms reached

comfort levels over 20 PPD in the early morning (0:00-6:00); however , the comfort

improved after 9:00 until about 18:00. The low level of comfort in the downstairs

rooms observed in the early morning would actually be advantageous. Since these

rooms are not occupied at this time, using additional energy to improve the comfort may be a waste.

5.2.3 MND

The Minimizing the Probability for Dissatisfaction (MND) strategy controlled the heating system by comparing the current discomfort in the house to the predicted discomfort found if the heating system was triggered. A flat 0.3°C temperature increase was used in all the room's predictions. Figure 5.5 shows the temperature plot of a typical day where the MND strategy was controlling the heating system. Figure 5.6 shows the comfort plot for the typical MND day.
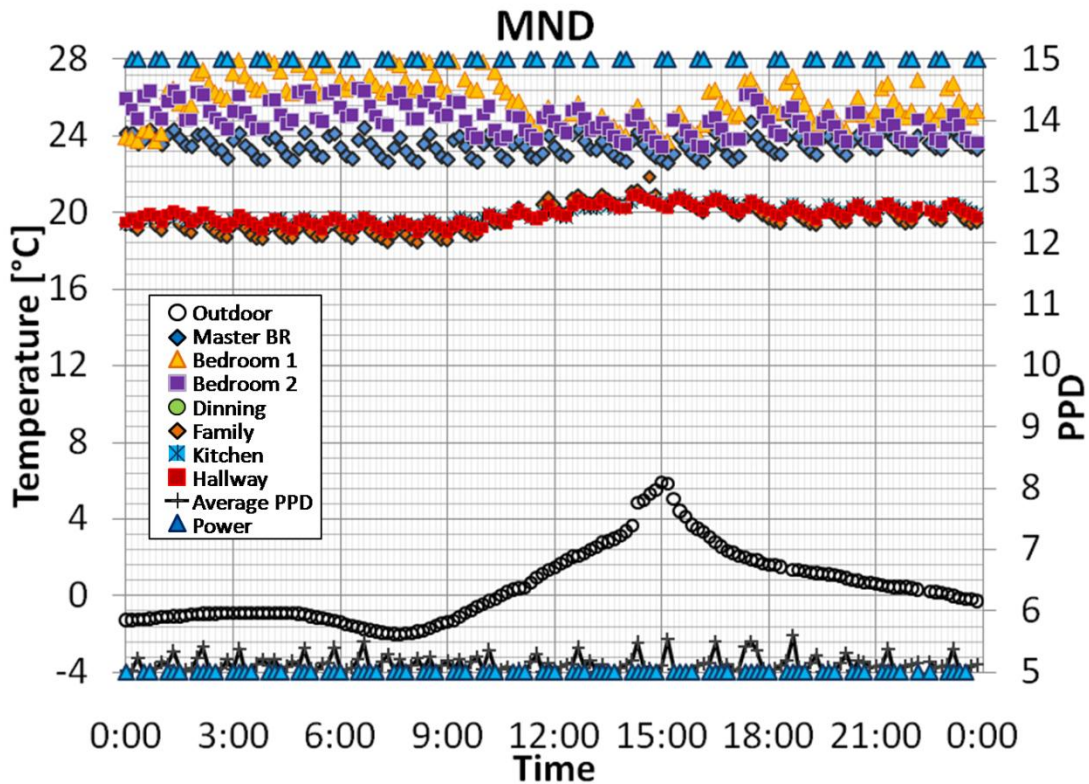
Figure 5.5 MND Temperature Plot
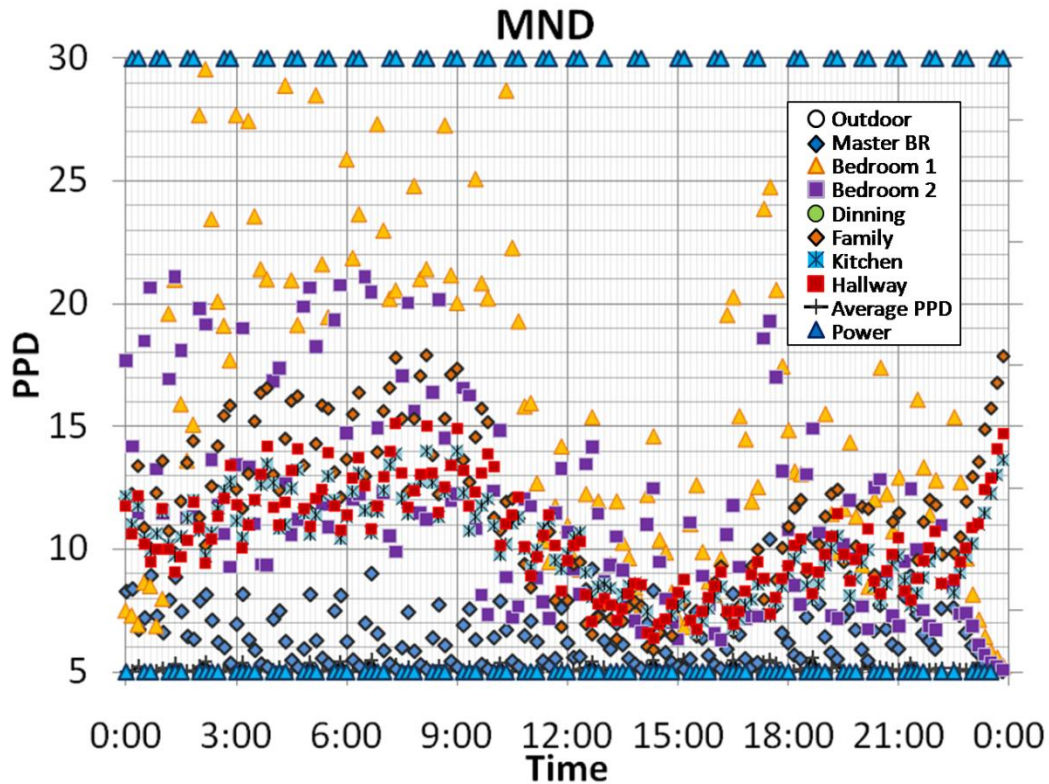
Figure 5.6 MND Comfort Plot

The MND strategy kept the house at the most optimal average conditions throughout the entire day by using a 10-20 minute ON and 30-40 minutes OFF duty cycle trend. At several periods in the day, bedroom 1 experienced warm conditions that resulted in PPD values over 20. The family room was the most uncomfortable room because of cool conditions, but still did not match the PPD value of the hot bedroom 1. Another observation of the MND strategy is how the comfort improved for every room starting after 9:00. This is because the strategy made a decision to improve the sum of every room's comfort, not the average like the PPD Average strategy. Averaging the comfort values has the warmer than optimal upstairs rooms balance with the cooler than optimal down stairs rooms. The average comfort in these strategies might be the same, but the MND will have a more comfortable house.

5.2.4 MXR

The Maximizing the Number of Rooms below a Threshold PPD (MXR) strategy controlled the heating by comparing the number of rooms below a threshold PPD value of 8, 10, or 12 PPD at the current and predicted future conditions. Figure 5.7 is the temperature plot of a typical day controlled by the MXR strategy with a threshold of 10 PPD. Figure 5.8 is a plot of the comfort for the typical MXR day.
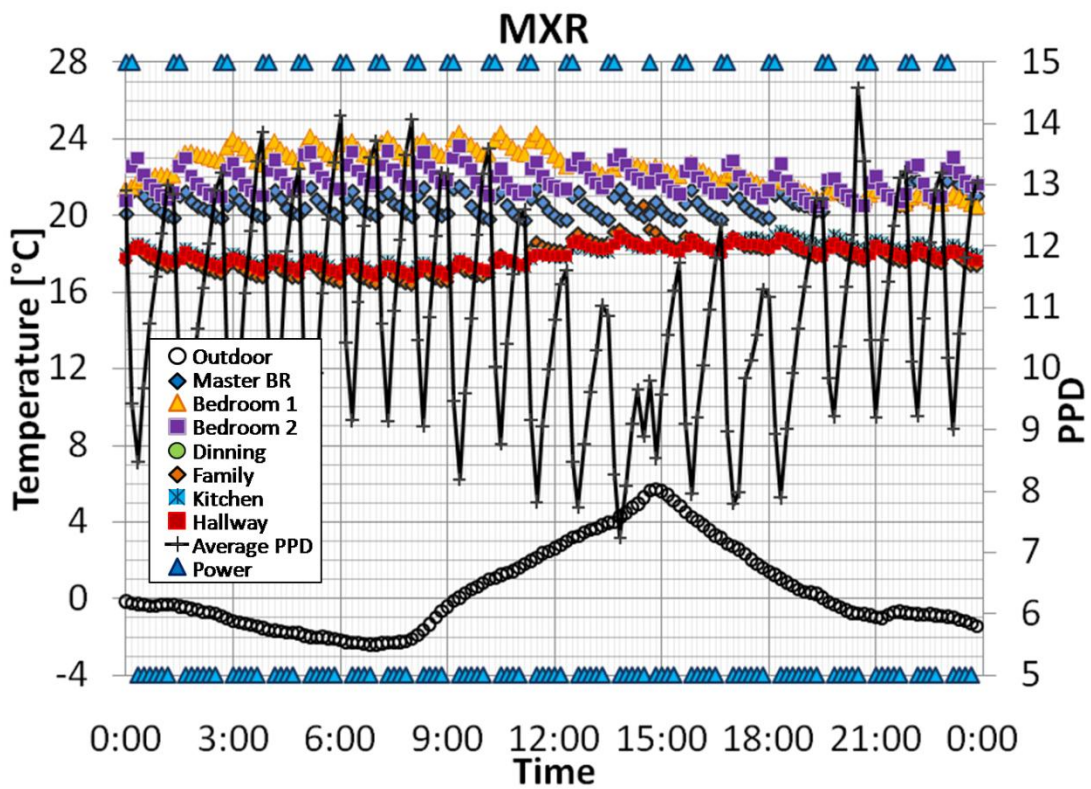
Figure 5.7 MXR Temperature Plot
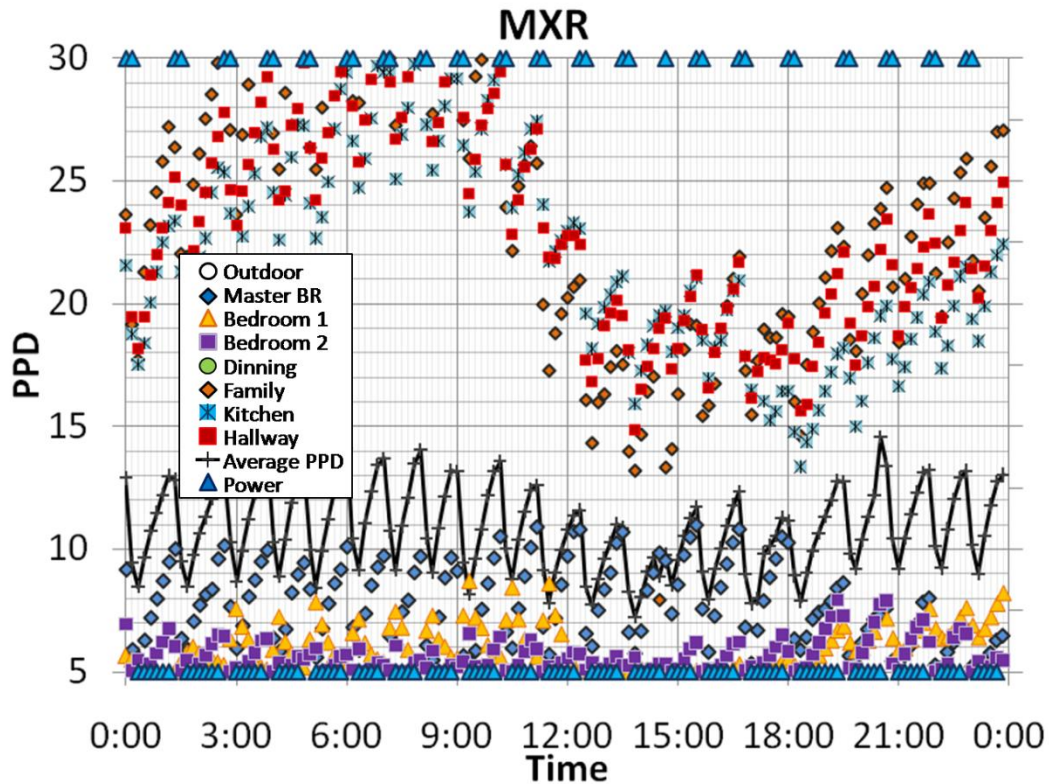
Figure 5.8 MXR Comfort Plot

When the threshold PPD value was 10 PPD the master bedroom was responsible for triggering all of the system position changes for the majority of the day. The other bedrooms stayed comfortable enough to avoid crossing the 10 PPD threshold and the downstairs rooms were too cold to have the predicted 0.3°C temperature increase push them over the threshold. In the evening the master bedroom became set below 10 PPD and the family room or kitchen were close enough to have the predicted heating value cross over the threshold, but the heating never lasted long enough to bring one downstairs room down to a PPD below 10. The same comfort improvement seen as the day progressed in the MND strategy was also observed with the MXR; both the upstairs and downstairs rooms increased in comfort, instead of only maintaining an average comfort level.

5.2.5 Thermal Comfort

The set points and thresholds of the strategies were varied to observe the performance at different levels of comfort. Figure 5.9 shows the average PMV of every strategy over the course of the winter heating experiment. The numbers accompanying the strategy names correspond to the temperature or PPD set points and thresholds. Averaging the PMV in a house was able to represent the ratio of discomfort due to being warm to discomfort due to being cool. Figure 5.10 shows the average PPD of the control strategies from the winter experiment.
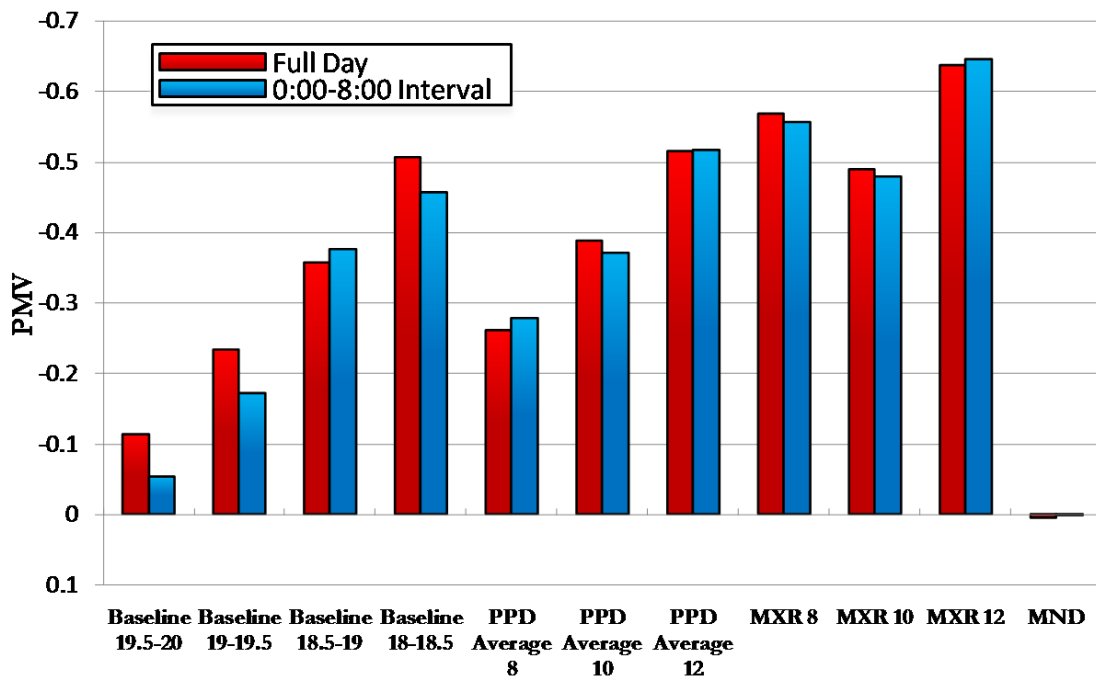
Figure 5.9 Average PMV
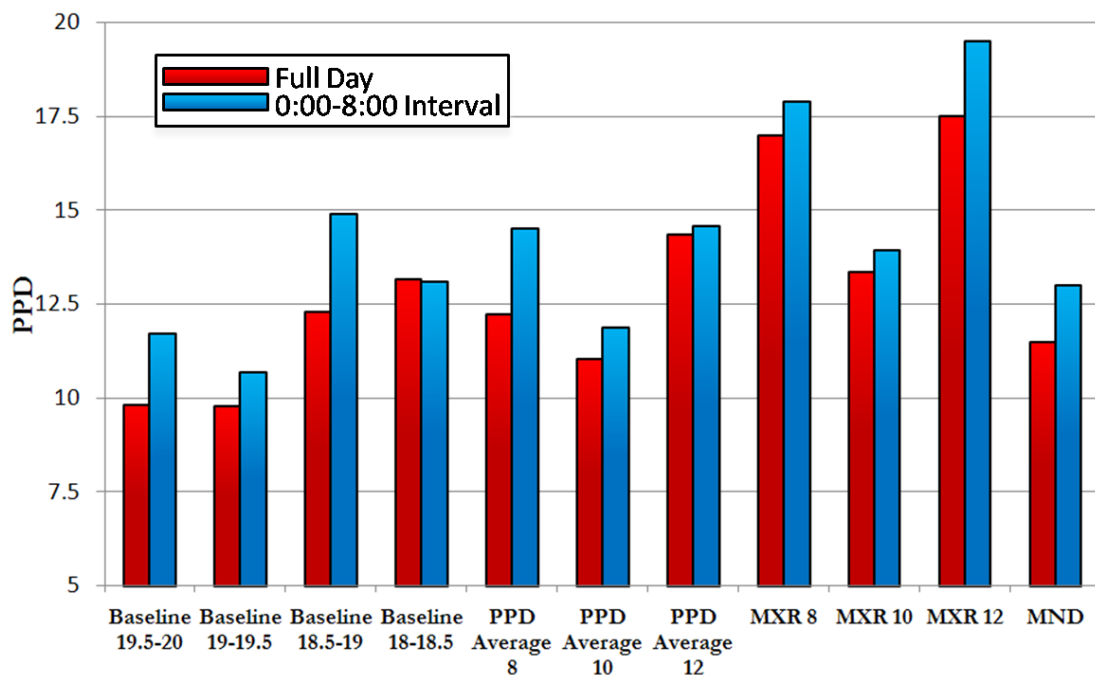
Figure 5.10 Average PPD

PMV and PPD are both metrics used to quantify thermal comfort, but the two

plots above show different trends for each strategy's average PMV or PPD. This is

because PMV has a direction built into its values (negative PMV equates to cooler

than optimal conditions and positive PMV equates to warmer than optimal

conditions). The winter heating strategies crossed over the optimal conditions

boundary many times; whereas, the summer cooling strategies only had a few times

where that occurrence was observed. The average PMV value describes the comfort

level of the average of the conditions in the home. The average PDD gives insight

into the average discomfort in the house.

The MND strategy was shown to have the most comfortable average PMV but

it did not have the lowest average PPD. The MXR 12 strategy was the least

comfortable with respect to both metrics because of the high threshold value. The

relationship in the same strategy PMV values with different set points appears to be

linear for the Baseline and PPD Average strategies. MXR did not show this relationship because of how the threshold and start conditions dictated how many, and what rooms, became the main drivers of the control. Figure 5.11 plots the average PPD of the 5 lowest average PPD strategies throughout the course of an entire day. Figure 5.12 plots the six highest average PPD strategies.
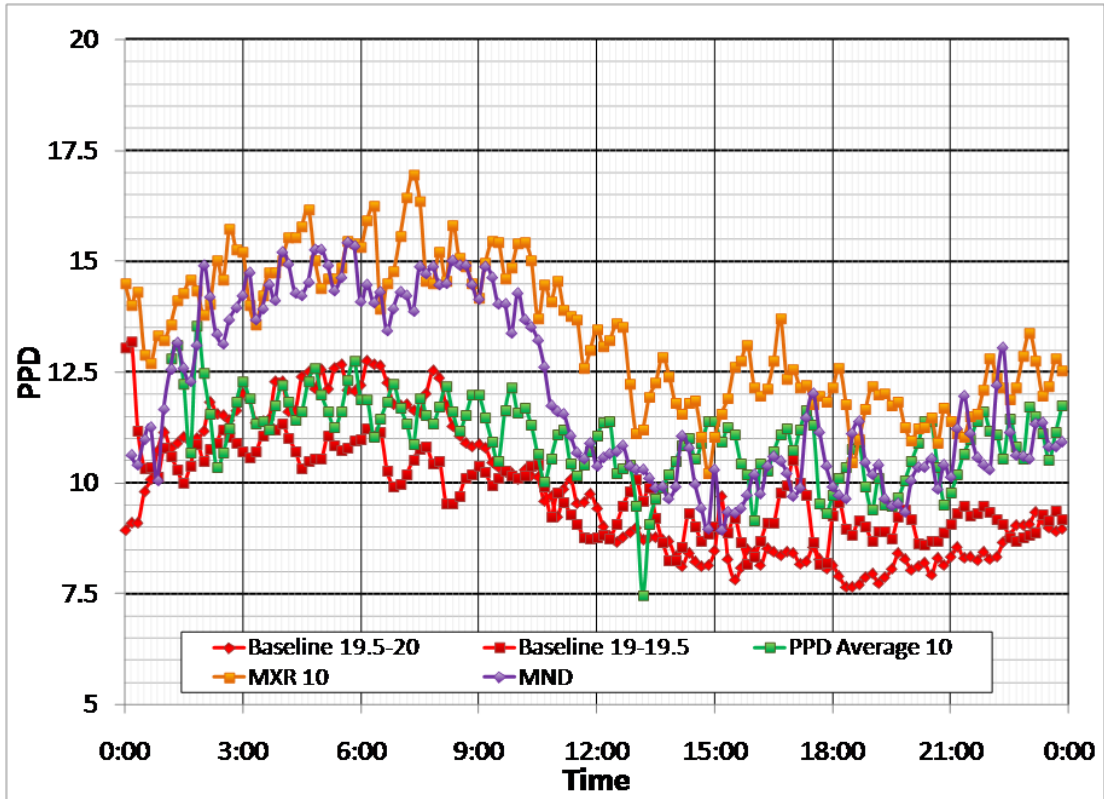
Figure 5.11 Average PPD over the Entire Day (low PPD)

118
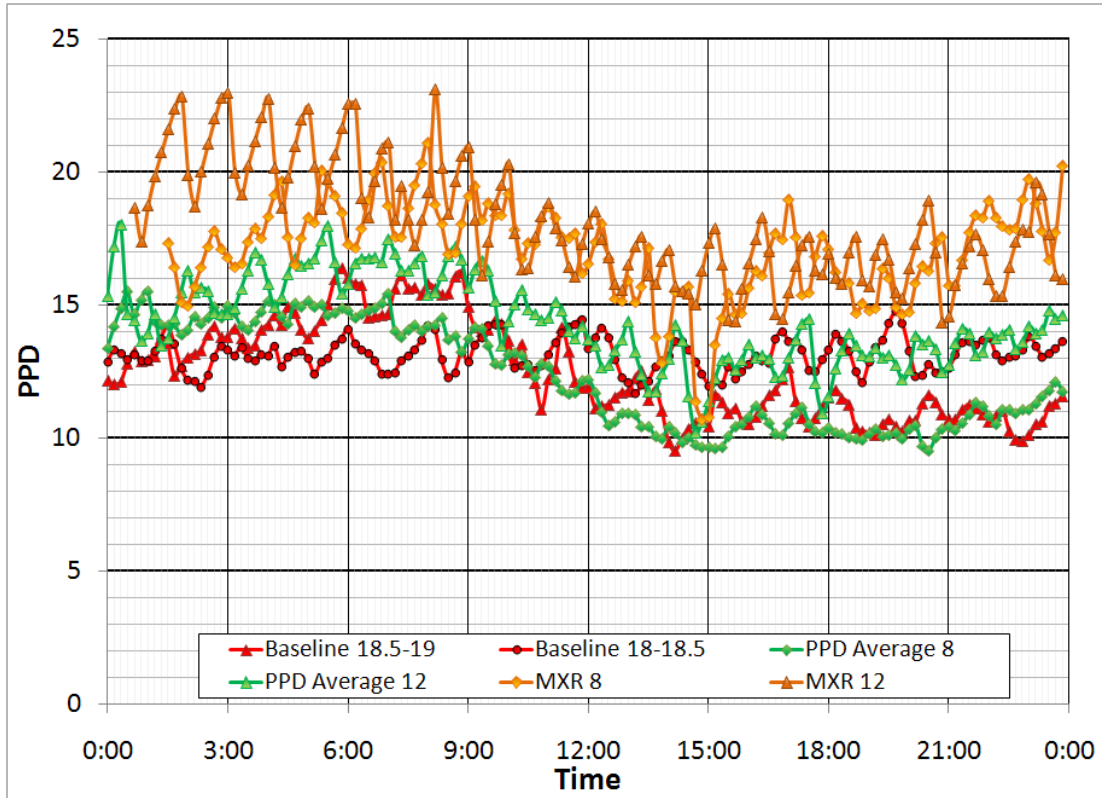
Figure 5.12 Average PPD over the Entire Day (high PPD)

Observing the average PPD over the course of the day is able to give more information than the average over the interval. Every strategy experiences higher discomfort in the early morning than the rest of the day. Figure 5.10 also shows the same result because the PPD values for the 0:00-8:00 interval are higher than the full day interval. The lowest PPD values were achieved around 15:00 for the majority of the strategies; several strategies kept the PPD down near that level for the rest of the day, while others made the PPD increase again. The MND and MXR strategies showed the greatest improvement in comfort starting at around 10:00. It is interesting to note that the PPD average with a threshold of 8 had higher PPD values than the same strategy with a threshold of 10 PPD. The average PMV of the PPD Average 8 strategy was lower than the 10 PPD strategy, so the explanation would be that more

119

of the rooms had discomfort from experiencing warmer than optimal conditions in the 8 PPD case than the 10 PPD case.

5.3 Energy Consumption

5.3.1 Daily Distribution and Start Time

There were 45 days tested that yielded worthwhile data in the winter heating experiment. Figure 5.13 shows the fraction of days the system was ON to the total number of days at a particular time step. The average outdoor temperature calculated over the entire test period is also shown to give a reference to when the highest and lowest temperature are usually observed in the day.
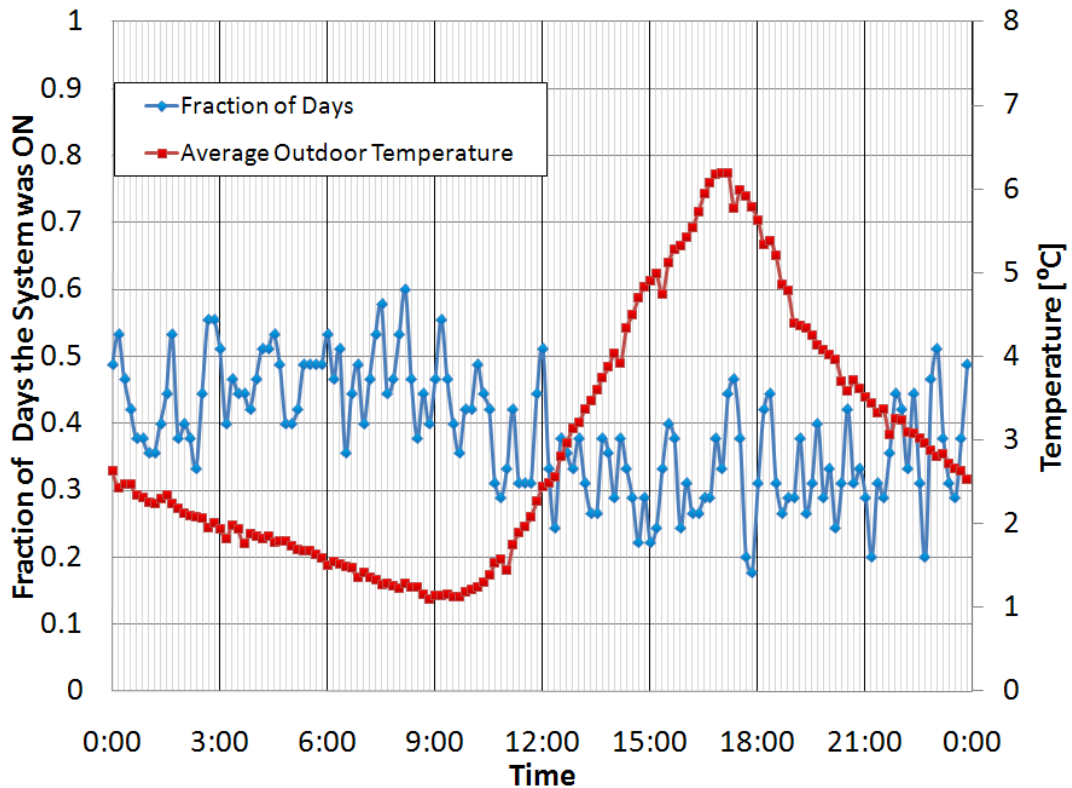

Figure 5.13 Fraction of Days the System was ON and Seasonal Average Outdoor Temperature

The fraction plot shows that the highest level of system ON time occurred during the 0:00-8:00 interval. This was the time when the outdoor temperature was the lowest and the sun was removed from the radiation transfer with the house. The heating system had to provide higher levels of heating to maintain the same level of comfort. A side effect observed is that the upstairs bed rooms are already warmer than the optimal conditions. Heating more to meet the higher demand actually raised the houses overall discomfort because the nonlinearity of the PPD function made a little more heat to an already warm room increase its discomfort significantly. There was not a significant increase in ON time seen right after the system switched control strategies at midnight. This is because the strategies all controlled around similar comfort levels and they did a better job than the summer control strategies at maintaining that comfort until the end of the day.

5.3.2 Duty Cycles

The normalized duty cycle metric was used to quantify the energy consumption of the control strategies during the heating experiment. The duty cycle was normalized by the HDD or HDI to account for a variety of outdoor conditions. Figure 5.14 shows the average normalized duty cycle for each strategy evaluated over each of the intervals. The error bars represent the 95 percent confidence interval of the data from each strategy.
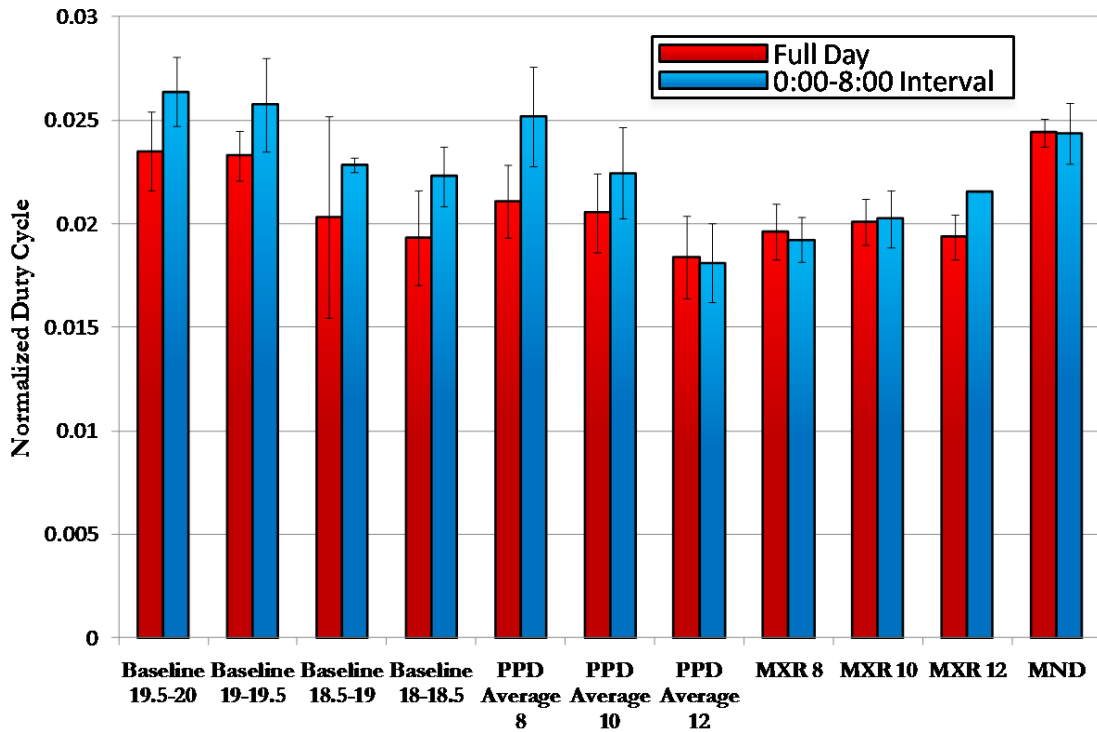
Figure 5.14 Average Normalized Duty Cycle

The normalized duty cycle plot gives the best representation of the individual strategies' energy consumption. The full day interval showed how the strategy behaved over the entire course of the day. The 0:00-8:00 interval gave a better representation of the control strategy because the solar load was different every day, and this would not always be reflected in the outdoor temperature and HDD. The 95 percent confidence interval was much smaller with respect to the normalized duty cycle value than what was observed with the control strategies in the summer cooling experiment. Several differences contributed to the tighter confidence, but the large temperature difference between the indoor and outdoor conditions was the underlying factor. This caused the system to be constantly heating throughout the entire day, and gave 24 hours of similar duty cycle periods. It also caused the transient response of

the house to be much faster and any difference in the initial conditions would be compensated for quickly, reducing their impact on the control.

The average NDC of the strategies with multiple set points and thresholds also changed linearly with the set points and thresholds. The highest temperature Baseline and lowest PPD PPD Average strategy consumed the highest amount of energy. The same trend was observed for the lowest temperature and highest PPD having the lowest average NDC. MXR did not have a set trend with the threshold values and this can explain why the comfort also did not follow one. MND consumed a lot of energy but it also had one of the lowest levels of discomfort.

5.3.3 Overall Strategy Performance Evaluation

The comfort of each strategy was expressed using the average PMV and PPD, and the energy consumption was quantified with the average normalized duty cycle. The set points and thresholds were varied to investigate the relationship between the comfort and the energy consumption. Figure 5.15 plots the normalized duty cycle verses the average PPD for every day over the 0:00-8:00 nighttime interval. Each individual control strategy is represented by a marker color, each day is marked with a symbol, and a trend line is found to fit the data for each strategy. Figure 5.16 divides the average normalized duty cycle from Figure 5.14 by the average PPD from Figure 5.10. This ratio embodies how much comfort is experienced with a strategy (at the particular set point or threshold) for a given amount of energy input. The higher the bar, the more efficient the strategy is at turning energy into comfort.
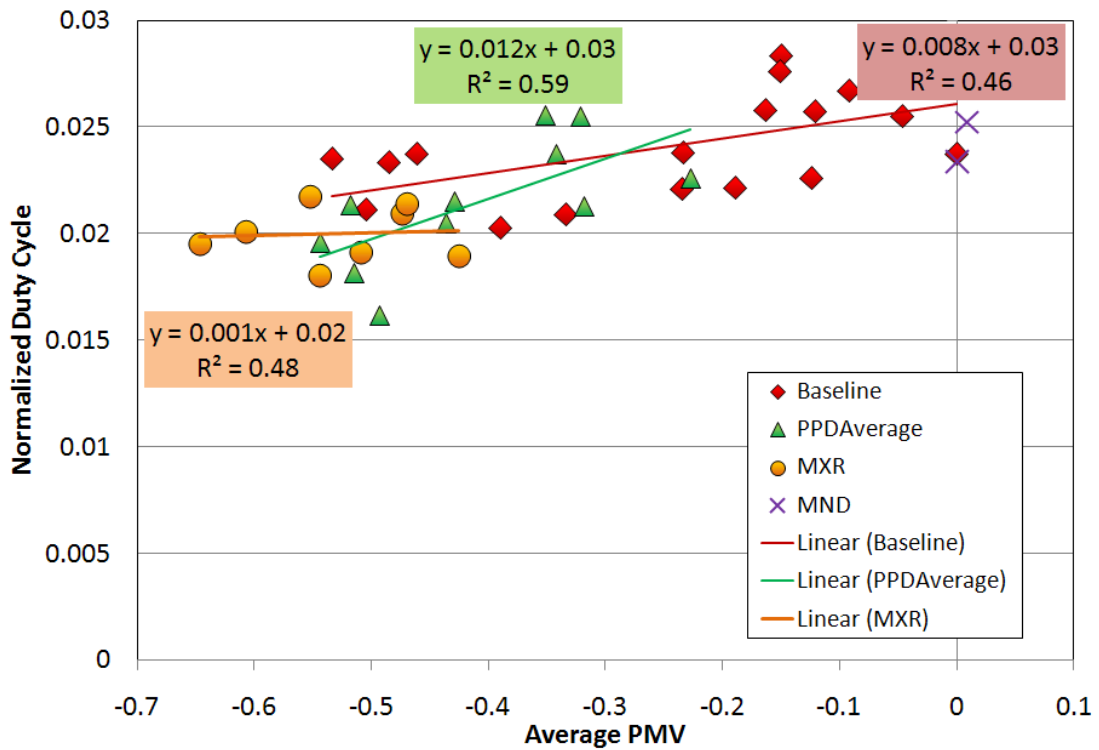
Figure 5.15 Normalized Duty Cycle verses the Average PMV (0:00-8:00 interval)
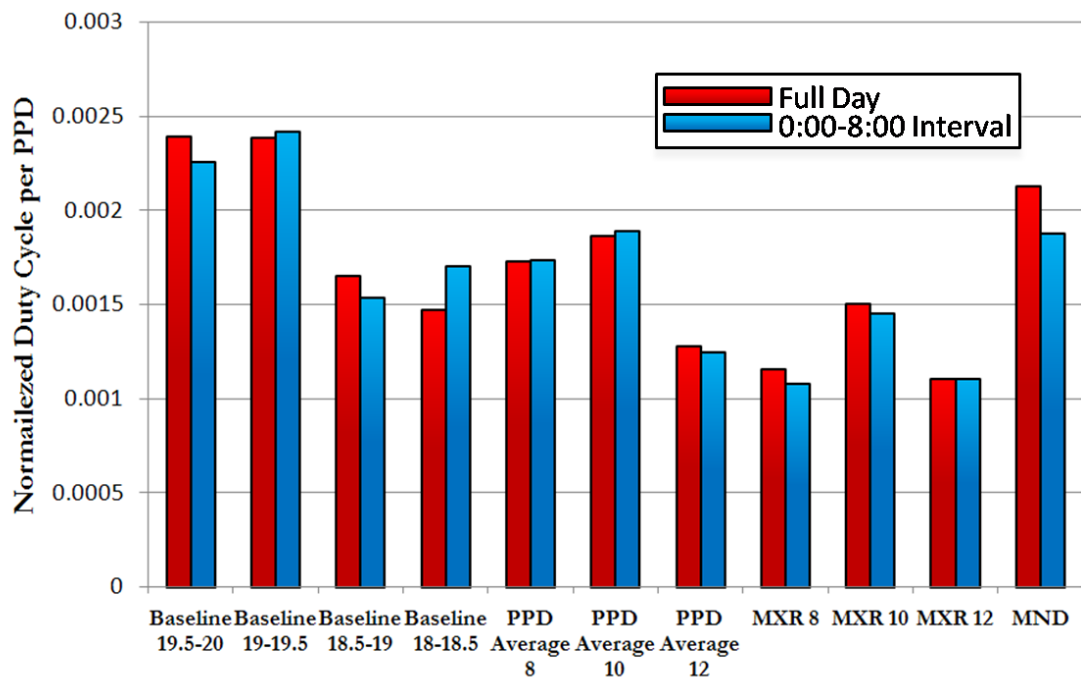

Figure 5.16 Normalized Duty Cycle per Average PPD

Plotting the normalized duty cycles verses the Average PMV for every day shows that the particular strategies perform differently at different comfort levels. The Baseline and PPD Average data sets showed a correlation between the NDC and the PMV. If the trend lines are extrapolated out to encompass the entire PMV range shown, the Baseline is superior at higher PMV values (more comfortable) because it would consume lower amounts of energy to deliver average PMV values from 0 to -0.3. At a PMV of -0.3 the two strategies would consume the same amounts of energy to deliver that average PMV. For lower PMV desired conditions, the PPD Average strategy would be superior. The MND strategy did not have enough data to make a meaningful correlation, and there was too much scatter in the MXR strategy data for the correlation to be significant.

The ratio of the PPD to the NDC was able to compare the performance of each of the strategies and the set points and thresholds used. The two highest temperature set point Baseline strategies (19.5-20 and 19-19.5) controlled with the least amount of discomfort per the energy they consumed. The MND and PPD Average 10 strategies followed behind in this category, and the MXR 8 and 12 strategies had the poorest efficiency.

Plotting the duty cycle verses the outdoor temperature is able to show the relationship of energy to outdoor temperature. Figure 5.17 plots the daily duty cycles and average outdoor temperatures for the 0:00-8:00 interval. Figure 5.18 shows how normalizing the duty cycle with a base of 15.5°C changes with the average outdoor temperatures.
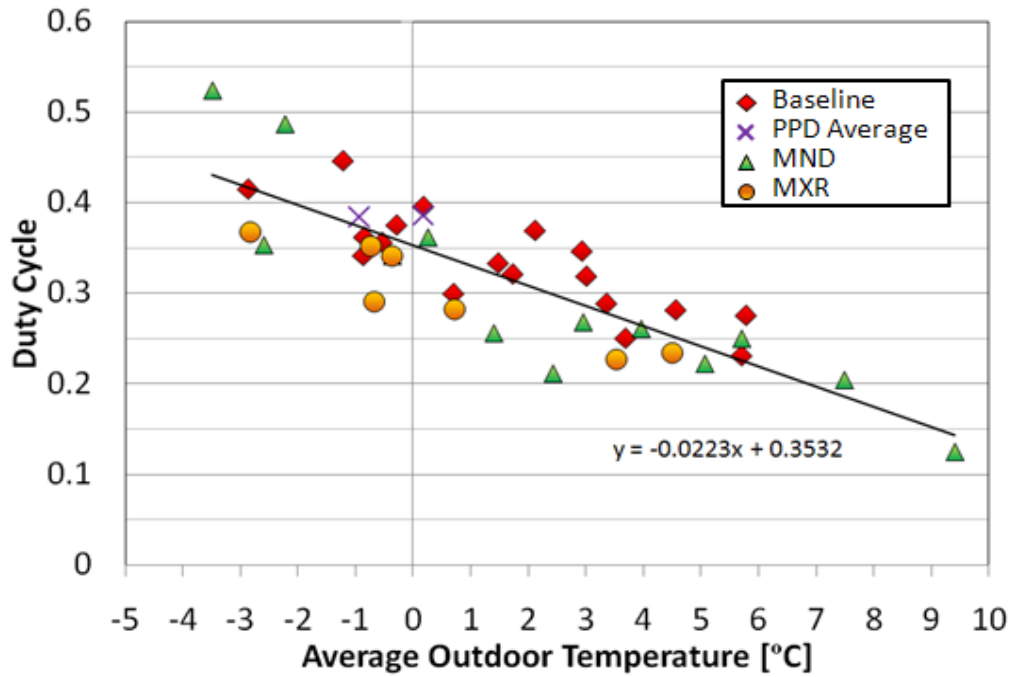
**Figure 5.17 Duty Cycle Verses Average Outdoor Temperature (0:00-8:00 interval)**
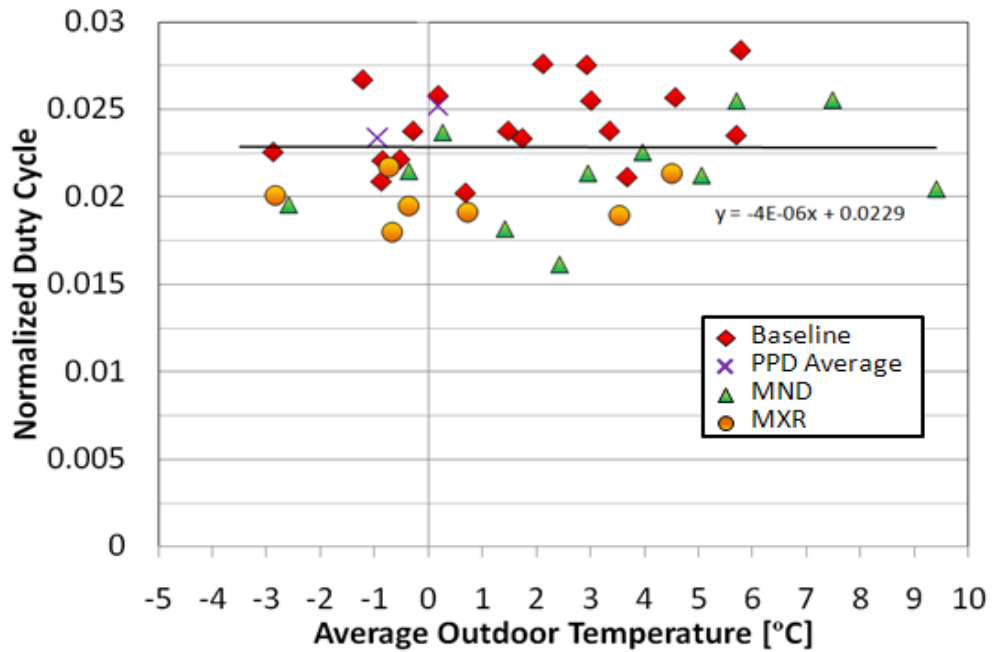
Figure 5.18 Normalized Duty Cycle verses Average Outdoor Temperature (0:00-8:00 interval)

126

The negative slope in the trend line of the duty cycle verses the average outdoor temperature plot is expected because lower outdoor temperatures translate to higher loads and the heating system will have to be ON longer to keep the house comfortable. The very small slope in the trend line in Figure 5.18 shows how 15.5 °C was a good choice to normalize the duty with. The various set points contribute to the scatter in the data points in the Y-direction of the plot, but the overall trend still shows how normalizing is able to allow days with different outdoor conditions to be compared evenly.

5.4 Discussion

The control strategies were shown to control the heating system in different ways. The Temperature Baseline strategy controlled the furnace with large temperature swings. The average comfort did not fluctuate as much when the right set points were used (19.5-20°C or 19-19.5°C) because the large temperature swings would move the majority of the rooms across the bottom of the PMV-PPD curve. This region is relatively flat compared to the rest of the curve, and increasing or decreasing the temperature here would not bring about high increases in the PPD. The baseline strategy did not fare as well when the set point was too low (18.5-19°C or 18-18.5°C) because changing the conditions would have more of an impact on the PPD.

The PPD Average strategy controlled the house by keeping an equivalent amount of warmer than the threshold conditions as cooler than the threshold conditions. This could have been done with very warm conditions upstairs and very cool conditions downstairs as long as the PMV scores balanced out to around the

score needed to achieve the threshold PPD. This could have also been done with more uniform and optimal conditions; however, the strategy's goal was not to minimize discomfort, it was to maintain an average level of comfort. Neither the lowest nor the highest threshold PPD yielded the best performance. The threshold of 8 PPD made several of the upstairs room too warm and more discomfit was observed than the threshold of 10 PPD. Using 12 PPD as a threshold kept the downstairs room too cool, and more discomfort was seen as well.

The MND strategy did not perform as well as it did in the summer cooling experiment with regards to minimizing the total discomfort because of the large temperature difference between the upstairs and downstairs rooms. In order to get the downstairs rooms close to the optimal conditions the strategy had to make the upstairs rooms more uncomfortable due to increasing the temperature in already warm conditions. This made the upstairs warmer than the house needed in the early morning. After the bedroom doors were opened and the energy demand in the house declined around 10:00, the MND strategy was able to improve the comfort of both the upstairs and downstairs rooms. The strategy was still able to deliver a high amount of comfort for the amount of energy input into the system.

A trend in how the MXR strategy controlled the house was not defined as the other strategies. The highest threshold (12 PPD) strategy consumed about the same amount of energy as the lowest threshold (8 PPD) strategy, and they had similar average comfort values. The 10 PPD threshold strategy was able to deliver the best comfort, but it did so requiring the most energy. Not having a direct relation between

the comfort level, threshold set point, and energy consumption made the MXR trend line in Figure 5.15 meaningless.

The system improved in the morning (around 8:00-10:00) because the outdoor temperatures and radiation conditions improved, and because the occupants open the upstairs bedroom doors. The lower density of the warmer air kept the majority of it upstairs; however, circulation occurred and more uniform temperatures were observed in the house. The multi-sensor strategies responded to the changes in the house better than the hallway controlled Baseline, and were able to achieve higher levels of comfort improvement between 9:00 and 15:00.

The single-sensor Baseline strategy with high temperature set points was the best winter heating strategy because the multi-sensor strategies did not have the proper weighting in the temperature increase used to predict the future conditions if the system is turned ON. The temperature increase of 0.3°C was calculated using the average increase in the home. At the time of the calibration, all 7 indoor motes were functioning properly. The temperature increases observed were averaged using 4 downstairs and 3 upstairs rooms. The upstairs rooms increase by more than 0.3°C and the downstairs rooms increase by less than 0.3°C. The multi sensor strategies would have had better predicting information if a larger temperature increase was used to reflect the distribution of sensors after the dining room mote was lost, or if the actual observed temperature increase in each room was used to calculate the predicted future value. This would have reduced over -heating the upstairs rooms to improve the downstairs marginally, and brought in the more uniform comfort observed in the summer cooling experiment.

5.5 Conclusion

The multi-sensors control strategies that were tested in the summer cooling experiment with an air conditioning system were tested in the winter with a natural gas furnace. Energy savings were also not observed in the heating experiment with these strategies when they were compared to a single sensor strategy. The set points and thresholds used by the strategies were varied to develop a better understanding between the set point and threshold, average comfort value, and energy consumption. Most of the control strategies operated by keeping rooms above and below the optimal conditions. This was rarely seen in the summer cooling experiment and resulted in differences between the average PMV and PPD calculated in the house for many of the strategies. The Baseline strategy with high set points was identified as exhibiting the best performance because it delivered the most amount of comfort per input energy. The PPD Average strategy was better suited to deliver lower levels of comfort because the amount of energy spent to over-heat already warm upstairs rooms would be less. The MXR and MND strategies also experienced a problem with heating the upstairs rooms beyond the optimal comfort point, but they were able to improve both the upstairs and downstairs comfort after the bedroom doors were opened better than the other strategies. The comfort prediction method could have been improved to yield better multi-sensor strategy results, but energy savings of any significance does not seem to be found with these strategies in the winter when the house is well insulated, the thermostat is located in a sufficient location, and the furnace is sized properly to meet the demand.

Chapter 6: Conclusions

6.1 Intellectual Contributions

This thesis is a collection of two seasonal studies of residential heating and cooling control strategies developed using a distributed wireless network. Reviewing the current literature suggested that the most promising technology that needed to be developed and tested were control strategies that utilized a wireless sensor network. If the technology is validated for a wide variety of climates, homes and heating and cooling systems, mass deployment across the country could bring about significant energy savings in the residential sector.

Initial work in the field was performed by the Center for the Built Environment at UC Beckley. Their experiment with a single-story house in Pleasanton, CA was performed in the late summer to evaluate the performance of wireless sensor network-based control strategies with air conditioning in a dry, hot climate. Energy savings on the order of 80 percent were observed when using these control strategies. The experiments performed in this study expand the knowledge of the field by investigating the performance of the control strategies in a variety of new conditions:

- Multi-floor home

- Humid subtropical and hot summer continental climates

- Winter heating

A multi-floor home can result in significantly larger room-to-room temperature and comfort differences if rooms from different floors are used, and the large comfort difference can result in the control to be primarily decided by a minority of the rooms.

The upstairs rooms can also suffer from significant overheating during the winter due to stratification effects. The mid-Atlantic climate introduced an opportunity to evaluate the cooling system in a season with high relative humidity.

A single senor strategy was developed to test the differences between actuating with a threshold logic based on temperature and one based on thermal comfort (combination of temperature and relative humidity). The results indicated that the comfort controlled strategy was shown with statistical confidence to be 36 percent less energy efficient on the 14:00-20:00 interval than the temperature controller as a result of using extra energy to dehumidify the air and reduce discomfort further. The MXR strategy was shown to statistically consume 13 percent more energy than the Temperature Baseline because it also reduced the average discomfort.

The cooling experiment failed to produce any multi-sensor strategies that could save a statistically significant amount of energy during the period of highest demand (16:00-19:00 interval). Overall thermal comfort during the two intervals was improved in the MND (by 3 PPD) and MXR (by 1 PPD) strategies at a nearly minimal additional energy cost, but a statistically significant energy savings was also not seen in the more uncomfortable PPD Average strategy. Varying the comfort set points of the strategies in the winter was able to show that the energy consumption depended more on the set point than the particular strategy.

This study was not able to produce the same energy savings seen in previous experiments. The same strategies were employed with very similar set points, but it appears the strategy used to benchmark in this experiment did not have the potential to improve as much as the previous study. All the strategies in this study operated

with 10 minute decision intervals to act as a deadband to prevent a high frequency of cycling the compressor ON and OFF. The CBE study used one minute intervals, and if the AveALL strategy shown in Figure 2.9 is supposed to exhibit the same patterns of the benchmark Standard strategy, it appears the system cycled up to five or six full times in an hour. This can be seen by closely looking at the fluctuations in the temperature of one of the rooms and how there were approximately five or six evenly spaced peaks. Five or six even cycles in an hour would translate to an average of five minutes of ON time. One would predict that this frequency was too high and that a large portion of the cycle's energy went to starting the compressor. The energy saving strategies appeared to have a lower cycle frequency, so this would result in a reduced amount of electricity use per length of a cycle. Other concerns addressed in Section 2.3.2 could have also contributed to the differences between the experiment performed by the CBE and this one. More data points were collected and tests were performed to determine statistical significance in the differences between the strategies in this experiment. The initial conditions and differences in set points were also accounted for to help make more informed conclusions.

6.2 Anticipated Benefits

This study can be used as a blueprint to develop, test, and analyze wireless senor network-based residential HVAC control strategies. Normalizing the duty cycle offered a new way to measure energy consumption for a variety of systems and outdoor conditions, and incorporating a statistical analysis was able to show the level of confidence the data should be taken at. The correlation between the energy consumption and comfort of the heating control strategies can also be used to

determine what strategy and set point would consume the least amount of energy for a particular level of comfort.

6.3 Recommendations for Future Work

Distributed sensing using a wireless sensor network is the first step on a path to significant residential energy savings. Coupling the sensing with a form of distributed control will be able to improve the demand response of a central HVAC system. This can be done with register or duct damper automation and developing control strategies that are able to maximize the comfort of individual rooms and minimize the energy required. Savings can be seen not only by avoiding over conditioning but also through the implementation of an occupancy pattern to determine ideal periods to set back the control levels. The wireless sensor network and control system from this study would make a perfect match for the future of this technology.

The current model can be improved with several adjustments to see if the control strategies still have the potential to improve the energy efficiency in this climate, style house, and for both winter heating and summer cooling. A suggested improvement would be to carefully calibrate the temperature difference used by the predictive strategies to determine if the system should turn ON. This could range from using a static value previously measured from that particular room to developing a model that would be able to correlate how much the conditions will improve with variables such as the previous ON time, current room conditions, and time of the day. The decision interval can be tuned more to work the best with the thermal lag in the sensors, battery energy capacity, and sustainable cycling of the compressor.

Improvements can also be made by having the thermal comfort model adapt to the time of the season and outdoor conditions. This will help if the strategies are ever evaluated in a shoulder season that sees both warm and cool conditions.

The duty cycle was able to show energy consumption by comparing the ON and OFF time of the strategies. Normalizing it was also able to compensate for any efficiency degradations introduced by higher outdoor temperatures in the summer. The one aspect of power consumption that it missed is in the spike seen in starting up the components such as the compressor and fan. A reliable power and gas meter would be the best way to fully quantify the energy consumption of the strategies, but if run properly there should not be an expected difference between it and using the duty cycle.

Several additional ideas can be investigated further using the data collected with this experiment. Performing a detailed room-to-room analysis would improve the understanding of how the strategies control and determine if several strategies are more desirable because they make the conditions more uniform. A building energy model simulation would also help determine if any important aspects of the house or cooling strategy were neglected in the analysis, so they can be corrected.

Chapter 7: Bibliography

Akyildiz, I.F. Su,W. Sankarasubramaniam Y. and Cayirci, E. (2002). Wireless sensor networks: a survey, *Computer Networks* **38**, pp. 393–422.

Akyildiz,I.F. Wang, X. and Wang, W. (2005). Wireless mesh networks: a survey, *Computer Networks Journal* **47**,pp. 445–487.

Annual Energy Review (2008). U.S. Energy Information Administration, U.S. Department of Energy, Washington, DC.

ASHRAE (2004). ANSI/ASHRAE Standard 55-2004, Thermal Environmental Conditions for Human Occupancy. Atlanta GA.: American Society of Heating, Refrigerating, and Air conditioning Engineers, Inc.

ASHRAE (2007). *ASHRAE Handbook: Applications.* Atlanta, GA.: American Society of Heating, Refrigerating, and Air conditioning Engineers, Inc.

ASHRAE (2009). *ASHRAE Handbook: Fundamentals.* Atlanta, GA.: American Society of Heating, Refrigerating, and Air conditioning Engineers, Inc.

Brown, C A. (2007). Multizone register controlled residential heating: Optimized forenergy use and comfort. M. S. Thesis, U. C. Berkeley.

Butcher, T., Y. Celebi, and G. Wei. (2006). The performance of integrated hydronic heating systems. In Proceedings of the 5th Aachener Ölwärme-Kolloquium, Aachen Germany, Sept. 13-14, 2006.

Çengel, Yunus A., and Michael A. Boles. (2008). "Chapter 14." *Thermodynamics: an Engineering Approach*. Boston: McGraw-Hill Higher Education.

Chen, Chi-Tsong. (1999). "Chapter 1." *Linear System Theory and Design*. New York: Oxford UP.

Crossbow MoteWorks Software Platform. <https://www.xbow.com/Products/productdetails.aspx?sid=154> 14 Apr. 2010.

Crossbow Wireless Modules. <http://www.xbow.com/Products/productdetails.aspx?sid=156> 14 Apr. 2010.

Cygwin. Version 1.5.25-15. Red Hat Inc., 2008 < http://www.cygwin.com > 14 Apr. 2010.

de_Dear, R. J., & Brager, G. S. (1998). Developing an adaptive model of thermal comfort and preference. *ASHRAE Transactions* **104**(1), pp. 1-18.

Dounis, A I, and Caraiscos, C. (2009). Advanced control systems engineering for energy and comfort management in a building environment—A review. *Renewable and Sustainable Energy Reviews* **13**, pp. 1246–1261.

EERE (2009). Building Energy Data Book 2009. Energy Efficiency and Renewable Energy, U.S. Department of   Energy, Washington, DC.

Energy Star (2010). http://www.energystar.gov/index.cfm?c=thermostats.pr_thermostats> 14 Apr. 2010.

Environmental Sciences Services Administration (1970), Heating and Cooling Degree Days. <http://www.lib.utexas.edu/maps/national_atlas_1970/ca000082.jpg> 14 Apr. 2010.

Fanger, P. O. (1972). Thermal comfort: analysis and applications in environmental engineering. New York, McGraw-Hill.

Fong, K.F, Hanby, V.I., and Chow, T.T.(2006). HVAC system optimization for energy management by evolutionary programming, *Energy and Buildings* **38**, pp. 220–231.

Gao, G. and Whitehouse, K. (2009). The Self-Programming Thermostat: Optimizing Setback Schedules based on Home Occupancy Patterns. In *First ACM Workshop On Embedded Sensing Systems For Energy-Efficiency In Buildings.*

Haines, R W., and Hittle, D. C. (2006). *Control Systems for Heating, Ventilating, and Air Conditioning*. New York: Springer.

Healy, W. M. (2005). Lessons Learned in Wireless Monitoring. *ASHRAE Journal.* **47**(10), pp. 54-58.

Humphreys, M. A., & Nicol, J. F. (2002). The validity of ISO-PMV for predicting comfort votes in every-day thermal environments. *Energy and Buildings* **34**(6), pp.667-684.

Hwang, Y, Radermacher, R, and Kopko, W. (2001). An experimental evaluation of a residential-sized evaporatively cooled condenser, *International Journal of Refrigeration* **24**, pp. 238–249.

Ingersoll, J, and Huang, J. (1985). Heating Energy Use Management in Residential Buildings by Temperature Control. *Energy and Buildings* **8**(1), pp. 27-35.

ISO (1994). International Standard 7730 Moderate thermal environments-determination of the PMV and PPD indices and specification of the conditions for thermal comfort. Geneva, International Standards Organization.

Karjalainen, S. (2007). Gender differences in thermal comfort and use of thermostats in everyday thermal environment, *Building and Environment* **42**, pp. 1594–1603.

Kolokotsa, D. (2003). Comparison of the performance of fuzzy controllers for the management of the indoor environment. *Building and Environment* **38**, pp. 1439-1450.

Kolokotsa, D. Saridakis,G. Pouliezos, A. Stavrakakis, G. (2006) Design and installation of an advanced EIB fuzzy indoor comfort controller using Matlab. *Energy and Buildings* **38**(9), pp. 1084-1092.

Lekov, Alex, Franco, Victor, & Lutz, James. (2006). Residential Two-Stage Gas Furnaces - Do They Save Energy?. Lawrence Berkeley National Laboratory: Lawrence Berkeley National Laboratory. LBNL Paper LBNL-59865.

Lin, C, Federspiel, C. C, and Auslander, D. M. (2002). Multi-Sensor Single-Actuator Control of HVAC Systems. International Conference for Enhanced Building Operations, Texas.

LogMeIn - Remote Access and Desktop Control Software for Your Computer. Web. <https://secure.logmein.com/US/home.aspx>.14 Apr. 2010.

Lund, J., B. Sanner, L. Ryback, R. Curtis, and G. Hellstrom. (2004). Geothermal (Ground-Source) Heat Pumps – A World Overview. *Geo-Heat Center Quarterly Bulletin* **25**(3), pp. 1-10.

Lutz, J., Franco, V., Lekov, A., Wong-Parodi, G. (2006). BPM Motors in Residential Gas Furnaces: What are the Savings? August. ACEEE Conference

MATLAB (2008) Version 7.6.0.320. Natick, Massachusetts: The MathWorks Inc.

Meyers, R.J. Williams, E. D. Matthews, H. S. (2009). Scoping the potential of monitoring and control technologies to reduce energy use in homes. *Energy and Buildings* **42**(5), pp. 563-569.

Nassif, N, Kajl, S and Sabourin, R. (2004). Evolutionary Algorithms for Multi-Objective Optimization in HVAC System Control Strategy. *IEEE NAFIPS* **1**, pp. 51-56.

Nicol, J. F. & Humphreys, M. A. (1972). Thermal comfort as part of a self-regulating system. In Proceedings of CIB W45 Symposium on Thermal Comfort and Moderate Heat Stress. pp.263-280.

Omer A M. (2008). Ground-source heat pumps systems and applications.

Renewable and Sustainable Energy Reviews **12**(2), pp. 344-371.

Oppenheim, P. (2002). Energy Saving Potential of a Zoned Forced Air Heating System. ASHRAE Winter Meeting, Anaheim, CA, USA, pp. 1247-1257.

Ota, N. (2007). The application of wireless sensor networks to residential energy efficiency and demand response. M. S. Thesis, U. C. Berkeley.

Ota, N, Arens, E, and Wright, P. (2008). Energy efficient residential thermal control with wireless sensor networks: A case study for air conditioning in California, *ASME IMECE Conference*, Boston, MA, Paper No. 76563.

Parsons, K. C. (2002). The effects of gender, acclimation state, the opportunity to adjust clothing and physical disability on requirements for thermal comfort. *Energy and Buildings* **34**(6), pp. 593-599.

Peel, M.C., Finlayson, B.L., and McMahon T.A. (2007): 'Updated world map of the Köppen-Geiger climate classification', *Hydrology and Earth System Sciences Discussions* **4**, pp. 439-473.

Phillips, B. A, (1984). Analysis of advanced residential absorption heat pump cycles. Proceedings of DOW/ORNL Heat Pump Conference, Washington D.C. pp.265-287.

Recovery.gov. Web. <http://www.recovery.gov/Pages/home.aspx>.14 Apr. 2010.

Renewable Energy Consumption and Electricity Preliminary Statistics (2008). U.S. Energy Information Administration, U.S. Department of Energy, Washington, DC.

Residential Energy Consumption Survey (2005). U.S. Energy Information Administration, U.S. Department of Energy, Washington, DC.

Roth, K. (2008). Wireless for controls: An update. *ASHRAE Journal* **50**(8), pp. 76-78.

Sanner, B, Karytsas, C. Mendrinos, H and Raybach, L. (2003), Current status of ground source heat pumps and underground thermal energy storage in Europe, *Geothermics* **32**, pp. 579–588.

Temple, K A. (2004). Field Performance of a Zoned Forced-Air Cooling System in an Energy Efficient Home. U.S. Department of Energy.

TinyOS Community Forum || An Open-source OS for the Networked Sensor Regime. Web. <http://www.tinyos.net/>.14 Apr. 2010.

Torcellini, P, Pless, S, Deru, M, and Crawley, D. (2006).Net zero energy buildings:

a critical look at the definition. *ACEEE Summer Study*, California.

Traister, J. E. (1990). *Residential Heating, Ventilating, and Air Conditioning: Design and Application*. Englewood Cliffs, N.J.: Prentice Hall.

Turns, S R.(2000). *Introduction to Combustion.* S.l. Mcgraw.

US Nuclear Plants (2009)- Palo Verde Nuclear Generating Station. *Energy Information Administration - EIA - Official Energy Statistics from the U.S. Government*. <http://www.eia.doe.gov/cneaf/nuclear/page/at_a_glance/reactors/palo_verde.html>. 14 Apr. 2010.

Vine, E. L., (1986). Saving energy the easy way: An analysis of thermostat management. *Energy* **11**(8), pp. 811-820.

Walker, I S. Register Closing Effects of Forced Air Heating System Performance. Lawrence Berkeley National Laboratory. 2003.

Walker, Iain S., & Lutz, Jim D.(2005). Laboratory Evaluation of Residential Furnace Blower Performance. Lawrence Berkeley National Laboratory: Lawrence Berkeley National Laboratory. LBNL Paper LBNL-58742.

Walpole, R E, Myers, R H, Myers, S L, Ye, K. (2007). *Probability & statistics for engineers & scientists*. Upper Saddle River, NJ: Pearson Prentice Hall.

Watt, J R. (1963). *Evaporative air conditioning*, The Industrial Press, New York

Weather Underground. <http://www.wunderground.com>.14 Apr. 2010.

Williams, E, Matthews, H S, Breton, M, and Brady, T. (2006). Use of a computer-based system to measure and manage energy use in the home. *IEEE International Symposium on Electronics and the Environment.*

Wills, J. (2004).Will HVAC Control Go Wireless? *ASHRAE Journal* **46** (7), pp. 46-52.